



**UNIVERSITÀ
DEGLI STUDI
DI TRIESTE**

UNIVERSITÀ DEGLI STUDI DI TRIESTE
XXXIII CICLO DEL DOTTORATO DI RICERCA IN
AMBIENTE E VITA

Borsa co-finanziata da Consiglio Nazionale delle Ricerche (CNR) - Istituto di Scienze Marine (ISMAR)

**DNA METABARCODIG AS A TOOL FOR
ZOOPLANKTON BIODIVERSITY ASSESMENTS IN
TRANSITIONAL ENVIRONMENTS**

Settore scientifico-disciplinare: **BIO/18 GENETICA**

**DOTTORANDA
ANNA SCHROEDER**

**COORDINATORE
PROF. GIORGIO ALBERTI**

**SUPERVISORE DI TESI
PROF. ALBERTO PALLAVICINI**

**CO-SUPERVISORE DI TESI
DR. ELISA CAMATTI**

ANNO ACCADEMICO 2019/2020

INDEX

SUMMARY	1
INTRODUCTION	4
1. DNA metabarcoding for biodiversity assessments	4
2. Biodiversity assessments in transitional environments	8
3. The study area	9
CHAPTER A: EVALUATING DNA METABARCODING FOR ZOOPLANKTON BIODIVERSITY ASSESSMENTS BY COMPARING IT WITH THE MORPHOLOGY BASED IDENTIFICATION	14
A.1 Aim	14
A.2 Material and methods	14
A.2.1 Data collection	14
A.2.2 Molecular and morphological analysis	15
A.2.3 Bioinformatic pipeline	16
A.2.4 Statistical analysis	19
A.3 Results	20
A.3.1 Taxonomical composition and richness	20
A.3.2 Spatial and temporal community patterns	26
A.4 Discussion	33
A.4.1 Molecular diversity and methodological concerns	33
A.4.2 Ecological evaluation of the two methods	39
CHAPTER B: APPLYING DNA METABARCODING ON HIGHER SPATIAL AND TEMPORAL FREQUENCY ASESSEMENTS	42
B.1 Aim	42
B.2 Material and Methods	42
B.2.1 Data collection	42
B.2.2 Molecular analysis	42
B.2.3 Bioinformatic pipeline	43
B.2.4 Statistical analysis	45
B.3 Results	46
B.3.1 Environmental characteristics	46
B.3.2 Molecular taxonomic assignment	46
B.3.3 Taxonomic composition and spatial and temporal community patterns	48
B.4 Discussion	54
CHAPTER C: COMPARING A DUAL COI MARKER FOR ZOOPLANKTON DNA METABARCODING	56
C.1 Introduction and Aim	56
C.2 Material and Methods	57
C.2.1 Data collection	57
C.2.2 Molecular analysis	57
C.2.3 Bioinformatics and statistical analyses	58
C.3 Results	59
C.3.1 Taxonomic assignment	59

C.3.2	Taxonomic richness	60
C.3.3	Relative abundances	61
C.4	Discussion	64
CHAPTER D: <i>IN-SITU</i> DIET ASSESSMENT OF THE INVASIVE CTENOPHORE <i>MNEMIOPSIS LEIDYI</i> BY DNA METABARCODING		68
D.1	Introduction and Aim	68
D.2	Material and Methods	70
D.2.1	Data collection	70
D.2.2	Molecular analysis	70
D.2.3	Bioinformatic and statistical analysis	70
D.3	Results	71
D.3.1	Biovolume of <i>Mnemiopsis leidyi</i>	71
D.3.2	Diet analysis	72
D.4	Discussion	77
CONCLUSION		82
ACKNOWLEDGEMENTS		86
REFERENCES		88
LIST OF FIGURES		104
LIST OF TABLES		108
SUPPLEMENTARY MATERIAL		110

SUMMARY

This thesis aims at evaluating the suitability of DNA metabarcoding for zooplankton biodiversity assessments. The high taxonomic and functional diversity of zooplankton, which occupies a variety of niches, significantly contributes to ecosystems functions and in the carbon flux. The Venice Lagoon and the Gulf of Venice were chosen as study area, as the elevated spatial and temporal variability of these ecosystems is advantageous for evaluation purposes. Both the taxonomic complexity of zooplankton as well as the environmental variability of transitional waters require high identification and sampling effort, which would particularly benefit from the rapidness and cost-effectiveness of DNA metabarcoding.

The taxonomic identifications and diversity patterns assessed with this molecular method, based on a COI marker proposed by Leray et al. (2013), were compared to the classical morphological analysis (CHAPTER A). On one side, in comparison to the morphological method, the molecular analysis resulted in higher taxa richness (224 vs. 88 taxa), discriminating better the meroplanktonic component, morphologically identified only up to order level. In addition, DNA metabarcoding was able to detect numerous non-indigenous species (NIS), highlighting its power as an early-detection system. On the other side, both methods revealed similar spatio-temporal patterns, and the sequence abundances were significantly correlated with individual counts for various taxonomic groups. The overall results of CHAPTER A indicate that DNA metabarcoding is an efficient tool for biodiversity assessments and laid the foundation for the subsequent applications of DNA metabarcoding. This study was already published in March 2020 in *Mar.Env.Res.* (<https://doi.org/10.1016/j.marenvres.2020.104946>).

The second chapter (CHAPTER B) describes the application of DNA metabarcoding on the zooplankton biodiversity in the Venice Lagoon by high spatial and temporal frequency sampling, testing the advantages of this fast and reliable method in increasing the monitoring effort. This large dataset revealed the presence of monthly patterns in the zooplankton community, confirming the importance of high temporal frequency

SUMMARY

assessments to detect community changes over the year and enabling a more precise description of the zooplankton biodiversity in the Venice Lagoon.

In CHAPTER C, an additional COI barcode was evaluated for zooplankton biodiversity assessment by comparing it with the COI barcode already validated in CHAPTER A. The results indicate that after a slight adjustment of the originally primer sequence proposed by Leray et al. (2013), the reverse mCOLintR primer, in combination with the jdgLCO1490 forward primer, performs very comparably to the much more widely used primer pair mCOLintF/dg+jgHCO2198. This comparability was verified in terms of level of taxonomic resolution, species detection and their relative abundance. This study was published in August 2021 in *Mar.Env.Res.* (<https://doi.org/10.1016/j.marenvres.2021.105444>).

The primer combination jdgLCO1490+mCOLintR has the advantage of not amplifying ctenophores. For this reason, it was found to be optimal for investigating on the diet of the highly invasive zooplanktivorous ctenophore *Mnemiopsis leidyi*. Up until now, to study the diet of *Mnemiopsis*, the gut content was mainly analyzed by morphological identification. In CHAPTER D, the first study investigating the feeding preference of this species utilizing DNA metabarcoding is presented. This study demonstrated the benefit of DNA metabarcoding methods, allowing to overcome the limitations in, e.g., identifying partially digested prey. The comparison of the gut content with the *in-situ* mesozooplankton community indicated that *Mnemiopsis* feeds on a variety of prey, mostly coinciding with the *in-situ* zooplankton assemblage. However, some groups, like decapod larvae and the slow-swimming larvae of gastropods and bivalves seem to be favored. Conversely, the relative abundance of copepods resulted being higher *in-situ* than in the gut content of *Mnemiopsis*.

In addition to the two articles mentioned above, during the course of this PhD, I was co-author of two other research articles on zooplankton ("*Zooplankton diel vertical migration in the Corsica Channel (north-western Mediterranean Sea) detected by a moored acoustic Doppler current profiler*" (Guerra et al., 2019; *Ocean Sci.*; DOI: 10.5194/os-15-631-2019) and "*The non-indigenous Oithona davisae in a Mediterranean transitional environment: coexistence patterns with competing species*" (Pansera et al., 2021; *Sci.Rep.*; DOI: 10.1038/s41598-021-87662-5).

INTRODUCTION

1. DNA metabarcoding for biodiversity assessments

Biodiversity assessment, that includes the estimation of species richness and the description of the community composition at different trophic levels, is a crucial element of environmental conservation and monitoring programs and finds application in several research fields, such as evolutionary, ecology and conservation biology (Gaston, 2009; Lodge et al., 2012). As the rate of biodiversity loss is constantly increasing, studying its variability in space and time is essential to carry out conservation actions (Cardinale et al., 2012). Taxonomic identification is fundamental to define management strategies for biodiversity protection, by predicting changes in communities, implementing ecological models, monitoring non-indigenous species (NIS), or by analyzing trophic pathways.

In the past, taxonomic identification has always been performed through the analysis of morphological features with the aid of supporting instruments such as stereo microscopes. This type of analysis requires great taxonomic expertise, especially in the framework of the extremely taxonomically complex group of zooplankton, where high taxonomic resolution is essential to forecast community responses to environmental alterations related to regime shifts or climate change (Sommer et al., 2017). However, the taxonomic knowledge varies among experts that are often specialized in particular taxonomic groups, reducing the consistency and comparability of different studies (Harvey et al., 2017; Sommer et al., 2017). In addition, specimens need to be well preserved, as missing or damaged parts could prevent a successful identification, especially with regard to gelatinous organisms. Moreover, the complexity of zooplankton assemblages, including cryptic and sibling species, and the lack of diagnostic characters for immature (larval) stages are key impediments to fully understand the patterns of biodiversity based on classical taxonomic identification methods (Bucklin et al., 2016; Schroeder et al., 2020). Correct morphological identification can be difficult not only due to species complexes with very similar morphological characters (e.g., *Paracalanus parvus complex*), but also in cases of high interspecific variability with phenotypic plasticity, risking to respectively under- or overestimate biodiversity. Furthermore, especially in large-scale studies, accurate

morphological assessments are very labor-intensive, explaining why the characterization of the spatio-temporal variability of zooplankton assemblages is scarcely investigated despite their ecological importance (Djurhuus et al., 2018). Regardless the rising necessity for taxonomic information across trophic levels to support ecological research and ecosystem-based management, morphological taxonomic expertise is in decline and its importance often underestimated (Hopkins and Freckleton, 2002; Kim and Byrne, 2006).

As these issues led to the rising need of more affordable, rapid and objective methods, new molecular techniques have subsequently been introduced. In 2003, a molecular method for metazoan species identification utilizing a short fragment of DNA used as a "barcode" was proposed (Hebert et al., 2003). The so-called DNA barcoding is a taxonomic method of identifying a single specimen based on sequencing a short DNA fragment (barcode), that is unique to each and can therefore be used for species discrimination. The sequence obtained by extracting, amplifying and Sanger sequencing (Sanger et al., 1977) will be compared with a reference database and eventually, if matching with a reference sequence, assigned to a species (Hebert et al., 2003). In fact, as molecular approaches are reliant on DNA barcode reference sequences from identified specimens, they do not entirely relieve from taxonomic identification and its possible impediments.

Especially since 2005, new technologies have been developed and improved. High-throughput sequencing (HTS) technologies, unlike Sanger sequencing, permitted massive parallel sequencing of multiple DNA amplicons at the same time, which significantly reduced sequencing times and costs (Bucklin et al., 2016). This new technology is the base of DNA metabarcoding (Taberlet et al., 2012) through the analysis of one or few orthologous DNA regions (Bucklin et al., 2016; Cristescu, 2014; Lindeque et al., 2013), which allows for large-scale taxonomic identification of complex samples.

Metabarcoding workflows include several laboratory and data analysis steps: i) sampling of complex samples (e.g. net sampling of plankton in case of bulk samples or water samples in case of environmental DNA (eDNA)), ii) DNA extraction, iii) amplification of the target region (e.g. using degenerate primers or taxa-specific primers) following a two-step protocol (regular PCR followed by an additional PCR to add the sample tags for

multiplexing samples and adapters necessary for the HTS platform) and lastly iv) sequencing. The obtained reads are finally subjected to a (v) bioinformatic analysis that will result in a taxonomic matrix, with which subsequently biodiversity analyses can be performed.

The estimation of biodiversity with DNA metabarcoding is becoming an important tool for surveying biodiversity: in fact, thanks to the broad taxonomic coverage and the possibility of increased sample processing speed it is possible to increase the sampling effort (frequency and spatial coverage) with sustainable costs (Brannock et al., 2014; Coissac et al., 2012), as rather than single individuals, complex bulk samples can be processed. An additional significant advantage, compared to the classical morphological identification, is the prospective to detect the 'hidden diversity' of zooplankton assemblages, including holo-, mero- and ichthyoplankton (Lindeque et al., 2013). As most marine species are planktonic at some point in their life cycle, this can give us new insights into the overall marine biodiversity (Bucklin et al., 2016). Several studies have now shown that DNA metabarcoding can be used as an efficient tool for zooplankton biodiversity assessments in various marine environments (e.g., (Bucklin et al., 2019; Deagle et al., 2018; Harvey et al., 2017; Stefanni et al., 2018). With constant progress in this technology, metabarcoding will be extremely helpful in the study of community changes, e.g., driven by climate change or habitat alterations, and studies of the ecology of cryptic taxa (Sommer et al., 2017). Also, DNA metabarcoding as rapid tool, subsequent flanked by a morphological validation, may permit the efficient prevention or mitigation of the spread of NIS by early-detection (Zaiko et al., 2015). Moreover, metabarcoding does not depend on the expertise of the single taxonomist and is therefore a more easily standardizable and comparable technique. Additionally, as the raw data consists of sequences, it can be easily re-analyzed in future studies, e.g., with new reference barcodes or improved bioinformatic pipelines, as well as, enhancing meta-analysis by sharing it with the scientific community.

In general, the mitochondrial cytochrome *c* oxidase subunit I (COI) gene is the most frequent DNA barcode region used (Hebert et al., 2003), as most taxa show a significantly different intra- versus inter-specific variability, allowing to discriminate between closely related species. The circular metazoan mitochondrial genome (mtDNA)

has a length of approximately 16 kb. However, some species have smaller mtDNA genomes, e.g., about 10-11 kb for the ctenophore *Mnemiopsis leidyi* (Pett et al., 2011). It is present in numerous copies per cell, which can be a beneficial feature compared with nuclear DNA when working on degraded samples, increasing the detection sensitivity (Deagle et al., 2006).

In the case of marine zooplankton, as this group consists of animals from almost all phyla, it is challenging to find an appropriate primer covering the immense biodiversity of zooplankton. Different gene regions have been used to describe with metabarcoding the diversity of mixed zooplankton assemblages: the four commonly used gene regions to describe patterns across different systematic levels are the mitochondrial 16S rRNA gene (Clarke et al., 2017; Lindeque et al., 2006), the nuclear genes 28S rRNA (Harvey et al., 2017; Hirai et al., 2020, 2013), and 18S rRNA (Blanco-Bercial, 2020; Chain et al., 2016; Lindeque et al., 2013; Sommer et al., 2017) and the mitochondrial COI gene (Carroll et al., 2019; Schroeder et al., 2020; Stefanni et al., 2018; Zaiko et al., 2015). The latter two are the most used ones: the 18S V9 region is a hypervariable region flanked by highly conserved sections, indicating a broad range of taxonomic groups (Amaral-Zettler et al., 2009; Medlin et al., 1988). However, the V9 region has been shown to probably not be optimal as 18S marker for zooplankton biodiversity assessment (Blanco-Bercial, 2020) and Questel et al. (2021), in fact, found the V4 region to have a greater taxonomic resolution. Due to the low genetic diversity and consequently limited taxonomic resolution of 18S rRNA regions, allowing family level identification at best, more and more zooplankton metabarcoding studies have begun to use the COI gene, which shows excellent taxonomic resolution, but with a drawback of reduced amplification success (Clarke et al., 2017). Indeed, several studies use a multi-marker approach to reduce the bias resulting from differing amplification success between various taxonomic groups. However, Clarke et al. (2017) demonstrated that COI resolved up to threefold more taxa to the species level than 18S rRNA. Also, COI has the benefit of a vast database for COI sequences (>3.5 million sequences deposited on GenBank), again increasing the suitability of COI as a genetic marker for metabarcoding. Therefore, this thesis focuses on the use of two COI barcodes based on the internal COI primers proposed by Leray et al. (2013).

2. Biodiversity assessments in transitional environments

Safeguarding the biodiversity of coastal and transitional waters is an environmental priority and a main objective of, e.g., European legislation frameworks (Water Framework Directive, WFD, 2000/60/EC; Marine Strategy Framework Directive, MSFD, 2008/56/EC). Transitional waters (estuaries, deltas, lagoons) belong to the most productive ecosystems and provide important habitats for a plethora of species, particularly during their juvenile and/or reproductive life stages (Milardi et al., 2018). Such waters also act as important nursery areas for many (commercially) important fish (Tournois et al., 2017), to which zooplankton is a very important food source. These distinct coastal ecosystems are characterized by composite gradients (Tagliapietra et al., 2009) that have a prominent role in the organization of biological communities (Reizopoulou et al., 2014), as they directly influence productivity, colonization and dispersal processes (Ghezzeo et al., 2015). In addition, they are strongly characterized by a temporal variability of hydrodynamic (freshwater inputs, meteo-marine conditions) and thermo-haline factors that lead to a high natural instability, consequently resulting in wide seasonal variations of species diversity (Reizopoulou et al., 2014).

Zooplankton occupies a variety of niches, and significantly contributes to ecosystems functions (Richardson, 2008; Steinberg et al., 2008) due to its high functional diversity (Morabito et al., 2018). Moreover, it plays a key role in the carbon flux (the biological pump) and transfers energy to higher trophic levels (Turner, 2015; Ward et al., 2012). Zooplankton significantly contributes to key ecosystems functions, not only as prey for juvenile fish species, but also as consumers of primary production. In general, in transitional environments the species are adapted to high habitat variability and show a decrease in species richness, an increase in abundance and a greater importance of small taxa along a confinement gradient (Belmonte et al., 2013; Riccardi, 2010). Due to its pronounced degree of unpredictability, however, the impact of local and large-scale environmental changes on planktonic population dynamics is hard to evaluate (Morabito et al., 2018). Therefore, especially in transitional waters, monitoring of zooplankton necessitates high sampling effort that accounts for the above-mentioned uncertainties (Hays et al., 2005; Richardson, 2008).

3. The study area

The studies presented in here were conducted in the Venice Lagoon (VL) and in the Gulf of Venice. The Gulf of Venice is a shallow coastal area located in the Northern Adriatic Sea, which is strongly influenced by the inputs of large rivers bringing water from the Alps and characterized by meso-eutrophic conditions and by a remarkable spatial and temporal variability of trophic and physico-chemical gradients (Bernardi Aubry et al., 2006). The VL has a surface area of about 550 km² with a mean north-south length of 50 km and a mean width of 10 km, and three inlets on the western side connecting the lagoon with the Adriatic Sea (Ghezzi et al., 2011). The lagoon is a heterogeneous and complex system, characterized by a number of environmental gradients involving salinity, marine water renewal (e.g. residence time), nutrients, depth and sediment structure (Tagliapietra et al., 2009) and by a mosaic of habitats and landforms (e.g. intertidal marshes, intertidal mudflats, and natural and navigation channels) that are the result of complex natural and man-induced drivers (Sigovini, 2011). It is characterized by a semi-diurnal microtidal regime with a mean range of 0.40 m during neap tides and about 0.80 m during spring tides. The amount of seawater that is exchanged during each tidal cycle is about one third of the total volume of the lagoon (Gačić et al., 2004). The residence times range from few days, in the proximity of the three inlets, to over 60 days in the inner lagoon areas (Cucco and Umgiesser, 2006). Hydrodynamics in the lagoon are driven mainly by tidal currents and affect basic parameters such as water exchange, dissolved oxygen, salinity, nutrients and sediment distribution. Only 25 % of the lagoon is deeper than 2 m and 5 % deeper than 5 m. The mean depth of tidal flats is -1.2 amsl, while it reaches -10/-15 m amsl in the natural tidal channels (Ghezzi et al., 2015, 2010; Molinaroli et al., 2007). The mean salinity ranges from 20 at sites influenced by freshwater to 33 close to the inlets, with high temporal fluctuations due to tides and river discharge (Zirino et al., 2014). The total freshwater discharge from the Lagoon river basin is about 35 m³s⁻¹ (Zuliani et al., 2005). The VL is also highly impacted by human activities (Lotze et al., 2006; Solidoro et al., 2010) and a hotspot of maritime traffic. Ballast water was recognized as a global vector in human-mediated invasions, inadvertently providing a fast and reliable dispersal mechanism for many marine taxa

and therefore massively increasing the risk of NIS introduction (Marchini et al., 2015; Vidjak et al., 2019).

The above-mentioned hydro-morphological characteristics of the VL determine a high temporal variability of variables such as salinity, nutrient concentration and dissolved oxygen. Those significantly fluctuate both on short-term (hourly/daily), depending on the weather condition and tidal phases (Sfriso et al., 1994), and on medium/long-term, including the seasonal and climate variability (Solidoro et al., 2004). Temporal and spatial fluctuation in these parameters, as well as the seasonal succession of the primary producers and their inter-annual changes (Bernardi-Aubry et al., 2020; Sfriso et al., 2003), result in substantial seasonal variability in the zooplankton community and in a variety of zooplankton species, ranging from holo- to meroplanktonic organisms, and from brackish to more typically marine species (Bandelj et al., 2008). Based on morphological identification, about 80% of the total zooplankton community in the VL is composed of copepods (with *Acartia* as the most abundant genus) and chordates with about 10%, mostly composed by Ascidiacea larvae, Appendicularia and Actinopterygii, followed by echinoderms and mollusks (Camatti et al., 2008; Schroeder et al., 2020). The composition varies from the inner parts of the lagoon with species more related to higher trophic conditions to groups, like cladocerans and other taxa (e.g., appendicularians), with more marine affinity, which are more frequent in the areas nearby the inlets (Solidoro et al., 2010).

The Gulf of Venice and the Venice Lagoon are subject of investigation within the Long-Term Ecological Research (LTER) network, the Biodiversity and Ecosystem Research LifeWatch-ERIC, and the European WFD and MSFD directives. In this context, there is a need to increase the knowledge on the zooplankton biodiversity and non-indigenous species to support the definition of Good Environmental Status (GES) and the identification of management strategies.

In the following chapters, a total of 16 stations within the VL and one in the nearby coastal area close to the research platform “Acqua Alta” were investigated (Figure 1, Table 1). Of these, five stations (st.1-5) in the VL and the one located in the Gulf of Venice (st.S) are part of the Long-Term Ecological Research (LTER; <http://www.lteritalia.it>) network (LTER_EU_IT_016 and LTER_EU_IT_057, respectively), while eleven additional stations, representative of different environmental conditions

INTRODUCTION

and habitats in the VL, were included for this study. The stations were grouped by location types (“lagoon”, “inlet” and “sea” for CHAPTER A). In CHAPTER B, including a higher number of “lagoon” stations, these were differentiated in “inner” and “med” stations, mainly based on residence time and salinity.

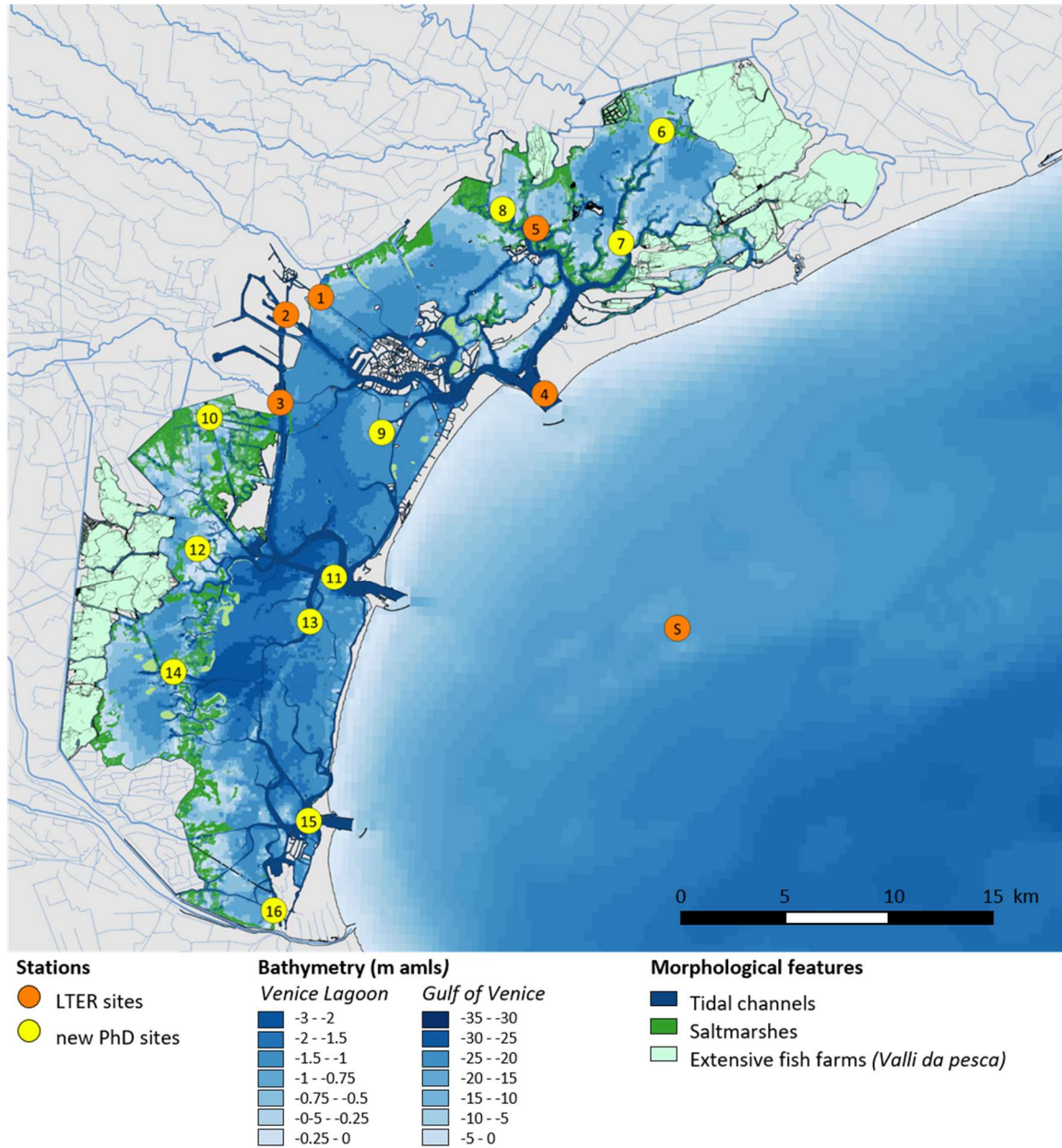


Figure 1: Study area - Overview and bathymetry of the 16 sampling stations within the Venice lagoon, and one in the Gulf of Venice. Orange dots: Long-Term Ecological Research (LTER) stations; Yellow dots: additional stations for the PhD project.

INTRODUCTION

Table 1: Name, coordinates, type, location, and chapter in which the stations were investigated.

Name	Coordinates	Station type	Location	Chapter
S	45° 18' 83.00" N; 12° 30' 53.00" E	ILTER_EU_IT_057	sea	A
1	45° 27' 55.44" N; 12° 16' 58.26" E	ILTER_EU_IT_016	lagoon/inner	A, B, C, D
2	45° 27' 25.56" N; 12° 15' 40.20" E	ILTER_EU_IT_016	lagoon/med	A, B, C, D
3	45° 25' 04.74" N; 12° 15' 34.50" E	ILTER_EU_IT_016	lagoon/med	A, B, C, D
4	45° 25' 32.94" N; 12° 25' 34.44" E	ILTER_EU_IT_016	inlet	A, B, C, D
5	45° 29' 57.12" N; 12° 25' 02.58" E	ILTER_EU_IT_016	inner	A, B, C, D
6	45° 32' 39.30" N; 12° 29' 42.12" E	PhD project	inner	B, C, D
7	45° 29' 38.40" N; 12° 28' 17.76" E	PhD project	med	B, C, D
8	45° 30' 25.50" N; 12° 23' 45.78" E	PhD project	inner	B, C, D
9	45° 24' 22.32" N; 12° 19' 27.06" E	PhD project	med	B, C, D
10	45° 24' 37.20" N; 12° 12' 54.36" E	PhD project	med	B, C, D
11	45° 20' 27.60" N; 12° 17' 50.02" E	PhD project	inlet	B, C, D
12	45° 21' 06.24" N; 12° 12' 37.68" E	PhD project	med	B, C, D
13	45° 19' 14.64" N; 12° 16' 58.56" E	PhD project	med	B, C, D
14	45° 17' 46.86" N; 12° 11' 52.68" E	PhD project	inner	B, C, D
15	45° 13' 56.28" N; 12° 17' 11.04" E	PhD project	inlet	B, C, D
16	45° 11' 31.02" N; 12° 15' 58.80" E	PhD project	med	B, C, D

CHAPTER A: EVALUATING DNA METABARCODING FOR ZOOPLANKTON BIODIVERSITY ASSESSMENTS BY COMPARING IT WITH THE MORPHOLOGY BASED IDENTIFICATION

A.1 Aim

The study presented in the first chapter aims at evaluating the suitability of DNA metabarcoding, compared to the traditional morphological method of species identification, in assessing zooplankton diversity patterns in a transitional environment along environmental gradients and over the year. A fragment (313 bp) of the cytochrome *c* oxidase subunit 1 (COI) corresponding to the second half of the universal animal DNA barcode was used (Leray et al., 2013). This is a DNA metabarcoding marker for which several studies have demonstrated its high value when studying marine metazoans (Carroll et al., 2019; Clarke et al., 2017; Stefanni et al., 2018; Zhang et al., 2018). The comparison includes measures of taxonomic richness and diversity and community composition, with the hope of highlighting promises and pitfalls of metabarcoding, giving the chance to improve those for future monitoring programs.

A.2 Material and methods

A.2.1 Data collection

The mesozooplankton community composition was seasonally investigated, from April 2016 to February 2017, at five stations in the Venice Lagoon (4 inner stations and 1 inlet station) and in the near shore coastal area in the Gulf of Venice (st.S) (Figure 1, Table 1). Surface horizontal hauls using an HydroBios Apstein plankton net (0.4 m opening diameter, 200 µm mesh size) and vertical hauls, from the bottom to the surface, using a WP2 net (0.57 m diameter, 200 µm mesh size) were performed at lagoon stations and at the marine station st.S, respectively. In order to reduce the impact of tidal phases on the monitoring results, the sampling was carried out during neap tides. The samples were divided in two equal parts: one was preserved in 4% borax-buffered formalin for

taxonomic and quantitative determinations performed by stereomicroscope, and the other part in 96% ethanol for genetic zooplankton community analysis. Contemporaneously, environmental data were measured with a multiparametric CTD probe (SBE 19plus).

A.2.2 Molecular and morphological analysis

Genomic DNA was extracted using the E.Z.N.A.[®] Mollusc DNA kit (Omega Bio-Tek) following the manufacturer's instructions by taking about one third of the total sample and increasing the initial reagents (lysis and binding buffer) provided by the kit proportionally to the sample volume. As an increase in the concentration of PCR inhibitors was previously noticed, the samples were not grinded, but the cell lysis was done overnight instead. The quality and quantity of the extracted DNA was assessed with a NanoDrop 2000 Spectrophotometer (ThermoScientific) and the amplification of the COI fragment was performed in triplicates (to reduce stochastic effects) for each sample individually using a combination of degenerated primers: mICOLintF, dgHCOI2198 and jgHCOI2198 (Table A2) with the Polymerase ready mix (2x PCR Bio HS Taq Mix) following a two-step protocol after Stefanni et al. (2018). The library was prepared for HTS by pooling an equimolar amount of all previously purified (MagBind HS) products after the secondary PCR. Next, emulsion PCR was conducted using the Ion One Touch System (Life Technologies) following the manufacturer's recommendations and DNA was bound to Ion Sphere particles (Life Technologies) for clonal amplification automatically enriched with the Ion OneTouch ES system (Life Technologies). For sequencing, the library was loaded on a 316™ chip with 650 flows in a PGM (Life Technologies).

For the creation of eight local reference sequences, belonging to four species, the DNA was extracted from morphologically identified individuals collected in station st.5 and st.S and the COI Folmer region (Folmer et al., 1994) was amplified using the primer combination LCO1490/HCO2198 (Table A2) following the manufacturer's instructions for the Polymerase ready mix (2x PCR Bio HS Taq Mix) by PCR Biosystems. DNA Sanger sequencing was performed at Macrogen (Macrogen Europe, Amsterdam, Netherlands).

For the morphological analysis, taxonomic and quantitative zooplankton determinations at the lowest possible taxonomic level (mostly species level for copepods and cladocerans) were performed using a Zeiss stereomicroscope. According to the International Council for the Exploration of the Sea (ICES) protocols (Harris et al., 2000), representative aliquots of the samples were analyzed, ranging from 1/3 to 1/40 of the total sample, while the entire samples were analyzed regarding species absent in the subsample. Other zooplankton were identified to phylum and, where possible, to class, order, or family level.

Table A2: Primers used in this chapter.

<i>primer</i>	<i>Sequence (5' - 3')</i>	<i>author</i>
mICOintF	GGWACWGGWTGAACWGTWTAYCCYCC	(Leray et al., 2013)
dgHCO2198	TAAACTTCAGGGTGACCAARAAYCA	(Meyer, 2003)
igHCO2198	TAIACYTCIGGRTGICCAARAAYCA	(Geller et al., 2013)
LCO1490	GGTCAACAAATCATAAAGATATTGG	(Folmer et al., 1994)
HCO2198	TAAACTTCAGGGTGACCAAAAATCA	(Folmer et al., 1994)

Table A3: Query for the creation of the marine metazoan reference database.

<i>Database</i>	<i>Query</i>
"Metazoa database"	((((((((((((((((((((coi) OR cox1) OR coxi) OR "cytochrome oxidase subunit 1") OR co1) AND Metazoa[Organism]) OR Chironomidae[Organism]) OR Gerrormorpha[Organism]) OR Carnoidea[Organism]) NOT Hexapoda[Organism]) NOT Tetrapoda[Organism]) NOT Arachnida[Organism]) NOT Myriapoda) NOT Onychophora) NOT Tardigrada) NOT environmental) NOT predicted) NOT unclassified) NOT unverified) AND 110:5000[Sequence Length]) AND (biomol_genomic[PROP]) AND mitochondrion[filter]

A.2.3 Bioinformatic pipeline

Raw COI reads were demultiplexed, truncated (tags and primers) and processed using the split_libraries.py script from QIIME 1 v. 1.9.0 pipeline (Caporaso et al., 2010) allowing 2 nucleotide mismatches in primers, a maximum length of homopolymers run of 8, while all other parameters were left as by default. The processing stage also included the removal of low-quality reads (minimum average Phred quality score >25) and sequences <200 bp or >1000 bp. Afterwards, the sequences were demultiplexed and dereplicated in QIIME 2 v. 2018 (Bolyen et al., 2019), chimeric feature sequences were identified and filtered with *q2-vsearch* (Rognes et al., 2016) excluding chimeras and "borderline" chimeras (Bolyen et al., 2019). Taxonomic assignment of the COI dataset was done by aligning the quality filtered reads against an in-house reference database for "marine metazoa" constructed from metazoan COI sequences that belong

to major metazoan groups that appear in marine environments deposited in GenBank (Table A3; date of download: 21.09.2018) with a naive LCA-assignment algorithm implemented in the MEGAN6 alignment tool (MALT) (Huson et al., 2016). First, an optimal similarity threshold was determined to provide a reliable basis for downstream analysis (Mohrbeck et al., 2015; Stefanni et al., 2018). Therefore, taxonomy assignment was conducted in a stepwise manner over a series of similarity thresholds (from 100% to 90%) decreasing by 1% at a time against the "marine metazoa" database. According to the relative abundance of assigned reads for various taxonomic groups at different similarity thresholds, the similarity thresholds of 97% and 94% were chosen (Figure A2).

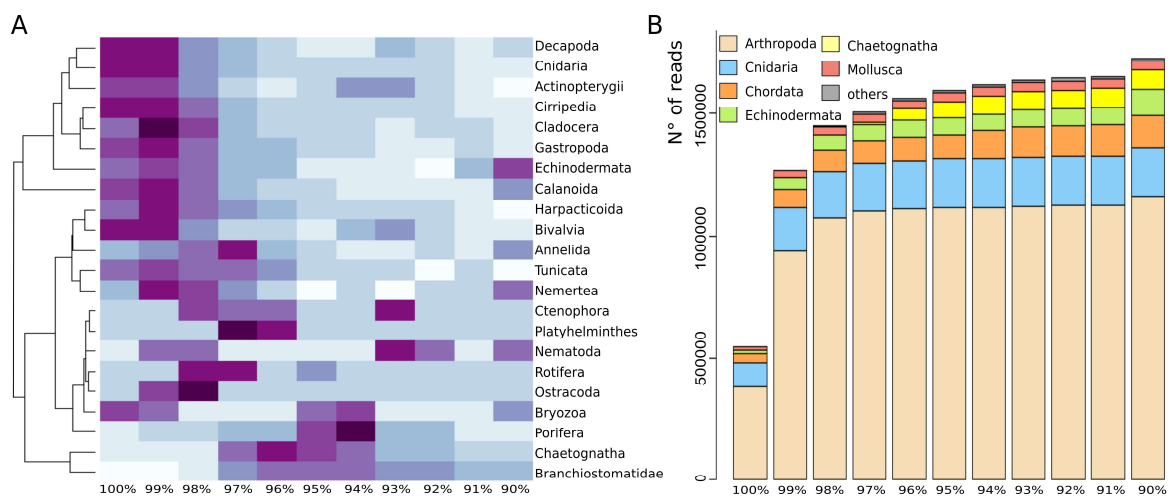


Figure A2: A) Heatmap based on the abundance of assignments for different taxonomic groups at similarity thresholds ranging from 100% to 90%, together with a similarity dendrogram. B) Barchart of summed taxonomic assignments of most the abundant phyla at different similarity thresholds (from 100% to 90%).

Above 97% similarity threshold hits were considered as species level operational taxonomic unit (OTUs) ("recovery 97%" dataset), however, if a taxon was first recovered between 97% and 94% similarity threshold, it was considered as less certain and so a "cf." was added to their taxonomy ("recovery 94%" dataset). Afterwards, both datasets were pooled together ("recovery 97% + 94%" dataset). The downstream analyses of the community diversity was performed following the suggestion of Stefanni et al. (2018), to include putative metazoan OTUs that could not be recovered above the 94% similarity threshold. For this, the remaining unassigned reads at the 85% similarity threshold were compared. Reads not matching any metazoan reference sequence at this threshold were considered as non-metazoan and were discarded, while reads with a hit were considered as putative metazoan reads (Figure A3). In the successive step, all the putative metazoan sequences were clustered *de-novo* with *VSEARCH* (Rognes et al.,

2016) using UCHIME *de-novo* approach at 97% similarity (“de-novo-recovery” dataset). VSEARCH was also used to select representative sequences for both the “de-novo-recovery” and for the “recovery 97% + 94%” datasets. To further deflate the number of OTUs and to fix erroneous OTUs, the two datasets were pooled together and curated with the LULU algorithm (Frøslev et al., 2017). After manually checking the LULU-curated OTUs, those de-novo OTUs that still remained unclustered (hence taxonomically unassigned) were blasted against the GenBank database with *BlastN*. The blasted taxonomy was checked manually and only considered when both the query coverage was above 90% and Max score above 100. If any of the blasted taxonomies matched taxonomies recovered in prior steps, they were pooled together, while blasted taxonomic assignments appearing here for the first time were only considered as “best match”. All datasets were manually checked regarding the known distribution of the corresponding taxa in the Adriatic Sea or in the Mediterranean Sea and regarding the reliability of the reference (e.g., “UNPUBLISHED” sequences from GenBank). A flowchart of the bioinformatic pipeline can be found in Figure A3.

Finally, additional reference COI sequences of the local community of three copepod species, *Labidocera brunescens*, *Centropages ponticus* and *Acartia margalefi* and for the cladoceran *Penilia avirostris* were created. Indeed, these species are expected to appear in and around the Venice Lagoon (and were also recovered with the morphological identification) but are missing or are not geographically well represented in GenBank. The GenBank accession numbers are: MN604219 and MN604220 for *Labidocera brunescens*, MN604215 and MN604216 for *Acartia margalefi*, MN604217 and MN604218 for *Centropages ponticus* and MN604221 and MN604222 for *Penilia avirostris*. The in-house reference database was expanded with these new local reference sequences. After evaluating the variation in the OTU table including and excluding the local reference sequences from the in-house reference database, the amount of the taxonomic assigned reads was manually added to the final OTU table (“local-barcodes recovery”).

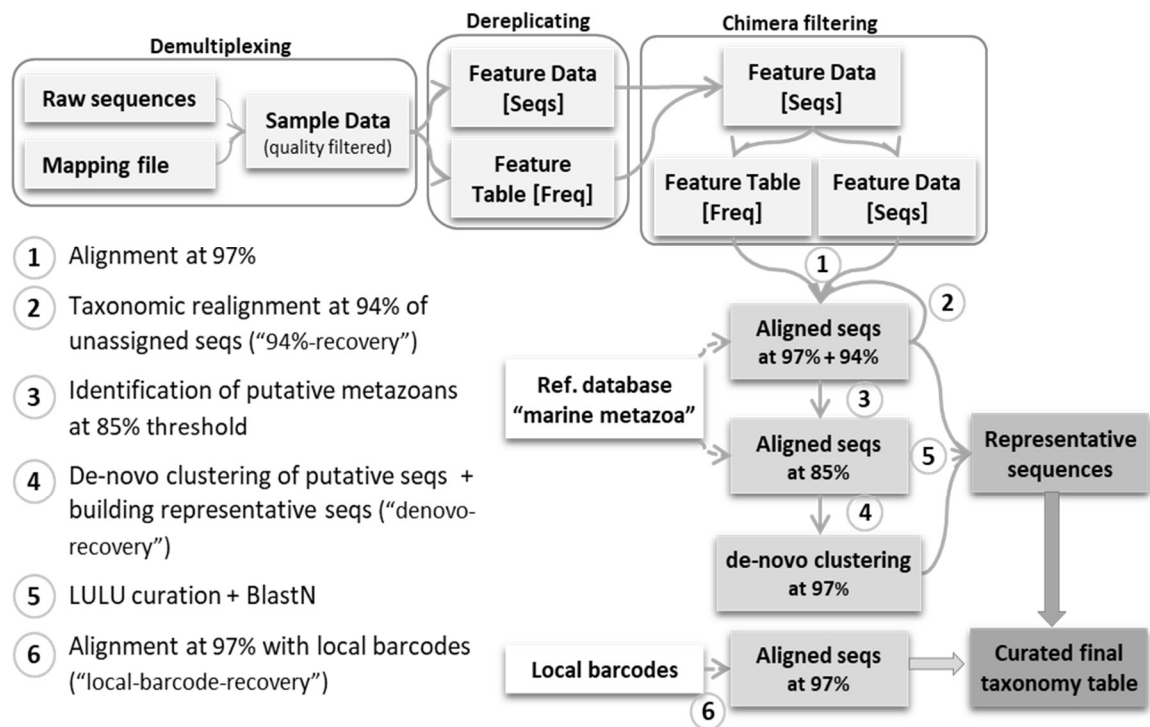


Figure A3: Flowchart of the bioinformatic multistep approach.

A.2.4 Statistical analysis

Diversity analyses were done with the R software (R Core Team, 2018). All calculations were done on square-root transformed data unless stated otherwise. Species richness per sample was quantified according to the measure of the first Hill number – MOTU/taxa richness ($q=0$) using the R package *iNEXT* (Chao et al., 2014; Hsieh et al., 2019). The taxonomic trees were created using the R package *ggtree* (Yu et al., 2017). Alpha diversity of individual communities was calculated according to the Shannon Wiener Index using the R package *vegan* (Oksanen et al., 2019). Alpha diversities of DNA metabarcoding data (hereon MBC) and morphological identification (hereon MOI) were compared with Pearson's correlation. The same comparison was done collapsing the MBC dataset to the same taxonomic level as the morphological dataset (e.g., all decapod OTUs collapsed to 1 OTU summing the reads) as proposed by Cahill et al. (2018). Finally, to evaluate the contribution of copepods to the total diversity, the estimation based on copepods only was compared to the overall diversity estimation. Differences between relative abundances (in percent) of the most abundant phyla (Arthropoda, Cnidaria, Echinodermata, Chordata, Mollusca, and Annelida) and the most abundant classes of arthropods (Hexanauplia, Malacostraca and Branchiopoda) over seasons and locations

(lagoon, including inlet, and sea) were assessed using the non-parametric Kruskal-Wallis Test, while correlations between the two methods were again tested with Pearson's correlation. Here, correlations over seasons and locations were done for the most abundant phyla and most abundant arthropod classes, while correlations for all species that were recovered in both datasets (21 species), were done by both pooling all the seasons and locations together. Pearson's correlations were evaluated from percentages of square-root transformed data after summation.

Beta diversity was evaluated from dissimilarity matrices built according to Bray-Curtis distances using the metaMDS script with the *autotransform* function (R package *vegan*) (Oksanen et al., 2019) and plotted using the function *ordiplot* superimposing the temperature and salinity values at the sampling sites using the function *ordisurf*, which fits a smooth surface for a given variable plotting it on the ordination diagram. Spatial and temporal patterns in the community composition based on Bray-Curtis similarity values were assessed using repeated-measure permutational analysis of variance (PERMANOVA) with season and location as fixed factors, and station nested within the location level (PRIMER 6+ and PERMANOVA software package; PRIMER-E, Ltd., UK) for both MBC and MOI. The correlation of the similarity matrices was calculated with the software package PRIMER6, utilizing the function *RELATE* (Spearman's correlations based on resemblance matrices) (Clarke and Gorley, 2006). The average dissimilarities between the MOI and the MBC were calculated applying *SIMPER* (on-way analysis based on Bray-Curtis similarities) using the software package PRIMER6 (Clarke and Gorley, 2006). The calculation of the combination of environmental parameters that explains the community composition was done using *BEST (BIOENV)* calculating the Spearman's correlation between both similarity matrices.

A.3 Results

A.3.1 Taxonomical composition and richness

The sequencing of the 24 samples resulted in more than 4×10^6 raw sequences. After quality check and chimera removal, the remaining 1.97×10^6 sequences had a mean length of 311.9 bp and a median length of 313 bp (Figure A4A).

At a similarity threshold of 97% mostly Arthropoda, followed by Cnidaria, Chordata and Echinodermata were identified, while the alignment at 94% similarity threshold resulted mostly in Sagittidae (Chaetognatha), Branchiostomatidae, Percomorphaceae (Chordata) and Echinoidea (Echinodermata) assignments (Figure A5). The final dataset included 1.5×10^6 assigned reads belonging to 258 OTUs. Of these, 205 OTUs (84% of assigned reads) were identified at 97%, 15 new OTUs were only identified at 94% similarity threshold (6% of assigned reads), 35 new OTUs and 4% of all assigned reads were identified by blasting the de-novo OTUs, and additional 3 OTUs and 6% of all assigned reads were assigned using the local barcodes. From the final dataset four singleton OTUs were removed as they did not have a confirmed presence in the Mediterranean Sea, while 24 singletons were kept in the dataset. Without considering the putative metazoan OTUs (“best matches”) 224 OTUs belonging to a total of 1.4×10^6 sequences were recovered.

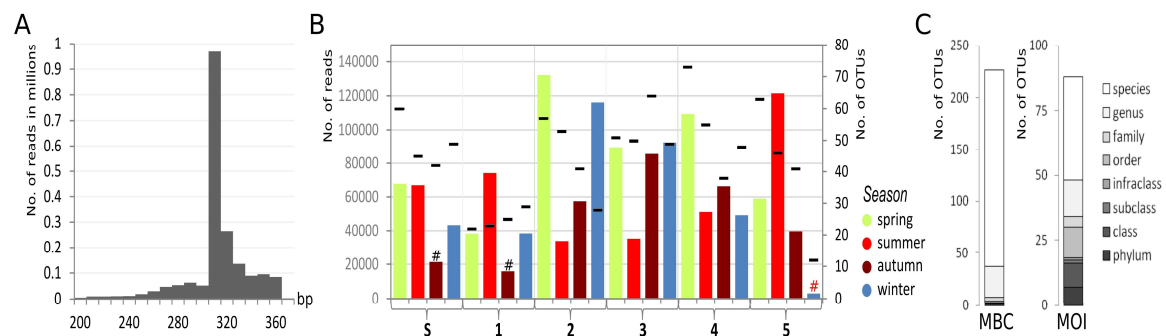


Figure A4: A) Histogram of read lengths after quality check and chimera filtering. B) Number of reads per sample of the 24 samples. Two samples (st.5 autumn; st.1, autumn) have less than 20% (black #) and one sample (st.5, winter) less than 5% (red #) of reads in relation to the sample with the highest number of reads. C) Taxonomic level of assignment using the molecular approach (MBC) and the morphological approach (MOI).

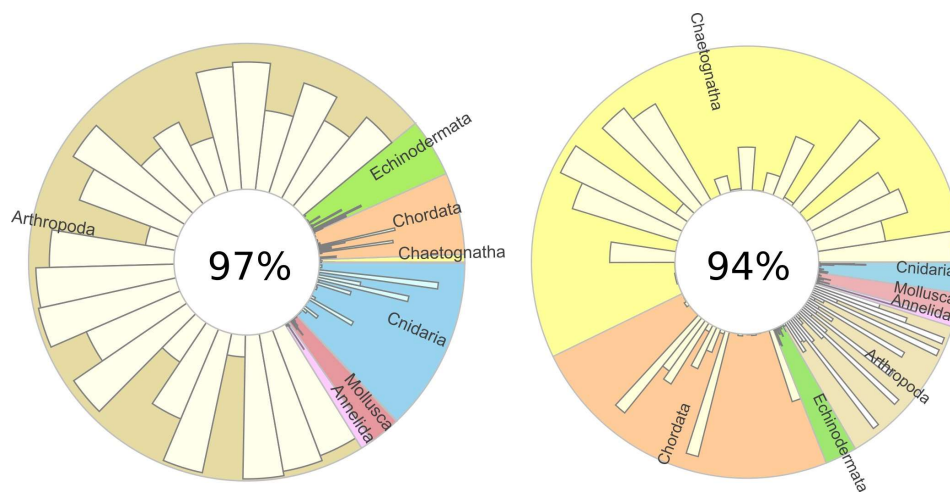


Figure A5: Pie chart of assignments with 97% (1.3×10^6) and 94% (0.94×10^6) similarity threshold of the 24 samples divided by phyla.

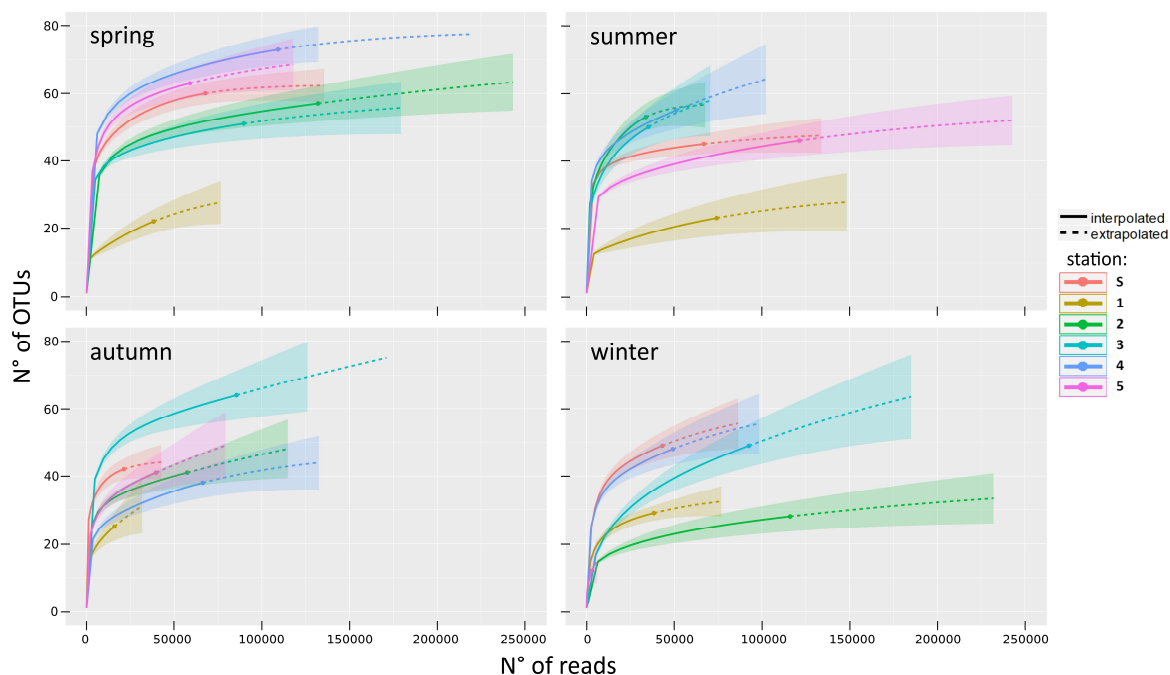


Figure A6: Sample-size-based rarefaction/extrapolation curves along with a bridging sample completeness curve of the 6 stations per seasons (R package *ggiNEXT*).

The number of reads per sample varies from 3×10^3 (st.5, winter) with 12 OTUs to 132×10^3 reads with 73 OTUs (st.2, spring) with a mean of $62.8 \times 10^3 \pm 34.3 \times 10^3$ reads and 44.3 ± 15.1 OTUs per sample (Figure A4B, Figure A6). Out of the 224 assigned OTUs identified with MBC, 188 were assigned at species level (83.6%), 29 at genus level (12.8%), while three OTUs were left unclassified (Bilateria, Protostomia, and Lophotrochozoa). The morphological identification (MOI) resulted in the identification of 88 taxa (level of taxonomic assignment: species: 40 (45.5%); genus: 14 (15.9%); family: 4 (4.5%); order: 12 (13.6%); infraclass: 1 (1.1%); subclass: 1 (1.1%); class level: 9 (10.2%); phylum level: 7 (7.9%) (Figure A4C).

The taxa richness with MBC was higher compared to the MOI (Figure A7). Using the MBC approach 188 species, 140 families, 30 classes and 15 phyla were identified (not including “best match <94%”); on the other hand, with MOI, 40 species, 23 families, 14 classes and 11 phyla were recovered. Compared to MBC, some phyla were not documented at all by MOI (Nemertea, Bryozoa, Rotifera, Gastrotricha and Platyhelminthes), some phyla were only recovered at phylum level (e.g. Ctenophora, Nematoda and Phoronida) and for some phyla, like annelids and mollusks could be assigned only to class level (polychaetes and gastropods/ bivalves). Also within arthropods, classes like Malacostraca showed much lower diversity according the MOI

approach, as for example amphipods and decapods could be assigned only to order level, while the MBC approach assigned seven amphipod OTUs and 24 decapod OTUs at species level. In addition, the MOI approach also performed poor in recovering chordates and cnidarians, namely, with MBC approach 28 chordate OTUs were identified (30 Actinopterygii, 7 ascidians and one Leptocardii, *Branchiostoma lanceolatum*) and only five with MOI approach – *Branchiostoma* larvae, Actinopterygii larvae, *Engraulis encrasicolus* eggs, Ascidiacea larvae, Appendicularia, Thaliacea. Nonetheless, the relatively abundant class Appendicularia could not be assigned molecularly and when not considering the “best matches <94%”, this approach also missed the phylum Phoronida (Figure A7).

In terms of relative abundance (read abundance) assessed by MBC approach, arthropods were the most abundant group ($67.5 \pm 26.6\%$), followed by cnidarians ($11 \pm 21.8\%$), echinoderms ($7.6 \pm 16.7\%$), chordates ($7.1 \pm 14.8\%$), mollusks ($4 \pm 7.3\%$), annelids ($1.9 \pm 4.6\%$) and other phyla (with less than 1%) ($0.1 \pm 0.6\%$) (Figure A8A). Also, the morphological analysis resulted in a dominance of arthropods in terms of number of individuals ($83.5 \pm 16.6\%$), followed by chordates ($10.9 \pm 4.1\%$), while all other phyla were much less represented (Figure A8B).

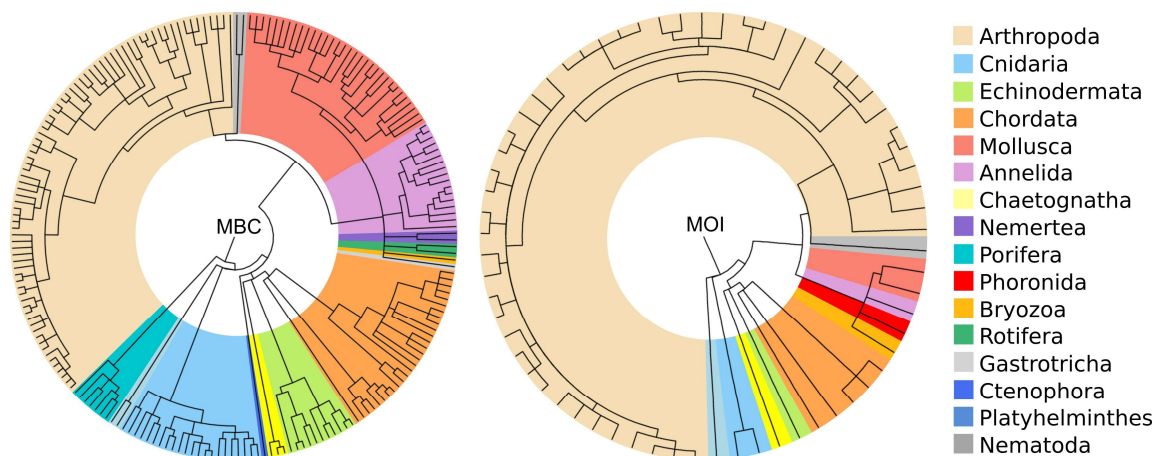


Figure A7: Taxonomic tree representing the taxonomic richness revealed with the molecular approach (MBC) and the morphological approach (MOI), respectively (R package ggtree).

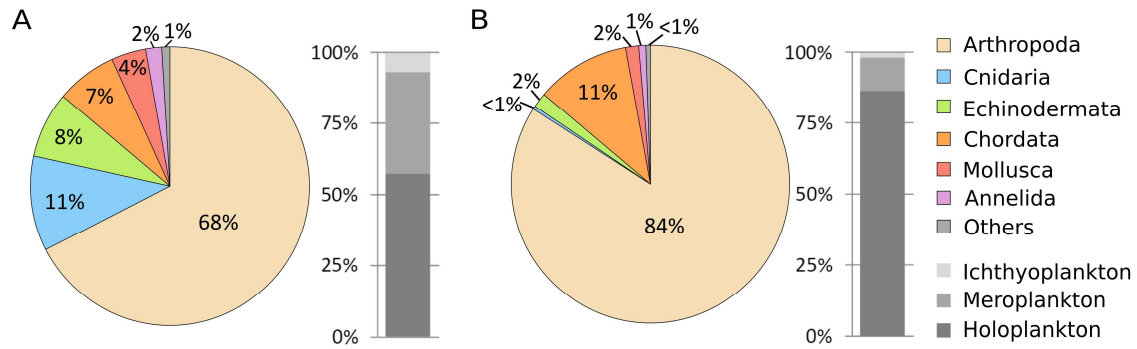


Figure A8: Relative read abundance of main phyla and of zooplanktonic groups by A) the molecular approach (MBC) and B) the morphological approach (MOI).

Although holoplankton resulted to be the most abundant group with both approaches, MBC (58%) and MOI (86%), in MBC data more than one third (35%) of the retrieved sequences belonged to meroplankton and 7% to ichthyoplankton (Figure A8A), whereas within MOI data, meroplankton contributed only with 12% to the total abundance and ichthyoplankton only with 2% (Figure A8B). In terms of species richness, in MBC data 69% of the taxa belonged to meroplankton (excluding cnidarians) and 9% to ichthyoplankton, while the morphological analysis was clearly dominated by holoplankton (80%) (mainly copepods and cladocerans) and only 10% were meroplanktonic taxa.

The species richness of copepods was similar with both methods; the molecular analysis allowed the identification of 41 taxa at species level and additional two at genus, one at family and one at order level, while the morphological analysis revealed 35 taxa at species level and additional ten at genus, four at family and four at order level. The contribution of copepods to the whole taxa richness resulted in 17.4% and 60.2% in MBC and MOI, respectively. At species level, only 18 taxa (31%) were shared by both methods; the percentage increased at genus level (57%; 16 genera) and at family level (62%, 13 families) (Figure A9A, B). Seventeen species of copepods were identified only with the morphological identification, e.g., *Clytemnestra scutellata*, *Labidocera wollastoni*, *Microsetella rosea*, *Candacia giesbrechti*, *Centropages kröyeri*, *Diaixis pygmaea*, *Oithona setigera*, *Oithona nana* and *Oithona tenuis*. Moreover, some problematic species discriminations have emerged: *Calanus helgolandicus* has been identified only by MOI and not with MBC where the sequences were assigned to reference sequences annotated as *Calanus euxinus*, known to be a population of *C. helgolandicus*. However, in the MOI dataset the abundance of adults was very low, with

only 2 specimens of *C. helgolandicus* found in 1 sample, but probably several not identified juveniles. A similar problem was observed in the *Paracalanus parvus* species complex. Here, MOI could identify only *Paracalanus parvus*, *Paracalanus nanus* and *Paracalanus sp.*, while MBC also identified *P. quasimodo* and *P. indicus*. However, according to both approaches, *P. parvus* was one of the most dominant species recovered; the mean abundance within copepods was 15.36% (up to 56%) in MOI, and 31.91% (up to 94%) in MBC. In the case of the genus *Clausocalanus*, two species were identified with both methods (*Clausocalanus furcatus* and *Clausocalanus jobei*), while MBC could identify four more species (*Clausocalanus mastigophorus*, *Clausocalanus parapergens*, *Clausocalanus lividus*, *Clausocalanus paululus*), all reported to be present in the Adriatic Sea. For two copepod families, Oncaeidae and Corycaeidae, the morphological identification stops at family level. For Oncaeidae, with MBC four species could be identified. Three of them reported for the Adriatic Sea (*Oncaea mediterranea*, *Oncaea scottodiarloi*, *Oncaea venusta*) and one species, *Oncaea waldemari*, reported for the Mediterranean, but not confirmed to be present in Adriatic Sea. For Corycaeidae, only *Ditrichocorycaeus anglicus* was identified by MBC. However, the morphological identification indicates that at least 2–3 different species of Corycaeidae could be present in the sample. Finally, *Pseudocalanus elongatus* was identified only with MBC, but it is known to be present in the Venice Lagoon from other studies (Camatti et al., 2008). The NIS species *Pseudodiaptomus marinus* was detected by both methodologies (15 samples with both methods, 3 samples only with MBC, 1 sample only with MOI). The mean zooplankton diversity measured by the Shannon Wiener Index was very similar for MBC and MOI data (2.67 ± 0.52 and 2.77 ± 0.36 , respectively). The correlation between H' -MBC and H' -MOI was $R^2 = 0.441$ ($p < 0.001$) with a slope of the line is 0.465 and a mean squared distance to 1:1 correlation line of $R^2 = 0.92$ (Figure A9C). After collapsing the molecular OTU table in order to match the morphological taxonomic resolution, the correlation between the mean of the two indices was much lower ($R^2 = 0.283$, $p < 0.01$; not shown graphically). When calculating the alpha diversity of only copepods, it resulted significantly higher with MOI data (2.25 ± 0.36) compared to MBC data (1.58 ± 0.39). Furthermore, the overall diversity and the copepod diversity were more correlated in MOI ($R^2 = 0.839$, $p < 0.001$) than in the MBC data ($R^2 = 0.533$, $p < 0.001$) (Figure A9D). The list of all detected taxa can be found in the SUPPLEMENTARY

MATERIAL with the information whether they were identified with MOI or MBC, respectively (Table S1).

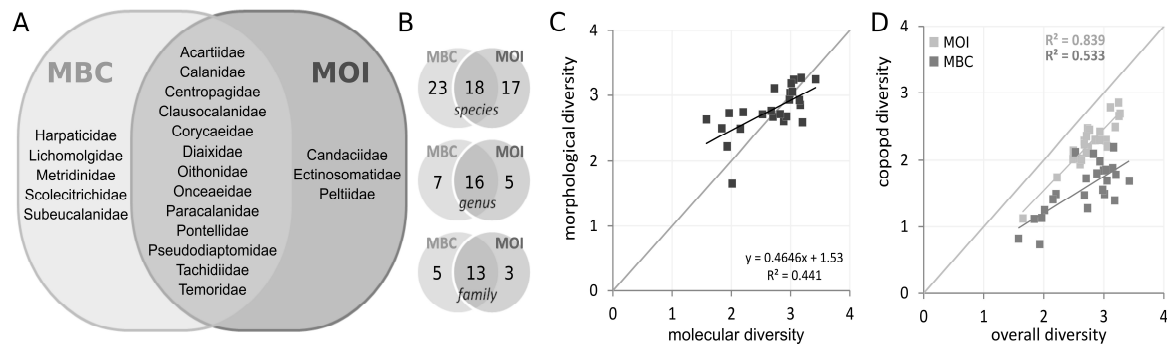


Figure A9: Venn diagram of A) list of copepod families; and B) number of taxa (species, genus, family) found with the molecular approach (MBC) and the morphological approach (MOI); and Shannon Wiener Index of C) MOI vs. MBC; and D) copepods vs. whole dataset.

A.3.2 Spatial and temporal community patterns

The relative contribution of each phylum and class to the total abundance was highly variable between locations and seasons with both methods (Figure A10). Both, MBC and MOI, indicated that arthropods are the dominant phylum in all six stations and over all seasons, and the abundances, sequence abundance for MBC and individual counts for MOI, were significantly correlated between the two methods (Table A5, Figure A11A). The annual mean of relative abundances of arthropods per station (averaged over the 4 seasons per station) calculated for MBC was $67.4 \pm 26.6\%$ and $84.1 \pm 17.4\%$ for MOI (Figure A10, Table A4). The relative abundance of arthropods was slightly higher, yet insignificantly, during winter with both methods compared to other seasons (Figure A10A, Table A4). High seasonal fluctuations in relative arthropod abundance were observed in MBC, while in MOI it was less variable (Table A4, Figure A10C, D). Comparing the mean seasonal abundance of the different classes of arthropods, MOI and MBC showed similar spatial and temporal patterns. Overall, the abundance of dominant classes of arthropods (Hexanauplia, Malacostraca and Branchiopoda) was highly correlated between the two methods and statistically significant (Table A5, Figure A11B). Hexanauplia were the most abundant class within arthropods, both with MBC ($83.7 \pm 24.5\%$ of arthropods) and MOI ($89.3 \pm 13.1\%$ of arthropods). During summer, MBC showed a decrease of Hexanauplia and a high increase of Malacostraca (Table A4). MOI showed somewhat smaller seasonal fluctuations: relative abundance of

Hexanauplia was $66.7 \pm 13.3\%$ and $78.1 \pm 21.4\%$ and of Malacostraca $11.8 \pm 15.4\%$ and $2.0 \pm 2.4\%$ in the summer and other seasons respectively (Table A4, Figure A10). In contrast to MOI, MBC showed significantly higher abundances in Malacostraca during spring-summer (Table A5). The molecular analysis resulted in a dominance of cnidarians in some samples (lagoon and inlet station), in contrast to the MOI data, where the abundance of cnidarians was overall very low (Figure A10, Table A4). However, in MOI, the relative abundance was significantly higher during summer. Indeed, the abundance of cnidarians did not result to be correlated between the two methods (Table A5, Figure A11A). Echinoderms were more abundant in the station located in the sea (st.S) than and the lagoon (st.1, 2, 3, 4, 5), but the significance for MOI was weak (Figure A10A, B, Table A4, Table A5). While in the MBC dataset echinoderms were present in all seasons, in the MOI dataset they were not present during winter (Table A4). Nonetheless, their abundance was significantly correlated between both methods (Table A5, Figure A11A). Chordates were mostly present in the lagoon stations in spring and summer in the MBC data (Figure A10A, Table A4), and mainly composed by Actinopterygii ($76.6 \pm 36.4\%$ of chordates), while with MOI, they were mostly composed by appendicularians ($55.6 \pm 44.5\%$ of chordates; Table A4). In fact, chordate abundances were not correlated between both methods (Table A5, Figure A11A). Although appendicularians were a well-represented class in the MOI data, MBC was not able to detect this class. The relative abundance of mollusks in the two methods was significantly correlated and higher in spring-summer according to both methods (Table A4, Table A5, Figure A11A).

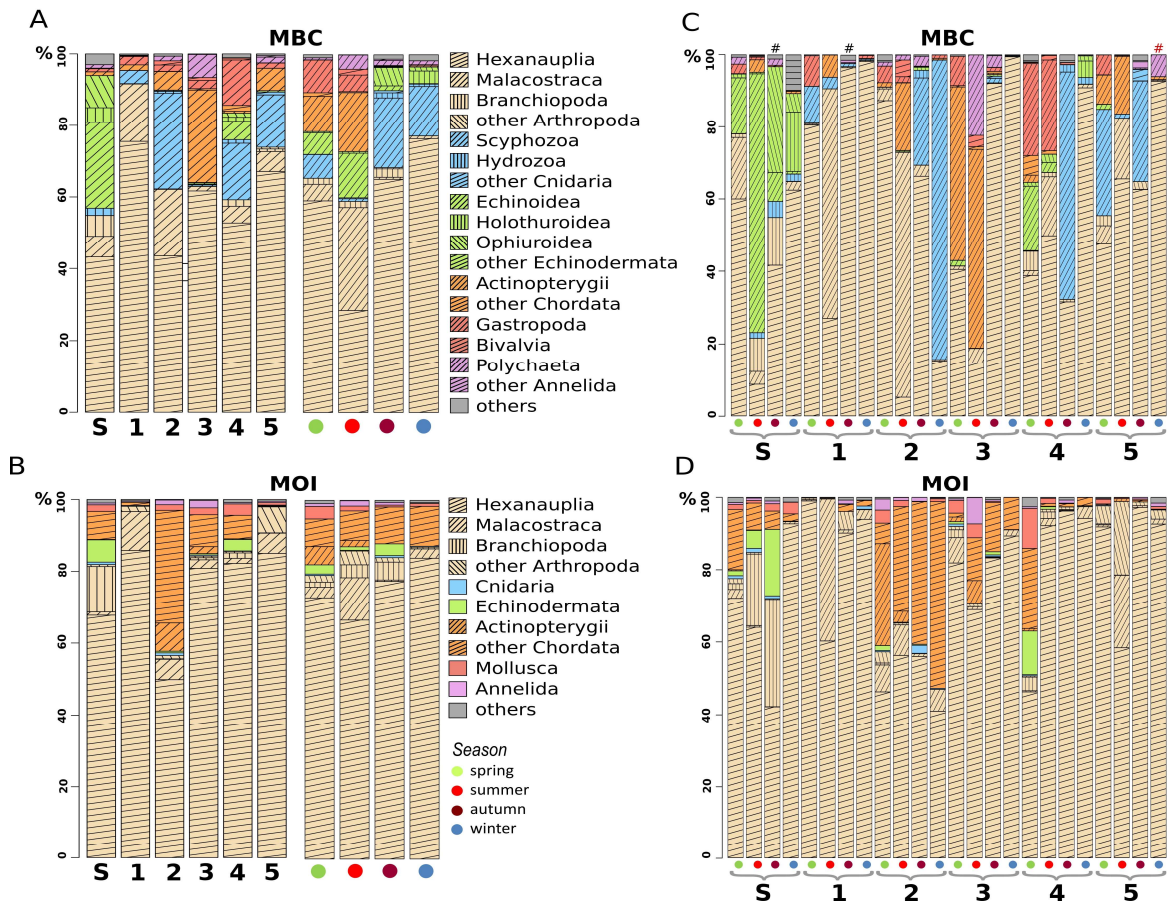


Figure A10: Barcharts of relative abundances grouped by phyla (colors) and classes (patterns) and averaged by stations (st.S, st.1–5) and by seasons with A) the molecular approach (MBC) and B) the morphological approach (MOI). Barchart of relative abundance per sample with C) MBC and D) MOI. Those samples are marked with a #, that have less than 20% (black) or less than 5% (red) of reads compared to the maximum number of reads in a sample (st.2 winter).

Also, for annelids, the two methods resulted to be correlated and showed the highest relative abundance in the same sample, st.3 during summer, with 7.4% in MOI and 22.3% in MBC (Table A5, Figure A11A). The number of sequences and the abundance counts based on morphological taxonomic identifications of selected species that are present in both datasets (19 copepods, 1 cladoceran, 1 fish species), show a significant correlation (Figure A11C), which is especially high for the most dominant of these 21 species: *A. tonsa* ($R= 0.84$, $p < 0.01$), *A. clausi* ($R= 0.8$, $p < 0.01$), *A. margalefi* ($R= 0.67$, $p < 0.01$), *C. ponticus* ($R= 0.8$, $p < 0.01$), *P. marinus* ($R= 0.89$, $p < 0.01$), *P. parvus* ($R= 0.51$, $p < 0.05$), *Temora stylifera* ($R= 0.75$, $p < 0.01$), *P. avirostris* ($R= 0.97$, $p < 0.01$), *Engraulis sp.* ($R= 0.55$, $p < 0.01$).

CHAPTER A: EVALUATING DNA METABARCODING FOR ZOOPLANKTON BIODIVERSITY ASSESSMENTS BY COMPARING IT WITH THE MORPHOLOGY BASED IDENTIFICATION

Table A4: Relative abundances in percent (mean value and standard deviation) of main phyla and of main classes of arthropods per station, location (sea, inlet, lagoon) and per season for molecular (MBC) and morphological (MOI) data.

Taxon	Tax. level	S	1	2	3	4	5	sea	inlet	lagoon	spring	summer	autumn	winter	
		mean sd	mean sd	mean sd	mean sd	mean sd	mean sd	mean sd	mean sd	mean sd	mean sd	mean sd	mean sd	mean sd	mean sd
MBC	Arthropoda	phylum	54.8 24.1	91.7 7.9	62.3 32.5	63.0 39.2	59.2 26.1	73.9 17.0	54.8 24.1	59.2 26.1	72.7 27.2	65.4 20.7	58.9 31.1	68.4 24.0	77.2 32.7
	Hexanauplia	class	43.2 24.8	75.5 33.3	43.5 27.4	61.7 40.9	52.7 26.5	67.1 18.8	43.2 24.8	52.7 26.5	61.9 33.0	59.1 20.7	28.5 24.3	65.1 26.1	76.5 32.9
	Malacostraca	class	5.8 7.7	16.1 31.7	18.6 33.1	1.3 1.9	4.7 7.8	5.6 7.9	5.7 7.7	4.7 7.8	10.4 22.0	4.6 6.3	28.7 29.2	0.6 1.2	0.8 0.9
	Branchiopoda	class	5.9 6.4	0.1 0.2	0.2 0.0	0.1 0.1	1.8 2.4	0.7 1.4	5.9 6.4	1.8 2.4	0.2 22.0	1.7 2.1	1.8 3.7	2.4 5.3	0.01 0.0
	Cnidaria	phylum	2.0 1.8	3.7 4.5	27.3 39.1	0.6 0.9	16.8 32.2	15.5 17.2	2.0 1.8	16.8 32.2	11.8 22.1	6.7 11.9	1.0 1.3	21.6 25.0	14.6 33.5
	Echinodermata	phylum	37.1 24.9	0.0 0.0	0.3 0.4	0.5 0.7	7.5 8.1	0.4 0.7	37.1 24.9	7.5 8.1	0.3 0.5	6.4 8.8	12.9 29.1	6.5 15.2	4.8 9.0
	Chordata	phylum	1.0 1.6	1.6 3.1	5.2 22.8	26.3 30.0	2.1 3.6	6.2 7.4	1.0 1.6	2.1 3.6	9.8 17.6	10.9 18.8	16.8 20.3	0.2 0.3	0.3 0.3
	Mollusca	phylum	1.0 1.1	2.5 4.1	2.2 4.0	2.2 3.6	2.3 14.9	1.4 2.7	1.0 1.1	2.3 14.9	2.5 3.1	9.2 8.4	6.2 10.2	0.4 0.4	0.3 0.4
	Annelida	phylum	1.0 1.0	0.5 0.4	0.5 1.3	0.3 10.7	0.3 0.1	0.5 2.8	1.0 1.0	0.3 0.1	2.5 5.5	0.6 0.8	4.0 9.0	1.8 1.2	1.1 2.4
	Other phyla	phylum	3.0 4.7	2.8 0.7	2.8 0.2	2.8 0.2	0.4 1.1	0.9 0.9	3.0 4.7	0.4 1.1	0.4 0.7	0.8 0.9	0.1 0.1	1.2 0.8	1.7 4.1
MOI	Arthropoda	phylum	81.9 9.2	98.1 2.0	56.5 7.5	84.3 9.9	85.6 23.3	97.9 1.1	81.9 9.2	85.6 23.3	84.2 18.4	79.1 21.1	86.0 15.1	84.1 16.9	87.0 19.8
	Hexanauplia	class	67.7 20.9	85.8 17.4	49.9 7.5	80.8 8.6	82.2 24.0	85.0 17.9	67.7 20.9	82.2 26.9	75.4 19.7	72.9 1.4	66.7 13.3	77.5 23.0	84.0 21.1
	Malacostraca	class	0.9 1.1	10.8 19.0	5.6 3.4	2.4 3.2	1.4 1.4	5.6 9.7	0.9 1.1	1.4 19.5	6.1 10.3	3.0 1.4	11.8 15.4	0.4 0.4	2.6 1.9
	Branchiopoda	class	12.8 14.4	0.01 0.0	0.1 0.3	0.6 1.1	1.5 1.7	0.1 0.1	12.8 14.4	1.5 14.8	0.2 0.5	1.4 1.4	3.6 8.0	5.0 12.0	0.04 0.1
	Cnidaria	phylum	0.7 0.4	0.2 0.5	0.7 1.0	0.3 0.3	0.1 0.2	0.1 0.1	0.7 0.4	0.1 0.2	0.3 0.6	0.4 0.3	0.2 0.5	0.6 0.9	0.3 0.3
	Echinodermata	phylum	6.2 8.4	0.0 0.0	0.5 0.6	0.4 0.4	3.2 5.9	0.0 0.0	6.2 8.4	3.2 5.9	0.2 0.4	2.6 4.7	1.0 2.0	3.3 7.4	0.0 0.0
	Chordata	phylum	7.9 6.4	0.9 1.0	39.3 8.8	10.8 6.8	6.7 10.8	0.4 0.3	7.9 6.4	6.7 10.8	12.8 17.1	12.7 14.1	10.0 12.9	10.2 15.1	11.1 20.1
	Mollusca	phylum	1.8 1.1	0.1 0.1	1.5 1.5	1.9 2.0	3.2 5.3	0.7 0.5	1.8 1.1	3.2 5.3	1.1 1.4	3.5 4.0	1.4 1.3	0.5 0.7	0.8 1.2
	Annelida	phylum	0.5 0.3	0.3 0.5	1.3 1.2	2.0 3.5	0.3 0.4	0.4 0.4	0.5 0.3	0.3 0.4	1.0 1.8	0.8 1.1	1.5 2.9	0.8 0.3	0.2 0.4
	Other phyla	phylum	1.0 0.6	0.4 0.4	0.2 0.2	0.3 0.3	0.9 1.2	0.5 0.7	1.0 0.6	0.9 1.2	0.3 0.4	0.9 1.0	0.1 0.1	0.5 0.4	0.6 0.7

Table A5: Differences between relative abundances (square-rooted data in percent) of the most abundant phyla and the most abundant classes of arthropods over seasons and locations (lagoon (st.1, 2, 3, 4) and sea (st.S)) and in specific cases, additional tests were assessed with the non-parametric Kruskal-Wallis Test. Correlations between the two methods were assessed with Pearson's correlation coefficient.

taxon	method	location (df=1)		season (df=3)		additional test (df=1)			Pearson's correlation between methods (df=22)		
		χ^2	p	χ^2	p	χ^2	p	test	r	t	p
Arthropoda	MBC	2.646	0.104	1.58	0.664	-	-	-	0.538	2.994	0.007
	MOI	1.015	0.314	0.89	0.848	-	-	-			
Cnidaria	MBC	0.096	0.757	6.77	0.08	3.24	0.072	summer vs other seasons	0.223	1.074	0.294
	MOI	1.8	0.18	4.84	0.184	4.578	0.032	summer vs other seasons			
Echinodermata	MBC	9.617	0.002	0.65	0.885	-	-	-	0.680	4.350	<0.001
	MOI	3.787	0.052	5.57	0.135	-	-	-			
Chordata	MBC	0.6	0.439	10	0.019	7.524	0.006	spring/summer vs autumn/winter	0.117	0.553	0.586
	MOI	0.096	0.757	0.1	0.992	0.0033	0.954	spring/summer vs autumn/winter			
Mollusca	MBC	0.054	0.816	12.8	0.005	12	0.001	spring/summer vs autumn/winter	0.628	3.783	0.001
	MOI	1.944	0.163	5.53	0.137	5.333	0.021	spring/summer vs autumn/winter			
Annelida	MBC	0.024	0.877	4.05	0.256	-	-	-	0.755	5.399	<0.001
	MOI	0.096	0.757	5.67	0.129	-	-	-			
Hexanauplia	MBC	3.174	0.075	8.06	0.045	6.084	0.014	summer vs other seasons	0.560	3.169	0.005
	MOI	0.486	0.486	5.42	0.144	3.24	0.072	summer vs other seasons			
Branchiopoda	MBC	3.462	0.063	6.23	0.101	3.419	0.064	spring/summer vs autumn/winter	0.752	5.350	<0.001
	MOI	2.988	0.084	6.29	0.098	3.341	0.068	spring/summer vs autumn/winter			
Malacostraca	MBC	0.096	0.757	15.1	0.002	9.818	0.002	summer vs other seasons	0.943	13.253	<0.001
	MOI	5.4	0.02	7.45	0.059	2.155	0.143	summer vs other seasons			

* p-values lower than 0.05 are highlighted in red

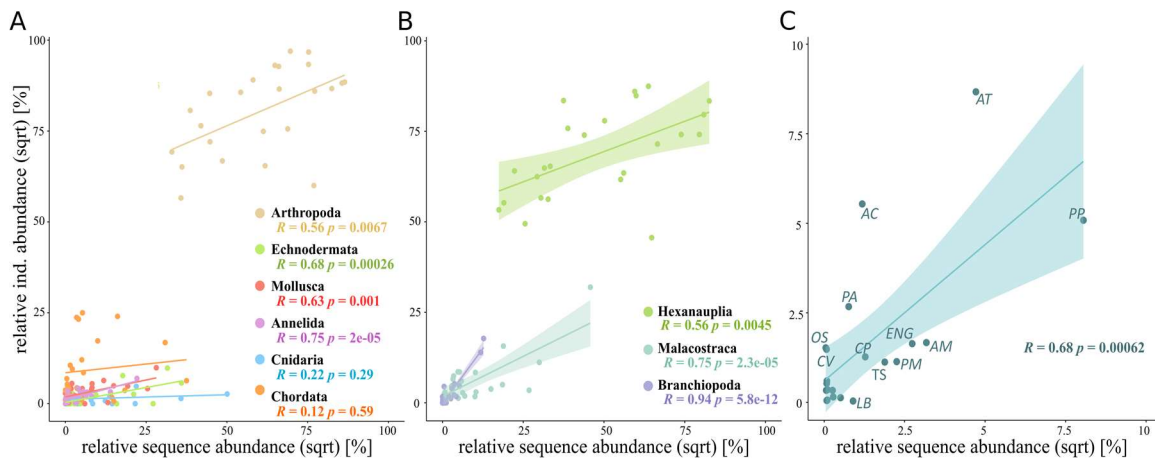


Figure A11: Relative abundance of reads for molecular data (MBC) and of individual counts for morphological data (MOI) (percent based on square-rooted data) of (A) most abundant phyla; (B) most abundant classes of Arthropoda (Hexanauplia, Malacostraca, Branchiopoda) and (C) 21 selected species present in both datasets (AT: *Acartia tonsa*, AC: *Acartia clausi*, PP: *Paracalanus parvus*, PA: *Penilia avirostris*, Eng: *Engraulis* sp., OS: *Oithona similis*, CV: *Ctenocalanus vanus*, CP: *Centropages ponticus*, TS: *Temora stylifera*, PM: *Pseudodiaptomus marinus*, LB: *Labidocera brunescens*; species with lowest abundances are not labelled (*Centropages typicus*, *Clausocalanus jobei*, *Oithona plumifera*, *Nannocalanus minor*, *Paracartia latisetosa*, *Temora longicornis*, *Clausocalanus furcatus*, *Diaixis* sp.). Pearson's correlations between the two methods are given in the corresponding color.

The beta diversity, visualized with non-metric multidimensional scaling plots (Figure A12), showed that the sample communities of MBC were clearly separated by season (PERMANOVA: Pseudo-F= 1.75, P(perm) 0.001), but not by stations (nested within location) or by locations. However, a separation of the categories, sea, inlet, and lagoon was evident. The dissimilarities between lagoon (excluding the inlet st.4) and sea stations were the largest (90.83%), followed by lagoon-inlet with 86.19% and sea-inlet (82.18%) (SIMPER on-way analysis based on Bray-Curtis similarities). Furthermore, this pattern was consistent with the ordination plot based on abundance counts (MOI), showing a separation between seasons (PERMANOVA: Pseudo-F= 2.21, P(perm) 0.001), but also location (PERMANOVA: Pseudo-F= 1.851, P(perm) 0.013). In fact, both similarity matrices, for MBC and MOI, were correlated with the environmental data (*PRIMER RELATE* - MBC: Spearman's rho= 0.494, p= 0.001; MOI: Spearman's rho= 0.308, p= 0.003). The dissimilarities of the MOI dataset were around 17% lower compared to the MBC data, with dissimilarities of 76.8% for lagoon-sea, followed by lagoon-inlet with 69.25% and sea-inlet (62.48%) (*SIMPER* on-way analysis based on Bray-Curtis similarities). The similarity between the two distance matrices (Bray-Curtis) could be confirmed as they were significantly positively correlated (Mantel statistic based on Spearman's rank correlation rho= 0.611, p= 0.001). Even though the stations were not significantly different, a differentiation following a salinity gradient was evident.

Especially in the MBC ordination plot, the stations 2 and 3 were more similar to the sea station and inlet station, compared to the two inner stations (st.1 and 5), as they are under higher marine influence being located in one of the main navigation channels for industrial transport connected to the sea (see Figure 1). The MOI ordination plot did not show such a clear discrimination (Figure A12). The combination of environmental parameters that was best explaining the community composition was salinity, temperature and Chlorophyll-*a* for the MBC data (Spearman's rho= 0.625) and salinity and temperature for MOI data (Spearman's rho= 0.495) (*PRIMER BEST*).

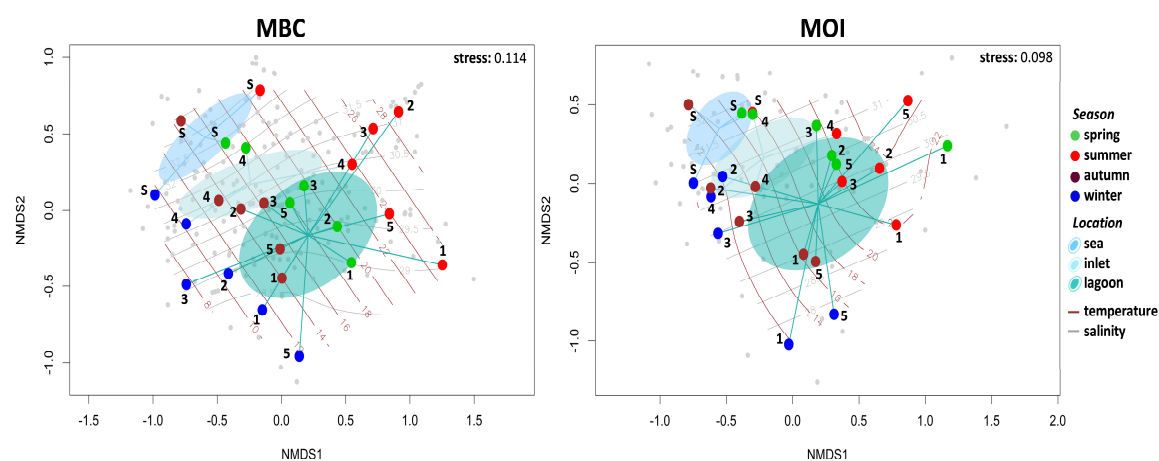


Figure A12: Beta diversity estimates based on Bray-Curtis similarities plotted on NMDS plots based on molecular (MBC) and morphological (MOI) data, respectively. Colors of points refer to the sampling season of each sample. The three locations (sea, inlet, lagoon) are highlighted plotting the distance to their centroid and the standard deviations of the points per location with the respective colors. Salinity and temperature are superimposed (brown and grey contour lines) on the NMDS plots according to the CTD measurements during sampling.

The temporal changes of relative zooplankton composition differed between MBC and MOI data. In the morphological data, most groups (typically meroplanktonic assemblages) presented an evident peak of abundance in the summer samples, over 85% for decapods, Actinopterygii, and polychaetes and for mollusks almost 70% of their total abundance (Figure A13B). Differently, the other groups showed smoother fluctuations in relative abundance; high relative abundances were found also in spring (Mollusca 70%, Actinopterygii 50%, Copepoda 35%) and in autumn (Cnidaria 37%, Copepoda 25%) and winter (Cnidaria 50%, Copepoda 28%) (Figure A13A). MBC data confirmed the summer peak found in MOI of decapod and polychaete abundance, while copepods and mollusks showed during summer their highest abundances in the MOI data and its lowest abundance in the MBC data (Figure A13A, B, Table A6).

The analysis of the three zooplanktonic groups, holo-, mero- and ichthyoplankton, showed a high peak in relative abundance during summer with MOI (close to 90%) (Figure A13D, Table A6). Also, MBC revealed mostly higher relative abundances of these groups in summer, but much less prominent (57% and 46%, respectively) (Figure A13C). In contrast, the holoplanktonic component showed an antagonistic seasonal oscillation comparing both methods, following the abundance of copepods (Figure A13C, D, Table A6).

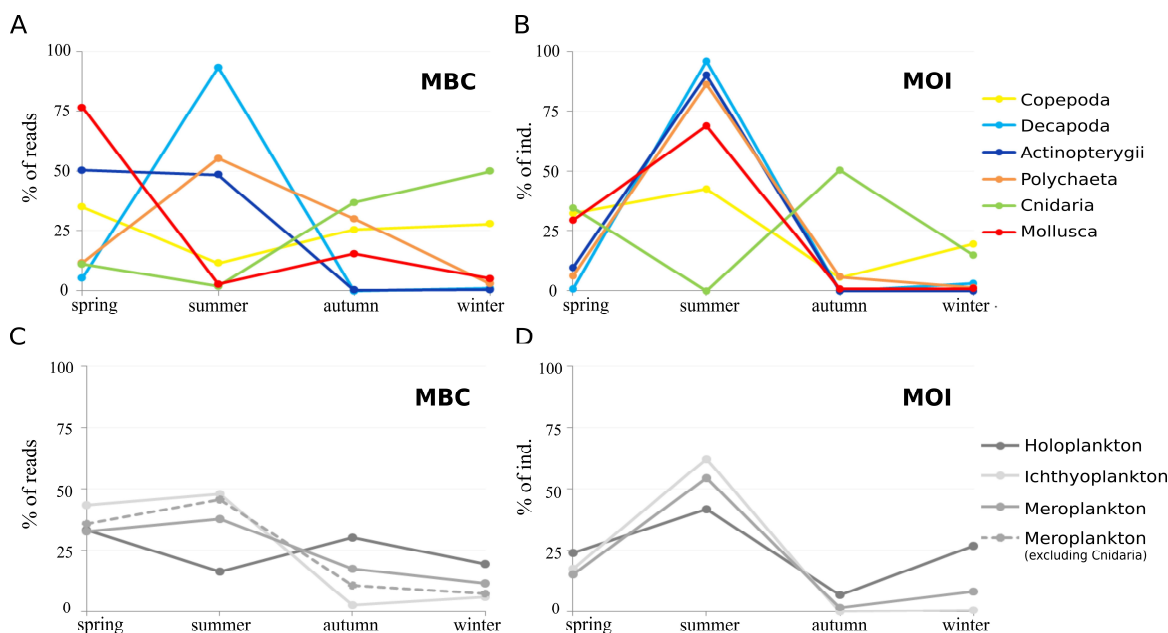


Figure A13: Relative abundance within specific taxa with A) DNA metabarcoding (MBC) and B) morphological identification (MOI); and of zooplankton groups with C) MBC and D) MOI divided by seasons calculating the fluctuation in abundances for each taxon along the year.

Table A6: Seasonal variation (relative abundances in percent) of selected taxa and of the three groups holo-, mero- and ichthyoplankton by metabarcoding (MBC) and morphological identification (MOI).

taxon/group	MBC								MOI							
	spring		summer		autumn		winter		spring		summer		autumn		winter	
	mean	sd	mean	sd	mean	sd	mean	sd	mean	sd	mean	sd	mean	sd	mean	sd
Copepoda	35.3	17.9	15.3	14.4	23.9	9.4	25.6	17.5	8.1	6.3	44.2	29.3	9.4	3.5	38.4	24.8
Decapoda	15.5	19.6	82.6	20.1	0.1	0.2	1.7	1.9	8.0	13.7	65.9	42.4	0.3	0.7	25.8	35.6
Actinopterygii	41.1	41.1	57.1	40.3	0.3	0.5	1.4	2.5	27.7	31.8	71.7	32.8	0.0	0.0	0.6	1.3
Mollusca	77.0	10.7	16.4	11.7	2.4	4.4	4.2	5.7	32.9	37.2	61.5	43.9	1.2	1.1	4.4	9.1
Polychaeta	29.5	26.7	18.6	31.0	28.1	15.7	23.8	23.9	29.0	34.7	38.4	51.8	19.4	31.7	13.2	26.5
Cnidaria	23.3	31.3	8.4	15.5	47.1	41.9	21.2	36.9	28.5	34.8	0.0	0.0	26.5	32.4	45.0	36.1
HOLO	36.7	15.1	14.7	10.1	23.9	12.7	24.7	5.6	31.1	30.5	61.5	36.1	5.6	7.6	1.9	3.7
ICHTYO	41.1	37.7	57.1	42.9	0.3	2.6	1.4	8.7	24.1	37.4	41.7	17.7	7.2	12.3	27.0	22.8
MERO	24.7	21.2	45.7	31.0	16.3	25.1	13.3	9.2	17.7	47.3	62.0	41.8	0.0	0.0	0.6	1.3
MERO (w/o Cnidaria)	23.3	25.9	8.4	18.7	47.1	48.5	21.2	28.4	15.4	40.8	54.3	36.7	1.7	3.4	8.5	14.2

A.4 Discussion

This study demonstrates that COI metabarcoding can be successfully applied to follow zooplankton biodiversity. The effectiveness of DNA metabarcoding was confirmed on three levels. First, this approach revealed a substantial level of often overlooked diversity of zooplankton, mostly due its ability in detecting the diversity of mero- and ichthyoplankton. Second, the ecological analysis revealed that the DNA metabarcoding approach gives similar spatio-temporal patterns as the morphological approach. Third, this study revealed highly significant positive correlations between total abundance counts from morphological taxonomic identification and metabarcoding sequence number for species recorded by both approaches.

A.4.1 Molecular diversity and methodological concerns

In this study, MBC was able to detect more taxa than MOI. The lower species richness in the MOI dataset was largely due to the difficulty of morphological identification of several taxa during larval stages (e.g., the larvae of decapods and mollusks or fish eggs) and to the lack of specific taxonomic expertise for some zooplankton groups; by contrast, the molecular method was able to detect sequences from cryptic early life stages (Djurhuus et al., 2018; Lindeque et al., 2013; Zaiko et al., 2015). Therefore, in MBC, a large proportion of the resulted species richness was composed by meroplankton (69%, excluding cnidarians) and ichthyoplankton (9%), while in MOI holoplankton (80%) was the dominant group (mainly copepods and cladocerans). It is therefore clear how the ability of metabarcoding to identify the mero- and ichthyoplankton can allow to study, for example, their spatial and temporal patterns and the larval dispersion, e.g., of bivalves or fish of economic interest (e.g., the three bivalves *Mytilus galloprovincialis*, *Ruditapes philippinarum*, *Chamelea gallina* or the fishes *Engraulis encrasiocolus*, *Atherina boyeri* and *Zosterisessor ophiocephalus* that were identified with MBC).

The “taxonomic bias” was especially evident when comparing the contribution of copepod diversity to the overall diversity estimated with the MBC and MOI approach. With MBC, more copepod species overall (41) were detected, but they accounted for only 22% of all recovered taxa at species level; while the 35 copepod species recovered

with MOI represent 88% of all recovered taxa at species level. Furthermore, this bias was also observed when comparing the Shannon Wiener Index based on only copepod diversity and overall diversity, as they were highly correlated and differed only slightly in the MOI dataset and were less correlated and considerably different according to the MBC dataset. Nonetheless the above-mentioned differences, both methods show that copepods dominate the zooplankton community and *Paracalanus* and *Acartia* are the most abundant genera in this study. This is in compliance with the finding by Bucklin et al. (2019) that metabarcoding analysis aligns with the morphological one. Even though only 31% of the detected copepod species were shared by both methods, those taxa comprise 98.5% of all copepod sequences obtained with MBC.

For some species, within the holoplanktonic copepods, the morphological identification of juveniles (nauplii and copepodites (C1–C4)) is not always possible at species level, e.g., for the highly abundant genera *Acartia* and *Clausocalanus*. Differently, MBC offers the detection and relative abundance including also the juveniles. However, it cannot distinguish between life stages. In this study, this may explain for example the presence of *Oithona davisae* in the MBC data, without the presence in MOI data, as the individuals could have been larval stages and therefore identified as copepod nauplii indet. Moreover, for some species, like *C. helgolandicus*, *C. euxinus* and the *P. parvus* complex, where the species status is not ultimately clarified (Kasapidis et al., 2018; Unal et al., 2006), MBC could give us new insights into the complexity of species discrimination. *Calanus helgolandicus* and *C. euxinus* are morphologically and genetically very similar, and therefore Unal et al. (2006) raised doubt about the species status of *C. euxinus* proposing that it may be a Black Sea population of *C. helgolandicus*. For the *P. parvus* species complex, Kasapidis et al. (2018) indicated that the morphological taxonomic characters are not adequate to discriminate between these species. This may have led to an inaccurate morphological identification, but at the same time the deposited sequences on NCBI may be misidentifications. This would explain why *P. parvus* is the dominant species within this complex, even though the dominant species in the Northern Adriatic may be *P. quasimodo* unlike previously thought (Kasapidis et al., 2018).

Also deficient preservation of specific groups, like some cnidarians, can limit their identification with morphological analysis, in addition to the missing expertise regarding

specific groups (Zaiko et al., 2015). Comparing the taxonomic resolution of Cnidaria for example, MBC was able to detect 29 taxa belonging to this phylum while MOI identified only four groups (Cnidaria indet., Hydrozoa indet., Scyphozoa indet. and Siphonophorae indet.). Nevertheless, it has to be taken into account that the detection of taxa only by MBC could also result from sequences derived of sloughed cells or fecal material (including organic material from adult benthic organisms) (Berry et al., 2019). Moreover, in contrast to morphological data, MBC analyses can sometimes fail, or the sequencing depth be too low and therefore, the obtained species richness and relative abundances are less reliable. In this study, three samples resulted in minor sequencing depth, but they have been kept even though probably under-sampled to not interrupt the time series.

Thanks to the bioinformatic multilevel approach used in this study, the taxonomic assignment could be improved. For example, in this way, the abundant copepod *A. margalefi* would have been recovered as “best match” from “de-novo recovery” even without the new local reference barcode. This also improves the alpha and beta diversity estimates, as in this way the diversity estimations are based also on putative metazoans, OTUs that were not assignments, but only “best matches”. While adding as much information as possible, this approach is still cautious enough, when it comes to taxonomic considerations as it considers the 94%-only species as “cf.”, and the blast hits only as “best-matches” and not as a proper taxonomic identification. MBC has the capability of identifying the taxa at lower taxonomic levels (188 vs. 40 OTUS at species level). However, identifications by MBC to species level should be interpreted carefully as the quality of the reference database is one of the most impacting aspects regarding the reliability of this method. In this study, missing reference sequences made it impossible to identify some taxa observed by microscopy, as for example eight copepod species identified only by MOI were not assigned by MBC as no species reference sequence was present on NCBI. For six of them only reference sequences of other species of the same genus were present on NCBI (*C. giesbrechti*, *C. kröyeri*, *D. pygmaea*, *O. setigera* and *O. tenuis*, and *L. wollastoni*), while for two of them not even the genus (*Clytemnestra*, *Microsetella*). In this study, three species, *C. ponticus*, *L. brunescens* and *A. margalefi* could only be identified with MBC after local barcodes were added to the reference database (“local-barcodes recovery”) (except from *A. margalefi* that would

have been also identified at 90% similarity as “best match”), highlighting again the rising need to improve and adjust to the own needs the reference database.

Missing reference sequences of congeneric species could create an erroneous identification at species level, when within a genus only one single species is present in the database. This was probably the case for the copepod *D. pygmaea*, as already mentioned by Stefanni et al. (2018). This species is missing in the NCBI reference database but confirmed for the Adriatic and present in the MOI dataset. However, as a reference sequence of the congeneric *Diaixis hibernica* was available, the MBC approach did erroneously assign the sequences to the latter. It might also be the case for the assignments of the echinoderm *Psammechinus miliaris* (found by MBC), which is the only species of that genus present on the reference database, while more probably it was *Psammechinus microtuberculatus*. In contrast, if a second congeneric species would have been present in the reference database, the LCA algorithm might have generated at least a correct genus level assignment (*Diaixis* sp. And *Psammechinus* sp., respectively), if the data sequence would have hit both reference sequences at the same similarity threshold. This highlights that metabarcoding requires taxonomically complete and geographically comprehensive reference databases (Bucklin et al., 2016). In fact, reference databases are often not representative of all taxonomic groups (Ardura et al., 2013; Ratnasingham and Hebert, 2013; Zaiko et al., 2015) resulting in possibly biased or hindered taxonomic assignments. To maximize phylogenetic representativeness and to provide an interim proximate taxonomic assignment, Weigand et al. (2019) proposed to fill the gaps producing reference barcodes of representative species first from missing orders, then missing families, and so forth down to genera in order to guarantee a broad taxonomic representation. Recently, a new COI sequence database for zooplankton communities called MetaZooGene Barcode Atlas and Database (MZGdb) (<https://metazoogene.org/database>) has recently become available (Bucklin et al., 2021), which has mined the extensive GenBank and BOLD repositories, removing errors found within these databases, and has created worldwide and geographically specific reference sequence databases for use in zooplankton metabarcoding studies.

Apart from the missing assignments due to absent reference sequences, nine copepod species were not detected by MBC even though reference sequences were available (*Mesocalanus tenuicornis*, *Isias clavipes*, *Calocalanus styliremis*, *Calocalanus pavo*,

Calanipeda aquaedulcis, *O. nana*, *C. helgolandicus*, *M. rosea* and *Goniopsyllus rostratus*), maybe due to high intraspecific variability and the fact that in most cases the reference sequences belong to specimens from the Atlantic or the Pacific Ocean or due to low abundances in the sample. However, two of them were not identified by MBC even though highly abundant (*O. nana*: max. 703.6 ind/m³ (st.S winter); *C. styliremis*: max. 487.9 ind/m³ (st.S winter)) and two others, *C. pavo* and *G. rostratus*, have been correctly assigned in another station nearby st.S in the sea (not part of this study), but not within the samples presented in this study. However, these two species showed low abundance also in the MOI data (max. 0.5 ind/m³ (st.S autumn) and max. 4.9 ind/m³ (st.S spring), respectively). It is also essential that reference specimens are correctly identified, as inaccurate identifications (including identification errors and sequence contaminations) remain a persistent impediment to the reliable use of metabarcoding for analysis of species-level zooplankton biodiversity (Bucklin et al., 2016). In some databases, including NCBI, the submission of sequences does not require to prove species identification. Therefore, special care must be taken with interpretation of the results when detecting rare or unexpected species (Djurhuus et al., 2018). In fact, when detecting a potential NIS with DNA metabarcoding, the reference sequence should be verified, as it could be a result of errors in the reference database. In this study, this was the case for example for the bony fish belonging to the family of Gobiidae, *Proterorhinus semilunaris*, a well-known highly invasive species, but not yet recorded in Venice Lagoon and adjacent coastal waters. More than 10,000 sequences were assigned to a reference sequence associated to this species. Investigating on that reference sequence (ID: EU444673), it resulted to be more similar to sequences of the family of Blenniidae than to other Gobiidae. In fact, it has as second best-match the Blenniidae *Salaria pavo*, a non-NIS fish species often recorded in Venice Lagoon. This is another example of the importance of a reliable reference database, especially when investigating on non-indigenous species. However, in this case, the risk of misidentification by MBC might have been due to the choice of the marker, as COI is probably not the best marker for the assessment of fish (ichthyoplankton) diversity as it does not offer sufficient resolution, while, e.g., CytB or the ribosomal markers 12S and 16S are probably more reliable (Evans et al., 2017; Hänfling et al., 2016; Miya et al., 2020; Vences et al., 2016). In fact, the choice of a specific barcode will alter the results in biodiversity (Clarke et al.,

2017; Piñol et al., 2019). A barcoding primer pair, which amplifies a marker sequence of short length for HTS for as many target taxa in the samples as possible, is the most critical component for successful assessments of bulk samples with DNA metabarcoding. However, finding appropriate primers for marine zooplankton assessment is difficult as most of them are prone to severe primer biases that prevent the detection of all taxa from the sample and limit the precise quantification of taxon biomass and/or abundances. Such primer biases may be even more common in the case of marine zooplankton as this group is composed by animals from almost all phyla.

To describe the diversity of mixed zooplankton assemblages using metabarcoding, different marker gene regions were used in the past. Frequently used gene regions to characterize zooplankton biodiversity patterns across different systematic levels are: the nuclear genes 18S rRNA (Chain et al., 2016; Hirai et al., 2015; Lindeque et al., 2013; Pearman et al., 2014) and 28S (Hirai et al., 2014, 2013), and the mitochondrial genes 16S rRNA (Goetze, 2010; Lindeque et al., 2006, 1999) and COI (Bourlat et al., 2013; Carroll et al., 2019; Machida et al., 2009; Schroeder et al., 2020; Stefanni et al., 2018; Zaiko et al., 2015). Indeed, several studies used a multi-marker approach for accurate species identification and discrimination, including the usage of group-specific primers (e.g. Bucklin et al., 2010) in order to reduce the bias resulting from differing amplification success between different taxonomic groups. The 18S V9 region is often the marker of choice in DNA metabarcoding studies of marine zooplankton (Bucklin et al., 2019; Stefanni et al., 2018), although recently the V4 region was shown to have a greater taxonomic resolution (Questel et al., 2021), as this hypervariable region is flanked by highly conserved sections, meaning it has a very broad amplification range (Amaral-Zettler et al., 2009) and can be considered as a “truly” universal marker for eukaryotes. Nevertheless, a very big draw of using this region for DNA metabarcoding is its low taxonomic resolution allowing family level identification at best. Therefore, more and more DNA metabarcoding studies of marine zooplankton are also relying on the COI marker, which shows great taxonomic resolution, but with a drawback of reduced amplification success. This may explain the number of copepod species that could not be identified despite the presence of reference sequences. Its limitations in quantification power, however, have so far not been evaluated thoroughly.

A.4.2 Ecological evaluation of the two methods

The analysis of alpha diversity measured by the Shannon Wiener Index gave similar results for MBC and MOI that were significantly correlated, similarly as reported by Bucklin et al. (2019) for 18S (V9). Collapsing the molecular OTU table in order to match the morphological taxonomic resolution, as proposed by Cahill et al. (2018), did not increase the correlation between the two methods regarding the alpha diversity. This is probably due to a compensation of different taxonomic groups in their contribution to biodiversity. In MBC, the contribution to the diversity resulted to be more equally shared by different groups than in MOI, coherently to the above discussed results concerning the effectiveness of MBC in detecting meroplankton and ichthyoplankton. In particular, the major contribution of the copepod diversity to the overall diversity in MOI, was a result of the minor proportion of mero- and ichthyoplankton compared to the holoplanktonic copepods. According to Bucklin et al. (2019) for 18S (V9), stating a distinction among geographic regions, both the metabarcoding data and the morphological abundance counts revealed an evidence of variation among the three locations and between seasons based on the NMDS analysis. As stated also by Harvey et al. (2017), in this study both methods show a similar spatio-temporal pattern, showing a separation by seasons in the NMDS analysis, following a gradient in temperature. The seasonality is slightly clearer with MBC, due to its capability to better detect the seasonal presence of, e.g., the decapods larvae peak during summer and the continuous decrease of mollusk larvae from spring to autumn/winter. The spatial pattern shows a noticeable differentiation along the sea-lagoon gradient (sea, inlet, lagoon) with both methods following a salinity gradient typical for transitional waters even if not statistically significant due to the high variability within the lagoon (Bianchi et al., 2004; Camatti et al., 2008; Solidoro et al., 2010). Also within the “lagoon” stations, the variability of the zooplankton community composition follows the salinity gradient, from sites with higher marine influence (st.2 and 3) to the more inner sites (st.1 and 5). However, for both biodiversity measures it has to be taken into account that the MBC data is based on the number of reads as a proxy of biomass (Harvey et al., 2017; Lindeque et al., 2013), while MOI is based on individual counts. Therefore, as for example some taxa may be larger in size (e.g. crustacean larvae) compared to others

(e.g. small copepods), their proportion in the MBC data might result greater compared to the individual based morphological data. This could result in different dominance of taxa and, mostly, in different species evenness. Correlations between sequence data and species abundance has been the focus of a number of studies (Hirai et al., 2014; Lindeque et al., 2013; Mohrbeck et al., 2015). In general, low associations between abundance or biomass and read number have been obtained (Evans et al., 2016; Harvey et al., 2017). But, similarly to the findings of Bucklin et al. (2019) for 18S (V9), where abundance counts were significantly correlated for Gastropoda, Calanoida and Chaetognatha, in this study, the COI marker was also shown to be very promising when it comes to the quantification of important taxonomic groups and a variety of taxa. The numbers of sequences and abundance counts based on morphological taxonomic identifications were significantly correlated for selected species (present in both datasets), as well as for the most abundant classes of arthropods and for most phyla, except from two, cnidarians (which seem to be overestimated by MBC) and chordates, which are composed mostly by fish sequences in MBC and by appendicularians in MOI, which could not be detected with MBC. The missing of appendicularians assignments, however, could also be due to the under representation of COI sequences deposited in GenBank database. As mentioned above, it has to be taken into account that the number reads are supposed to better correlate to the biomass than to the number of counts, as for example copepod nauplii are significantly smaller than adults and also as the sizes between copepod species do differ. In fact, for example the copepod *L. brunescens*, relatively large in size, results to be overestimated with MBC in comparison to smaller species. A reliable estimation of biomass or abundance data is still a critical issue which is a fundamental aspect in the suitability of MBC in the framework of biodiversity assessment related to water management.

The Venice Lagoon, as a transitional water body with high anthropogenic activities, is a hotspot of introduction of NIS, and the combination with special local environmental conditions makes it a highly “invadable” site (Camatti et al., 2019; Marchini et al., 2015). Several studies based on MBC successfully detected NIS, both from bulk samples (e.g. Darling et al., 2018; Flynn et al., 2015) and from eDNA (Comtet et al., 2015; Zaiko et al., 2015). In this survey, metabarcoding revealed the possible presence of several NIS, among others *Paranais frici*, *Polydora cornuta*, *A. tonsa*, *O. davisae*, *P. marinus*,

Paracaprella pusilla, *Palaemon macrodactylus*, *Dyspanopeus sayi*, *Tiaropsis multicirrata*, *Mnemiopsis leidy*, *Ostrea stentina*, *Arcuatula senhousia*). With MOI, only two non-indigenous copepod species, *P. marinus* and *A. tonsa*, have been detected in this study, and vice versa no NIS has been detected only with MOI. However, even though missing in the MOI data in this study, also the non-indigenous copepod *O. davisae* has been regularly reported with MOI in other studies in the Venice Lagoon (Pansera et al., 2021; Vidjak et al., 2019). These findings confirm that metabarcoding is a promising alternative to traditional methods for assessing the presence of NIS and their early detection. This will also help when studying the effect on recipient communities, on the ecosystem functioning and consequently on the ecosystem's services as well as predicting secondary spreads and when assessing the environmental status within the Marine Strategy Framework Directive (MSFD) (Lehtiniemi et al., 2015).

CHAPTER B: APPLYING DNA METABARCODING ON HIGHER SPATIAL AND TEMPORAL FREQUENCY ASSESSMENTS

B.1 Aim

After having successfully evaluated the suitability of DNA metabarcoding for zooplankton biodiversity assessments by comparing it with the morphological identification (CHAPTER A), this chapter aims at fully exploiting the power of this method by applying it on a zooplankton biodiversity assessment with higher spatial and temporal frequency in the Venice Lagoon.

B.2 Material and Methods

B.2.1 Data collection

The number of stations in the Venice Lagoon was increased to 16, st.1-16, (Figure 1, Table 1) and the sampling was conducted monthly in a one-year period from April 2018 to March 2019 to capture the intra-annual variability. The sampling was conducted with the same sampling method described in CHAPTER A, by surface horizontal hauls using an Apstein net with 0.4 m opening diameter and 200 μm mesh size, during neap tides, preserving the zooplankton samples in 96% ethanol for genetic analyses, and measuring in the same stations environmental data with a multiparametric CTD probe (SBE 19plus).

B.2.2 Molecular analysis

In order to allow homogenization and therefore ensure an equal extraction success, in this study, differently to the study presented in CHAPTER A, the AccuStart II PCR ToughMix (2X) Polymerase was applied, instead of the Polymerase ready mix (2x PCR Bio HS Taq Mix), as it is more resilient to possible PCR inhibition. Hence, after removing the ethanol from the representative subsamples (about one-third of the total sample) by centrifugation and rinsing with PBS (1x), the samples were homogenized by bead-beating. According to CHAPTER A, the genomic DNA was extracted using the E.Z.N.A.®

Mollusc DNA kit (Omega Bio-Tek) following the manufacturer's instructions and increasing the initial volume of reagents (lysis and binding buffer) provided by the kit proportionally to the sample volume. The quality and quantity of the extracted DNA were assessed with a NanoDrop 2000 Spectrophotometer (ThermoScientific). The amplification of the COI fragment was performed in triplicates using a combination of degenerated primers: mICOLintF, dgHCOI2198 and jgHCOI2198 (Table A2) following a two-step protocol after Stefanni et al. (2018) with the AccuStart II PCR ToughMix (2X) polymerase. The library preparation, purification, and sequencing with the Ion Torrent PGM System (Life Technologies) was performed equivalently to CHAPTER A.

B.2.3 Bioinformatic pipeline

The bioinformatic pipeline was slightly adjusted compared to CHAPTER A, by including, e.g., two types of sequencing error corrections appropriate for sequencing with Torrent PGM, while omitting the *LULU* curation due to computational limits working with a dataset of this size. The raw COI sequencing reads were first demultiplexed, truncated (tags and primers), sequences <200 bp were excluded, and sequences were trimmed to 320 bp using the CLC Genomics Workbench 20.0 (Qiagen). Afterwards, as suggested by Song et al. (2017), two different sequence corrections were sequentially applied. First, *pollux*, a *k*-spectrum-based method that divides reads into *k*-mer lengths and generates a *k*-mer depth profile (Marinier et al., 2015), was used to detect and remove homopolymers and indel-errors (insertion/deletion), typical for In Torrent PGM (Bragg et al., 2013) and then *fiona*, a suffix array/tree-based method that uses a suffix tree to detect and correct substitution errors (Schulz et al., 2014). The filtering of chimeric feature sequences on previously dereplicated data was performed with *q2-vsearch* (Rognes et al., 2016) excluding chimeras and "borderline" chimeras, and lastly, the sequences were rereplicated.

To achieve the optimal exploitation of the sequence data and therefore guarantee an assessment that is taxonomically as inclusive as possible and taking into account a series of intrinsic difficulties, e.g., complete absent or geographically not representative reference sequences, a multistep approach based on the recovery of putative metazoan sequences was performed, enabling a more reliable taxonomic assignment. A graphical representation of the bioinformatic workflow can be found in Figure B14.

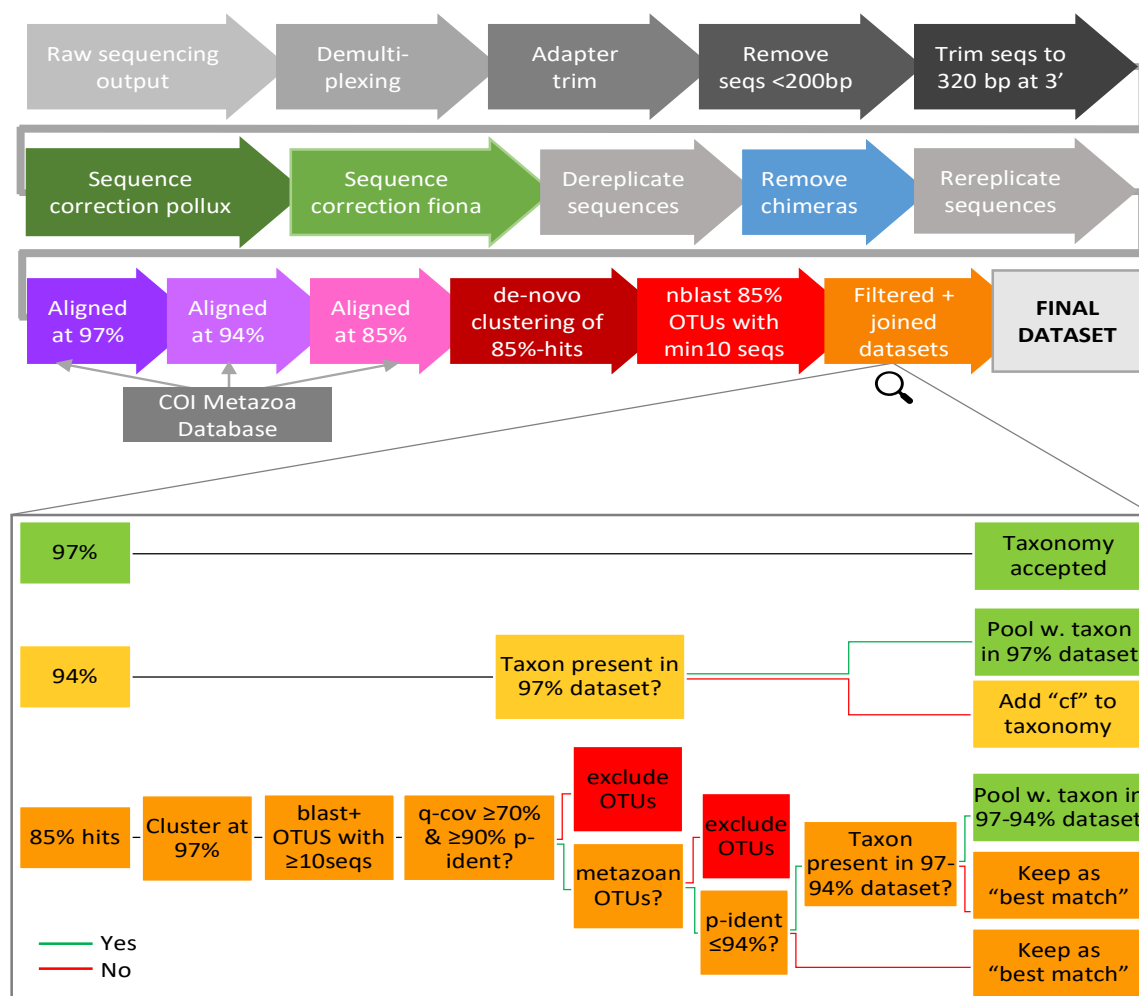


Figure B14: Bioinformatic workflow. Green boxes: taxa considered as "confidential", yellow boxes: considered as less confidential ("cf." taxa), orange boxes: even less confidential and therefore not considered in some analyses ("best match"), red boxes: OTUs were excluded as they were not considered putative metazoan sequences.

The taxonomic assignment of the quality filtered COI reads was performed by aligning them against a COI reference database of marine metazoan sequences deposited in GenBank (Table A3; date of download: 17.11.2020) with a naive LCA-assignment algorithm implemented in the MEGAN6 alignment tool (MALT) (Huson et al., 2016). First, sequences were aligned at a similarity threshold of 97%, while sequences not aligned at 97% were again aligned at 94%, and sequences not aligning at 94% were again aligned at 85% to include putative metazoan OTUs that could not be recovered above the 94% similarity threshold. Reads not matching any metazoan reference sequence at a threshold of 85% were considered non-metazoan and discarded, while reads with a hit were deemed to be putative metazoan reads. Those OTUs were clustered *de-novo* at 97% (*q2-vsearch*) (Rognes et al., 2016) and only those OTUs counting at least 10 reads in the whole dataset were kept and compared against the GenBank database with *BlastN+* (Camacho et al., 2009). Metazoan assignments that had a query cover of at least 70%

and an identity of at least 90% were kept, while all others were discarded. Finally, the three datasets were pooled together: above 97% similarity hits were considered as confidential OTUs, while, taxa firstly recovered between 97% and 94% similarity, were considered as less reliable and so a “cf.” was added to their taxonomy, and taxa detected both with 97% and 94% similarity threshold were merged. Also, putative metazoan taxonomy with a *BLASTn* p-identity of at least 94% were joined to the corresponding taxa in the pooled dataset, while OTUs with a *BLASTn* p-identity of <94% and >90% were considered as “best match” (Figure B14).

B.2.4 Statistical analysis

Spatial and temporal patterns of the environmental factors based on Euclidean distances of normalized data were assessed using the repeated-measure permutational analysis of variance (PERMANOVA) with the sampling months as fixed factor and the stations as random factor (PRIMER 6 + and PERMANOVA software package; PRIMER-E, Ltd., UK). To visualize the similarities between the samples in terms of environmental conditions a PCoA (Principal coordinates analysis) was computed and differences between months and stations were tested by the Kruskal-Wallis Test (R Core Team, 2018).

Analogously to CHAPTER A, the beta diversity was evaluated based on Bray-Curtis distances using the *metaMDS* script with the *autotransform* function and plotted using the function *ordiplot* superimposing the temperature and salinity values at the sampling sites using the function *ordisurf*. To better visualize the temporal variability, the NMDS plots were divided by the three locations (“inner”, “med”, “inlet”), and to highlight the temporal succession, a circle, colored according to the months, was manually added. The taxa best describing the ordination pattern (correlation $r^2 > 0.2$ and $p = 0.001$) are plotted as vectors using the R function *envfit*. Alpha diversity of individual communities was calculated according to the Shannon Wiener Index and plotted against temperature and salinity, and the Pearson’s correlation was calculated. Both diversity estimates were calculated using the R package *vegan* (Oksanen et al., 2019). While for the analysis of the taxonomic composition the “best matches” were excluded, the analysis of the two diversity estimates was performed including those putative metazoans.

B.3 Results

B.3.1 Environmental characteristics

The environmental parameters, measured at the sampling sites, differed significantly both spatially following a salinity and turbidity gradient, as well as temporally, between the months, following the temperature fluctuation (Figure B15A, Table B7).

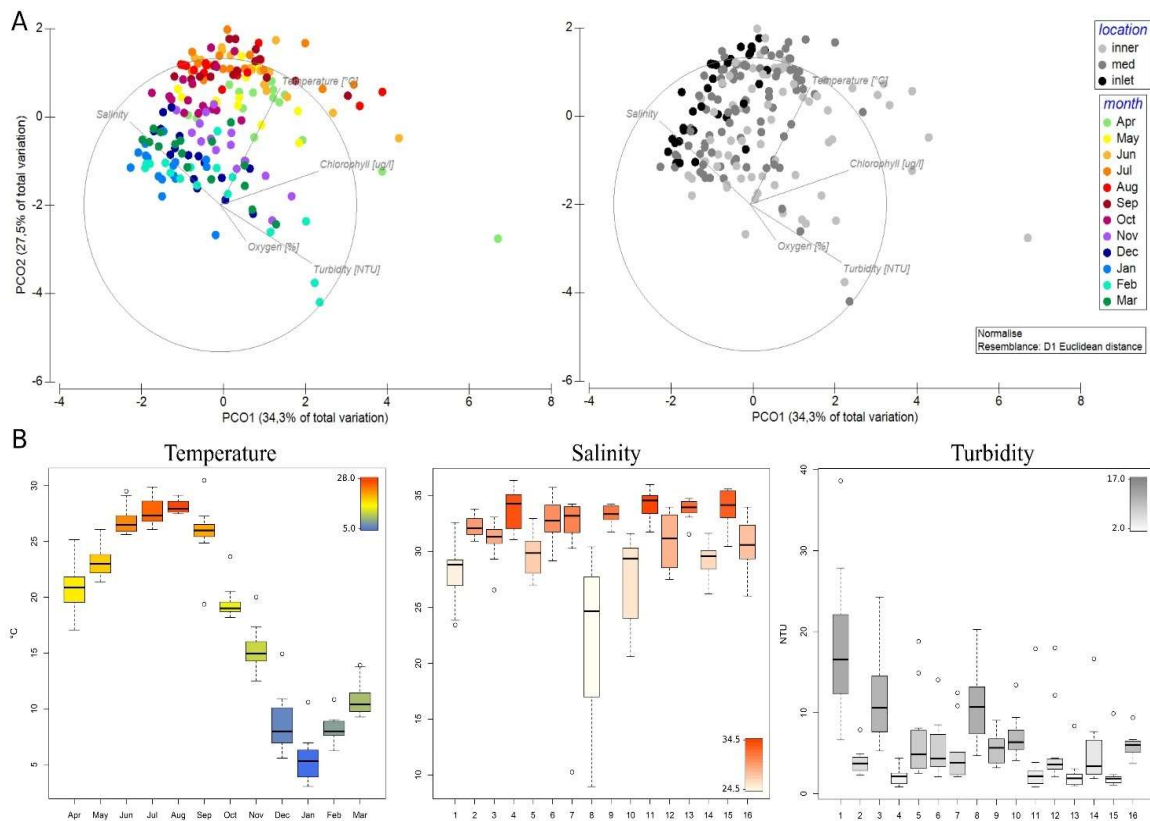


Figure B15: A) PCoA (Principal coordinates analysis) of environmental parameters colored by sampling month (left) and by location (right). B) Boxplot of Temperature, Salinity and Turbidity measured during sampling activities.

Table B7: Spatial and temporal patterns of the environmental factors based on Euclidean distances assessed using repeated-measure PERMANOVA with the sampling months as fixed factor and the stations as random factor.

	df	SS	MS	Pseudo-F	P(perm)	Unique perms
month	11	344.88	31.4	14.7	0.001	996
station	15	257.98	17.2	8.1	0.001	995
Res	165	352.14	2.1			
Total	191	955				

Especially the temperatures showed a high temporal variability owed to the general low depths in the Venice Lagoon water and exhibited the typical seasonal trend (KW: $\chi^2=180.63$, $df=11$, $p<2.2e-16$). In the months with lower temperature values, Chl-*a* was lower too. In contrast, turbidity and salinity was more related to the location, with higher salinities (KW: $\chi^2=122.54$, $df=15$, $p<2.2e-16$) and lower turbidity values (KW:

$\chi^2 = 112.7$, $df = 15$, $p < 2.2e-16$) in the inlet stations (4, 11 and 15) and the nearby areas (Figure B15B). Overall, the temperatures ranged from 3.0 to 30.5 °C ($18.3 \text{ °C} \pm 8.2$), the salinity from 9.0 to 36.3 (30.9 ± 4.2), the Chl-*a* from 0.7 to 49.3 $\mu\text{g/l}$ ($5.1 \mu\text{g/l} \pm 6.9$), the turbidity from 0.8 to 38.5 NTU ($6.3 \text{ NTU} \pm 5.6$) and the oxygen from 56.9 to 188.2% ($102.3\% \pm 17.4$).

B.3.2 Molecular taxonomic assignment

Starting with more than 10×10^6 raw sequences, after trimming, the 9,407,399 remained sequences had a mean length of 310.9 bp. The pollux correction resulted in 3,523,213 OTUs, while the successive fiona correction lowered again the variability resulting in 2,985,746 OTUs (99% similarity clustering). The chimera filtering slightly reduced both the number of sequences to 9,355,818 and 2,961,389 OTUs.

While 3,085,703 sequences (32.98%) could not be taxonomically assigned to metazoans (e.g., not (marine) metazoans, phytoplankton, or low-quality reads), a total 6,270,115 sequences were assigned to metazoans, with 489 different taxa (45 singleton taxa) (6,258,371 sequences and 447 taxa when not considering “best match” assignments). Of these, 411 taxa (84.0%) and 6,257,495 sequences (99.8%) were considered confidential assignments as they were assigned at up to 97% similarity threshold, and 36 taxa (7.4%) and 876 sequences (0.01%) were only assigned at up to 94% and therefore a “cf.” was added to their taxonomy. In addition, 43 taxa (8.8%) and 11,801 sequences (0.19%) were considered putative metazoans (“best-match”) as comparing them with the total GenBank database resulted in a similarity between 90-94% and a query cover of <70%, but the corresponding taxa were not already detected at 97% or 94% similarity (Figure B16B, Table B8).

Table B8: Number and percentage of taxa and sequences at different degrees of taxonomic assignment.

type of assignment	taxa		sequences	
	N	%	N	%
unassigned	-	-	3 085 703	32.98%
assigned	489	-	6 270 115	67.02%
Confidential taxa	411	84.0%	6 257 495	99.80%
“cf.” taxa	36	7.4%	876	0.01%
“best match”	43	8.8%	11 801	0.19%

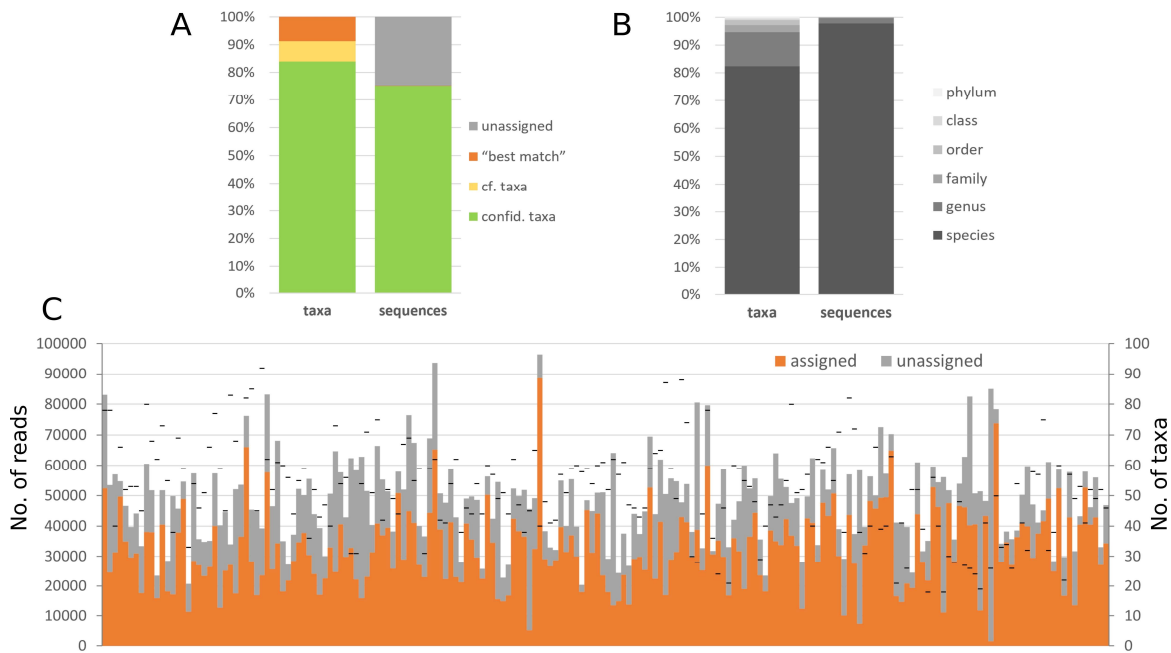


Figure B16: Proportion of taxa and sequences of A) the different degrees of taxonomic assignments and B) different taxonomic level of assignment. And C), number of sequences per sample, divided by assigned and unassigned ones, and number of taxa per sample (black bar).

Regarding the taxonomic resolution, the main proportion was composed by species level assignments (386 taxa; 82% of taxa; 97.5% of sequences) and genus level assignments (55 taxa; 12% of taxa; 2% of sequences) (Figure B16B).

The number of total reads per sample varied between 20×10^3 and 96×10^3 (mean $48,740 \pm 14,183$). The number of unassigned reads per sample ranged between 1,159 and 83,373 (4% - 98%) with a mean of $16,071 \pm 11,514$ sequences (32%), while 1,575 to 88,559 (2% - 96%) sequences per sample were assigned to metazoans with a mean of $32,668 \pm 13,186$ (63%). The number of OTUs per sample ranged from 18 to 104 (mean 51.5 ± 15.5) (Figure B16C).

Excluding the "best matches" assignments, the final dataset of 447 assigned taxa consists of 15 phyla (as in CHAPTER A), 36 classes, 93 orders, 250 families, 339 genera and 368 species (almost twice the amount compared to the 188 species detected in CHAPTER A).

B.3.3 Taxonomic composition and spatial and temporal community patterns

The taxonomic composition varied greatly between the 192 samples (Figure B18). Arthropoda was again the by far most abundant phylum, with similar amounts between the 16 investigated stations in the lagoon. Hexanauplia (mostly Calanoida) was the most

abundant class (73.1% ± 22.9), followed by Branchiopoda (composed exclusively by cladocerans) (6.6% ± 15.1) and Malacostraca (5.6% ± 8.8) (mainly composed by decapods) (Figure B17, Figure B18). While Branchiopoda showed slightly higher abundances in the inlet stations, Decapoda showed relatively consistent presence in all stations. Regarding the temporal variability, Branchiopoda showed higher abundances during late-summer and Decapoda showed mostly a spring and an autumn peak (Figure B17). Cnidarians, with Scyphozoa as the most abundant class (2.3% ± 9.6), showed singularly high abundances, but with highest consistency during winter (Figure B17, Figure B18). Gastropods (mean 2.3% ± 8.4) showed their highest relative abundance during spring and early-summer, similarly to Actinopterygii (mean 2.2% ± 6.2), while ctenophores (mean 2.9% ± 7.6), almost exclusively composed by *Mnemiopsis leidyi*, showed the highest abundances during summer and early-autumn (July-October) (Figure B17, Figure B18).

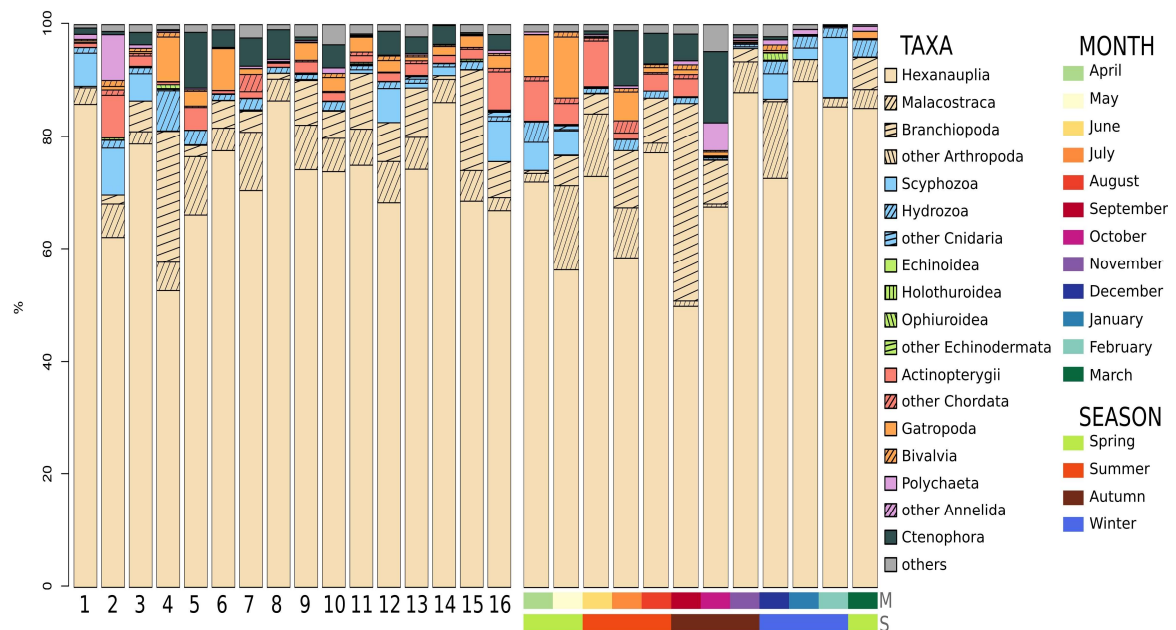


Figure B17: Barchart of mean relative abundances grouped by phyla (colors) and classes (patterns) averaged by stations (left) and by months/seasons (right).

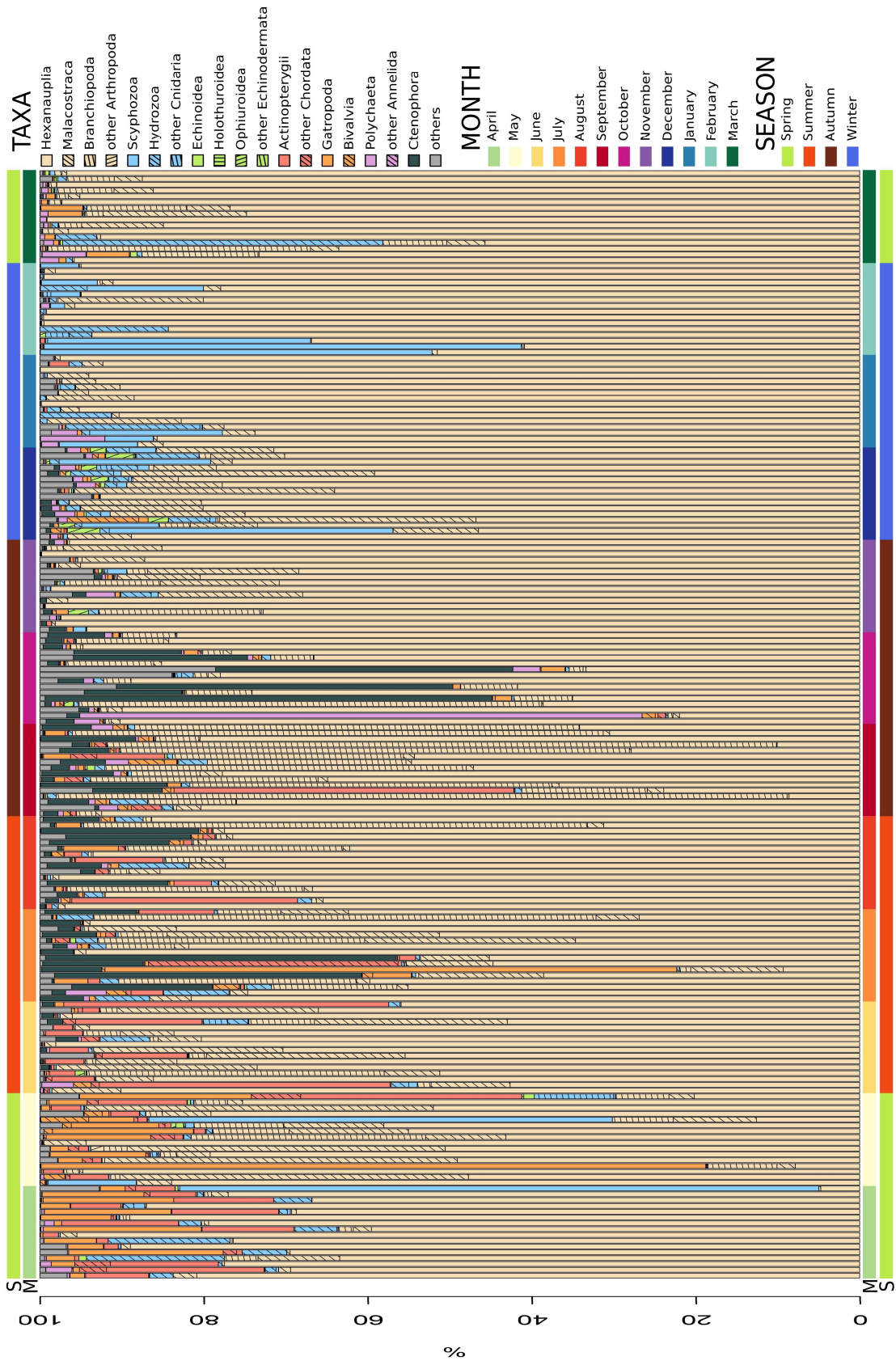


Figure B18: Barchart of relative abundances of all 192 samples grouped by phyla (colors) and classes (patterns).

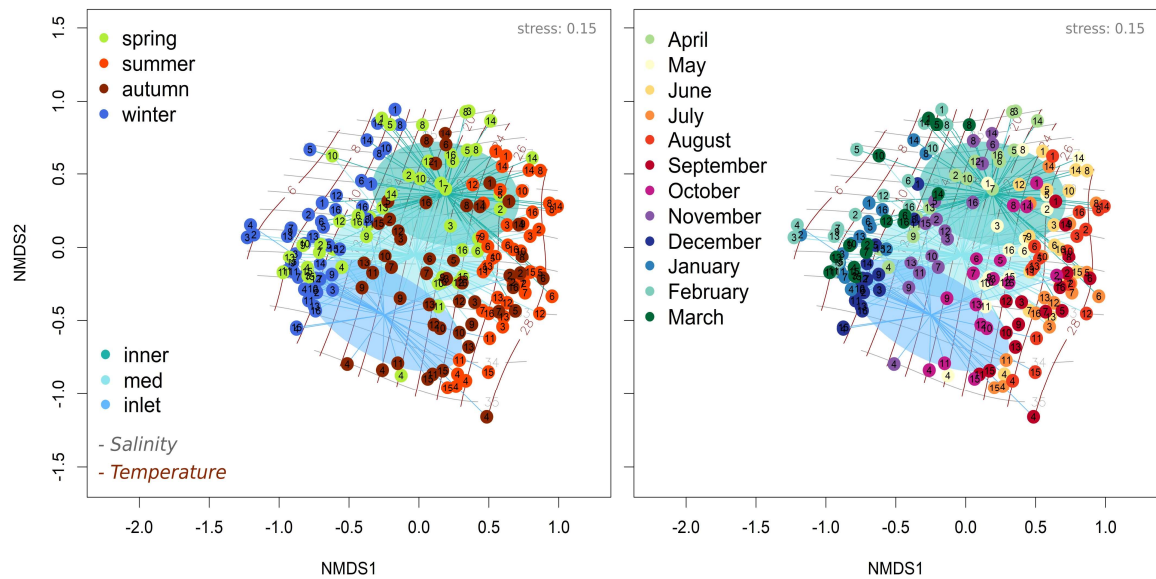


Figure B19: Beta diversity estimates based on Bray-Curtis similarities plotted on NMDS plots. Colors of points refer to the sampling season (left) and sampling month (right). The three locations (inner, med, inlet) are highlighted plotting the distance to their centroid and the standard deviations of the points per location with the respective colors. Salinity and temperature are superimposed (brown and grey contour lines) according to the CTD measurements during sampling.

The beta diversity visualized with non-metric multidimensional scaling (NMDS) plots showed that the sample communities are moderately separated by locations (inner, med, inlet), following the salinity gradient, as well as by season and partially by month of sampling, following a temperature gradient (Figure B19). However, the differences between months was less evident, as partially masked by the spatial variability. Therefore, NMDS plots divided by location were computed to better visualize the temporal variability, which in fact, showed an almost perfect circular succession of the months regarding the community composition (Figure B20). This is especially true for the med and inlet stations, and less evident for the inner stations. The division also enabled to better investigate on the species best explaining the pattern in the NMDS plots. Accordingly, in the “inner” stations, the spring and early-summer is characterized by the copepod *Acartia tonsa* and the barnacle *Amphibalanus eburneus*, followed in the late-summer by *Centropages ponticus* and *Mnemiopsis leidyi*. During winter, the inner stations are characterized by the copepods *Euterpina acutifrons*, *Oncaea*, *Calanus helgolandicus/euxinus*, the *Paracalanus parvus complex*, and by the decapod *Carcinus aestuarii*, followed by *Acartia clausii*.

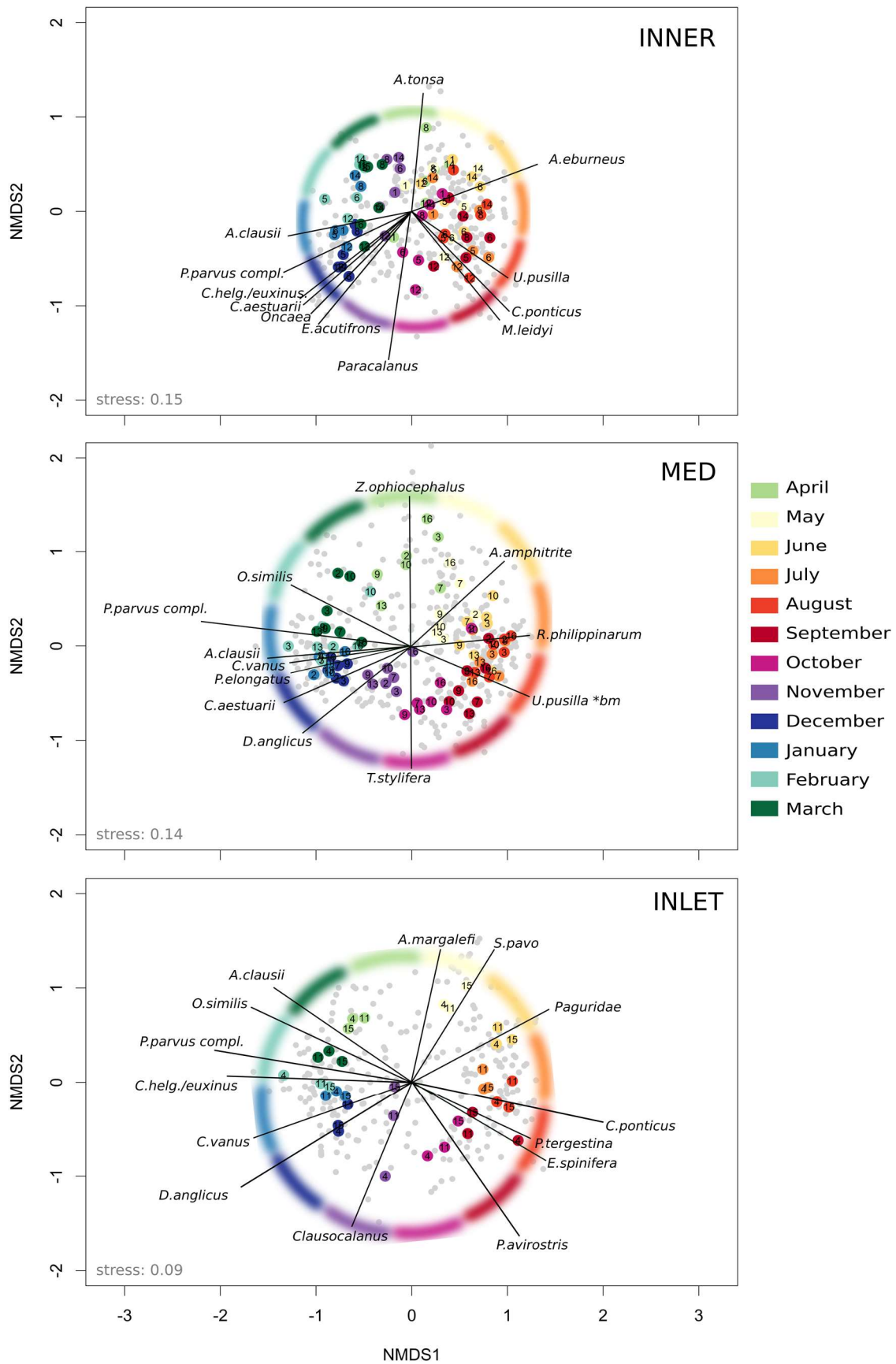


Figure B20: Beta diversity estimates based on Bray-Curtis similarities plotted on NMDS plots divided by sampling location, inner (top), med (center) and inlet (bottom) stations. Colors refer to the sampling month. To highlight the circular succession of months, a colored ring was manually added. The taxa best describing the ordination pattern ($r^2 > 0.2$ and $p = 0.001$) are plotted as vectors.

The “med” stations are characterized in spring by the gobby *Zosterisessor ophiocephalus* and the barnacle *Amphibalanus amphitrite*, during summer by the manila clam *Ruditapes philippinarum* and by the mud shrimp *Upogebia pusilla*, during autumn by the copepod *Temora stylifera* and during winter by the copepods *Ditrichiocorycaeus anglicus*, *Pseudocalanus elongatus*, *Ctenocalanus vanus*, and the *P. parvus* complex and again by the decapod *C. aestuarii*. Finally, the “inlet” stations are characterized during spring by the presence of the copepod *A. margalefi*, the blenny *Salaria pavo* and Paguridae, during summer by *C. ponticus* and during autumn-winter by the cladocerans *Pseudoevadne tergestina*, *Evadne spinifera* and *Penilia avirostris*, and the copepods *Clausocalanus*, *D. anglicus*, *C. vanus*, *C. helgolandicus/euxinus*, the *P. parvus* complex and *Oithona similis* (Figure B20).

The alpha diversity, measured by the Shannon Wiener Index, is only weakly significantly correlated to temperature ($R= 0.22$, $p= 0.002$), but highly significantly to salinity ($R= 0.5$, $p= 2.5e-13$), indicating that with increasing connectivity to the sea, from the inner areas of the lagoon towards the inlets, the alpha diversity increases (Figure B21).

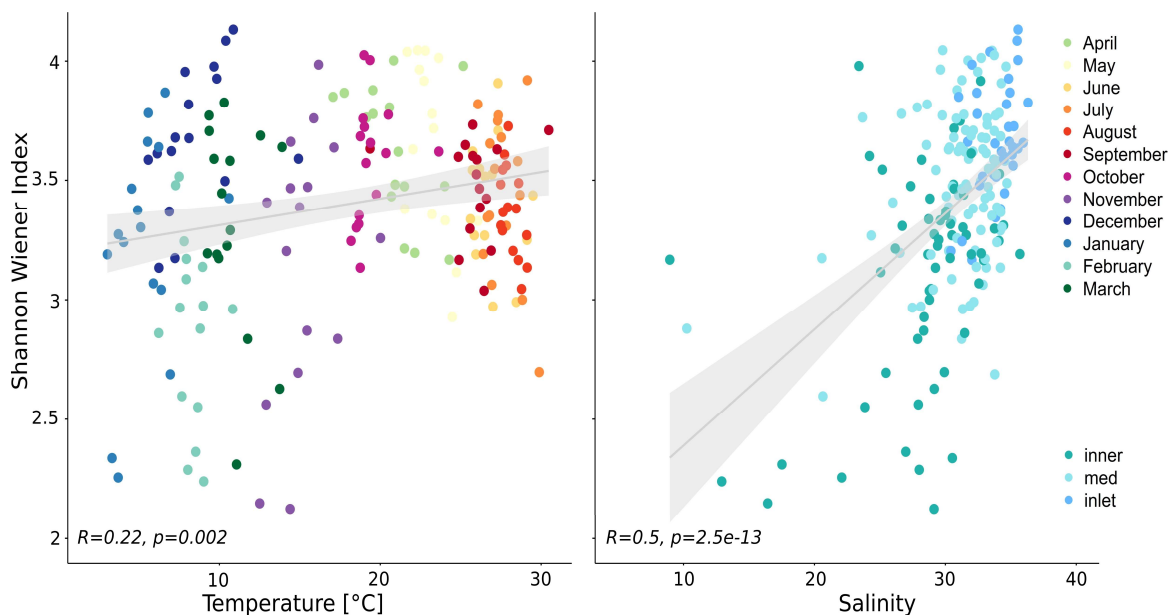


Figure B21: Correlation between alpha diversity (Shannon Wiener Index) and the two environmental parameters, temperature, and salinity. Colors of points refer to the sampling month (left) and location (right).

B.4 Discussion

The Venice Lagoon, as a transitional environment, exhibits both a high temporal as well as spatial variability. To enable a more precise description of the zooplankton biodiversity in this habitat and to fully exploit the benefit of this method in being fast and cost-effective, DNA metabarcoding was applied on a higher spatial and temporal scale.

As expected, the percentage of taxa per confidence level (“confidential taxa”, “cf. taxa”, and “best matches”), as well as the percentage of taxa and sequences assigned at the different taxonomic levels (species, genus, family etc.) was similar between CHAPTER A and B.

However, the large dataset obtained by this study enabled a more precise description of the zooplankton biodiversity in the Venice Lagoon. In comparison to CHAPTER A, where 224 taxa (excluding “best matches”) were detected in 24 samples (seasonal sampling of five stations within the VL and one in the nearby coastal area), in the assessment presented in CHAPTER B, the 192 samples (monthly sampling in 16 stations within the VL) resulted in 447 taxa. This already highlights the added value of high sampling effort in this complex environment for ensuring a reliable analysis of biodiversity patterns.

The data from monthly samples (Figure B18) confirm the expected intra-seasonal variability in the relative abundance. DNA metabarcoding combines the advantage of enabling high sampling frequency and high taxonomic resolution, providing information of short-term temporal changes of, e.g., of meroplanktonic larvae or eggs. For example, the spring peak of Actinopterygii would have been underestimated, if sampled only as seasonal sample in May (like in CHAPTER A), as they show highest abundances in April (mostly *Z. ophiocephalus* and *Engraulis encrasicolus*) and in June (mostly *E. encrasicolus* and *S. pavo*). Another example is the detection of short recruitment periods that might be overseen, e.g., of Ophiuroidea and *Atherina fragilis* (Pinnidae) in December and of *Bittium reticulatum* in May.

The NMDS plots by location (Figure B20) highlight the presence of monthly patterns of the zooplankton composition (especially for inlet and med locations - see the circular succession of months), confirming the importance of high temporal frequency assessments to detect the community changes over the year.

Regarding the spatial variability, the data from the 16 stations confirm the patterns in the zooplankton composition already observed and discussed in Chapter A, following an inlet-med-inner gradient (Figure B19). The “inlet” location is characterized by higher diversity (Figure B21), as well as richness (mean 62 taxa), followed by “med” (53) and “inner” (42) locations (data not shown). Nevertheless, the dispersion around the centroids in Figure B19 indicates the high intra-location variability of zooplankton composition, that is not completely explained by the temporal variability. Indeed, the above-mentioned dispersion follows both the temperature (proxy of seasons) and salinity (proxy of location) trajectories. Therefore, redundancy of stations for each location is essential for provide a robust assessment of zooplankton biodiversity at lagoon scale.

The overall results highlight the risk of under-sampling the highly diverse and variable group of zooplankton. In the framework of large-scale monitoring, lowering the sampling effort is often a necessary compromise due to time, human resource, or budget limitation. Indeed, by the morphological approach the analysis of 200 samples would require at least one year (approx. 1-3 days for each sample). In contrast, especially once the protocol (extraction, amplification, sequencing, bioinformatic) is defined, the metabarcoding could allow to overcome these limitations. The analysis of 200 samples would require approximately one working month, an order of magnitude lower compared to the morphology-based approach. Moreover, both laboratory and bioinformatic analyses will probably become faster in the near future, by automating of the procedures, coding optimization and improving the computational power.

To further investigate the impact of sampling effort on zooplankton community indicators (e.g. richness, diversity, target species abundance), additional analyses of this 192 sampling will be carried out, e.g., simulating lower frequency and/or number of stations by subsampling the dataset.

This large dataset, characterized by a wide spatial distribution of sampling stations covering the entire Venice lagoon, will be used for more detailed study on specific topics concerning the zooplankton dynamic, e.g., the larval dispersion of target species by coupling the metabarcoding data with hydrodynamic modeling.

CHAPTER C: COMPARING A DUAL COI MARKER FOR ZOOPLANKTON DNA METABARCODING

C.1 Introduction and Aim

The COI gene shows excellent taxonomic resolution, but with a drawback of reduced amplification success (Clarke et al., 2017). Indeed, several studies used a multi-marker approach to reduce the bias resulting from differing amplification success between various taxonomic groups. The study presented in this chapter focuses on the use of two COI barcodes, based on the internal COI primers proposed by Leray et al. (2013), mICOLintF and mICOLintR (5'-GGRGGRTASACSGTTCASCCSGTSCC-3'), which were utilized in several studies. However, as Leray et al. (2013) found "the reverse primer to perform poorly", almost all studies implemented the forward primer in combination with HCO2198 (or its degenerate versions dgHCO2198 and jgHCO2198). Only few studies, mainly on terrestrial arthropods, started utilizing the proposed reverse mICOLintR primer with contrasting success: Brandon-Mong et al. (2015), which excluded this primer after weak amplification success, and Krehenwinkel et al. (2017) utilized the mICOLintR primer as proposed by Leray et al. (2013). Other authors instead, adapted the mICOLintR sequence by modifying, e.g., all "S" nucleotides to: "W" as Günther et al. (2018) (on marine eDNA), to "N" as Wang et al. (2019), or to an "I" as Shokralla et al. (2015), as in fact, the originally proposed primer sequence is not the proper reverse complement to mICOLintF.

This chapter describes a study aiming to test the efficiency of the reverse mICOLintR primer in combination with the degenerated forward primer jdgLCO1490 (herein) by comparing it with the barcode that has been previously evaluated in Chapter A (based on the forward mICOLintF primer). The variety of zooplankton species in the study area, ranging from holo- to meroplanktonic organisms, and from brackish to more typically marine species, makes these samples an excellent application for comparing the abilities of the two COI barcodes in assessing the zooplankton community.

C.2 Material and Methods

C.2.1 Data collection

For this study, a subset (44) of the previously described 192 mesozooplankton samples (see CHAPTER B) was used to compare the efficiency of the two COI primers. These 44 samples correspond to those, where also *Mnemiopsis leidyi* individuals were collected for gut content analyses (see CHAPTER D).

C.2.2 Molecular analysis

For each of the 44 selected samples, the DNA extracts from the study presented in CHAPTER B were utilized for the amplification of the COI fragment based on the new set of primer pair: the amplification was performed in triplicates using a degenerated forward primer jdgLCO1490 (herein) in combination with the internal reverse primer mICOLintR proposed by Leray et al. (2013) (target length: 319 bp; position: 0-319) (hereon called P1). However, the mICOLintR primer was modified compared to the original to match the forward internal primer mICOLintF by interchanging the “S” with “W” nucleotides: 5'-GGRGGRTAWACWGTTCWCCWGTWCC-3' instead of 5'-GGRGGRTASACSGTTCASCCSGTSCC-3'. The amplification, library preparation, purification, and sequencing in Ion Torrent PGM System (Life Technologies) was done equivalently to CHAPTER B.

For the comparison of P1 with the barcode used in the study presented in the Chapters A and B (hereon called P2), which is based on the internal forward primer mICOLintF with a combination of degenerated primers dgHCOI2198 and jgHCOI2198 (target length: 313 bp; position: 345-568), the P2 data of the same 44 samples of the study of CHAPTER B were used (Table C9).

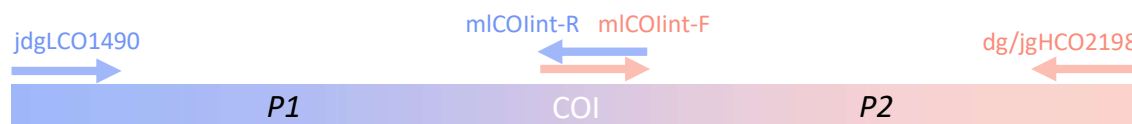


Figure C22: Schematic representation of the primer regions.

Table C9: Primers used in this chapter.

<i>primer</i>	<i>Sequence (5' - 3')</i>	<i>author</i>	<i>barcode</i>
jdgLCO1490	TCAACAAAYCAYAARGAYATYGG	herein	Forward P1
mlCOlintR-mod	GGRGGRTAWACWGTTCAWCCWGTWCC	herein	Reverse P1
mlCOlintF	GGWACWGGWTGAACWGTWTAYCCYCC	(Leray et al., 2013)	Forward P2
dgHCO2198	TAAACTTCAGGGTGACCAAARAAYCA	(Meyer, 2003)	Reverse P2
jgHCO2198	TAIACYTCIGGRTGICCRARAAYCA	(Geller et al., 2013)	Reverse P2

C.2.3 Bioinformatics and statistical analyses

The bioinformatic pipeline corresponded to CHAPTER B (Figure B14). As the two barcodes are almost of the same length (319 bp for P1 and 313 bp for P2), the bioinformatic pipeline did not differ between the two barcodes.

Based on the final dataset, the number of sequences and OTUs that were detected at each of the steps of the taxonomic assignment and the number of OTUs detected at the different taxonomic levels were calculated and plotted as a barchart. All following analyses did not consider the “best match” OTUs, as they are not reliable taxonomic assignments but rather a representation of putative metazoans. To investigate on the number of OTUs detected by the two barcodes (P1 and P2), only the OTUs assigned at species and genus level were taken into consideration. Furthermore, this analysis was repeated but aggregating those taxa to family level. To investigate if low abundances could explain the detection of some taxa with only one of the two barcodes, the taxa were divided into three categories of detection (P1, both barcodes, and P2) and the mean abundance and standard deviation per category were calculated.. Moreover, for those taxa that were detected only with P1, the presence in two other existing P2 datasets, the dataset of CHAPTER A and the extended dataset of CHAPTER B was checked. The taxonomic tree was visualized and edited using the R package *ggtree* (Yu et al., 2017). Diversity estimates, alpha-diversity based on Shannon Wiener Index and beta-diversity based on Bray-Curtis similarities, were calculated on square-root transformed data and the correlation between the two barcodes was evaluated based on Pearson’s correlations. Pearson’s correlations of relative abundances of phyla, selected classes and orders between the two barcodes were evaluated from percentages of square-root transformed data.

C.3 Results

C.3.1 Taxonomic assignment

The number of raw sequences of the 44 samples was about 3.2×10^6 (mean length of 348 bp \pm 34) for P1 and about 2.3×10^6 (384 bp \pm 35) for P2, while after trimming, sequence correction and chimera filtering, 2,267,551 reads (98.9%) and 795,027 OTUs for P1 and 2,061,251 (99.5%) and 943,983 OTUs for P2 were retained and used as input for the taxonomic assignments (Table C10).

The taxonomic assignment resulted in comparable proportions of sequences and OTUs at the different levels of assignments (Figure C23A, B). With P1, 1,486,969 sequences (65.6%) could be assigned to metazoans, out of which, 1,464,182 sequences (98.5%) and 177 OTUs were assigned at 97% similarity threshold (“confidential” taxa), 641 sequences (0.04%) and 36 OTUs were assigned only at 94% similarity (“cf.” taxa), 22,146 sequences (1.49%) and 20 OTUs were considered putative metazoans (“best matches”). While with P2, 1,432,433 sequences (69.5%) could be assigned to metazoans. Regarding the different levels of assignments, 1,429,240 sequences (99.8%) and 246 OTUs were considered as confidential, 238 sequences (0.02%) and 10 OTUs were assigned at 94% similarity threshold only, 2,655 sequences (0.19%) and 28 OTUs were considered as putative metazoans (Figure C23A, B, Table C10). Per sample, the mean number of assigned sequences was 35×10^3 ($\pm 15 \times 10^3$) for P1 and 33×10^3 ($\pm 11 \times 10^3$) for P2. The unassigned reads, 34.4% and 30.5% for P1 and P2, respectively, belong most probably to the SAR supergroup, non (marine) metazoans, or low-quality reads.

Table C10: Stepwise change in number of sequences and OTUs through bioinformatic analyses and taxonomic assignment.

process	step	P1			P2		
		sequences	% of sequences	OTUs	sequences	% of sequences	OTUs
Sequence preparation	Raw reads	3,204,993	-	-	2,330,003	-	-
	After trim and seqs corr.	2,293,472	71.6%	815,369	2,071,489	88.9%	952,422
	After chimera filtering	2,267,551	98.9%	795,027	2,061,251	99.5%	943,983
Taxonomic assignment	Confidential taxa	1,464,182	98.5%	177	1,429,240	99.8%	246
	cf. taxa	641	0.04%	36	238	0.02%	10
	“best match”	22,146	1.49%	20	2,655	0.19%	28
	assigned	1,486,969	65.6%	233	1,432,433	69.5%	284
	unassigned	780,582	34.4%	-	628,818	30.5%	-

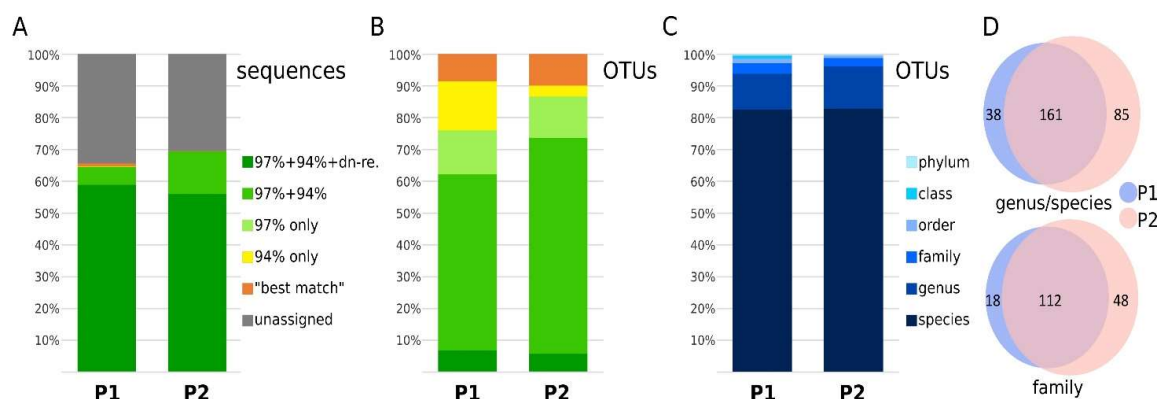


Figure C23: Barchart of proportion of A) sequences and B) OTUs for each degree of taxonomic assignments, and C) of OTUs for each taxonomic level of assignment, for each barcode, P1 and P2. D) Venn diagram of OTUs assigned at species or genus level (above) and, below, those aggregated at family level, detected with P1 only, with both barcodes, or with P2 only.

C.3.2 Taxonomic richness

In terms of the number of detected taxa, the taxonomic richness showed similar results for both barcodes, with slightly higher values for P2. The barcode P1 resulted in 213 taxa (233 taxa including “best matches”), while P2 resulted in 256 taxa (284 taxa including “best matches”). Also, the taxonomic resolution shows comparable results, with the main proportion composed by species level (both 83%) and genus level (11% and 13%, respectively) assignments (Figure C23C).

In terms of shared taxa, considering only species and genus level assignments and excluding “best matches”, the two barcodes share 161 taxa, while 38 taxa were only detected by P1 and 85 taxa only by P2. However, the 161 shared taxa represent the vast majority, 97.3%, of the sequences, while the non-shared taxa are composed by 0.02% and 2.7% for P1 and P2, respectively. To further investigate if taxa that are not shared by both barcodes have in general low abundances, the mean for each category (P1-only, shared and P2-only taxa) were calculated (excluding absence in samples), resulting in considerably higher mean abundances for the shared taxa in comparison to the non-shared taxa: 18-fold higher than P1-only and 9-fold higher than P2-only taxa. Similarly, 112 families were identified by both barcodes, while 48 only by P2 and 18 only by P1 (Figure C23D).

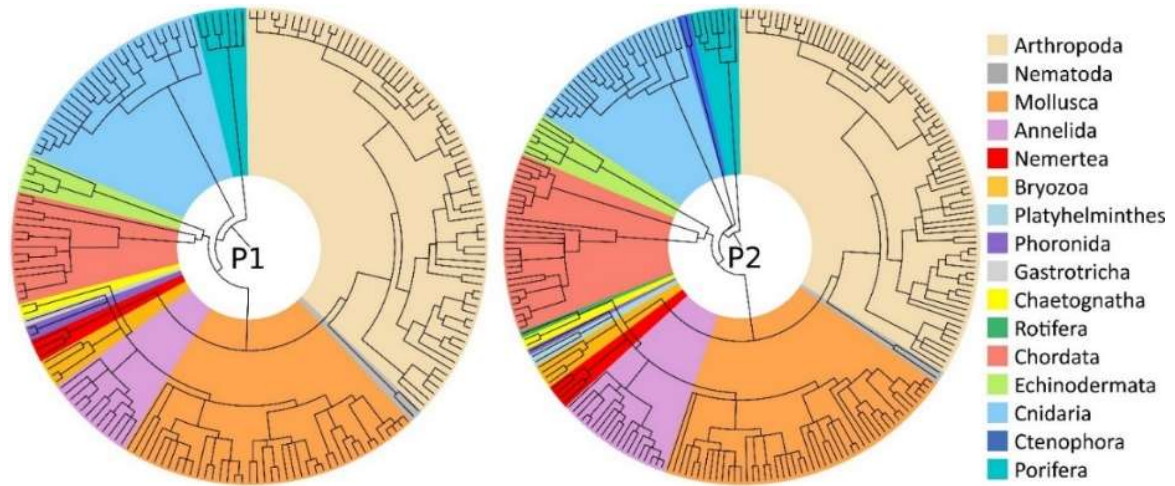


Figure C24: Taxonomic tree representing the taxonomic richness revealed with the barcodes P1 and P2, respectively.

As graphically evident in Figure C24, the taxonomic richness is comparable between the two methods as almost all phyla present a similar number of branches. The P1 barcode, however, in contrast to the P2, was able to detect the phylum Gastrotricha, while P2 in contrast to P1 did detect the phyla Rotifera, Platyhelminthes and Ctenophora. At species level, examples of species detected with P1 only are the shrimp *Palaemon macrodactylus*, the decapod *Pilumnus spinifer*, the fish *Sprattus sprattus* and *Serranus hepatus*, the anemone *Anemonia viridis* and the order of sponges Haplosclerida. On the other side, taxa detected with P2 only were, e.g., the gobies *Knipowitschia panizzae*, *Ninnigobius canestrinii* and *Pomatoschistus marmoratus* as well as the sea needle *Belone belone*, and the bivalves Teredinidae, *Lithophaga lithophaga* and *Pinna nobilis*. Within copepods, *Paracartia latisetosa*, *Ditrichocorycaeus anglicus*, *Oithona plumifera* and *O. davisae* and *Mesocyclops pehpeiensis* were not detected with P1, and the genus *Candacia* was not detected using the P2 system in this dataset (Table S2) even though previously spotted in the dataset presented in CHAPTER B (Table S1). Further details regarding the species detection with P1 and P2 can be found in the SUPPLEMENTARY MATERIAL (Table S2).

C.3.3 Relative abundances

In terms of relative abundances, the two barcodes show similar patterns at class and phylum level (Figure C25). As expected, containing the very abundant group of copepods, Arthropoda is the dominant phylum ($89.4\% \pm 16.6$ and $87.9\% \pm 11.8$ with P1 and P2, respectively).

Also, some seasonal patterns can be noticed with both barcodes, especially in the winter samples in December and January, where the zooplankton community slightly differs from the rest of the dataset as well as the higher fish abundance in the same two samples (July station 16 and August station 2), as well as the single appearance of, e.g., Hydrozoa and Ophiuroidea in the same samples.

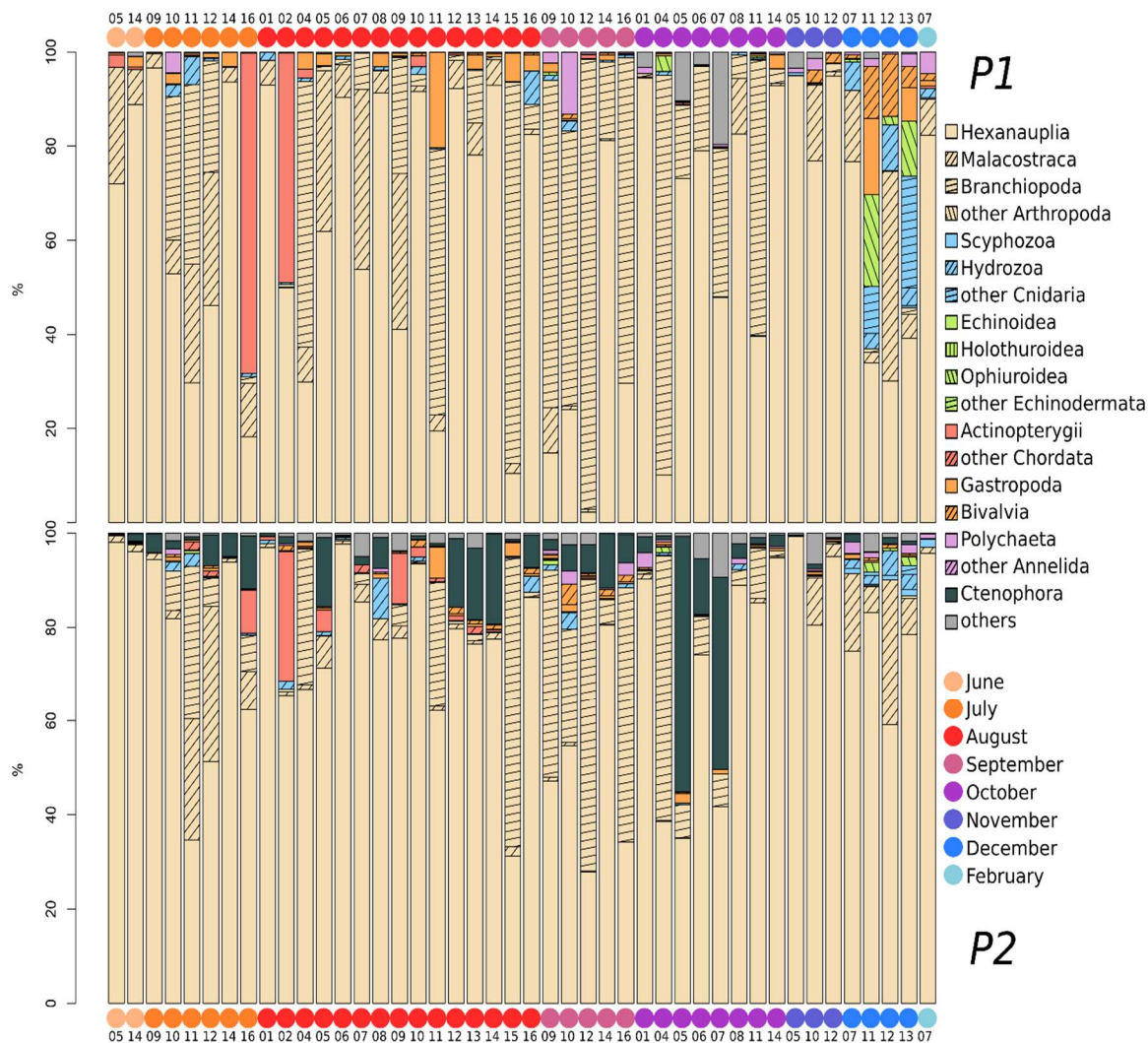


Figure C25: Barchart of relative abundance of the most abundant phyla (colors) and their classes (pattern) for each sample for P1 and P2.

Moreover, for almost all phyla, and selected classes and orders, the relative abundance in the two barcodes is significantly correlated (Table C11). The only groups where the two barcodes are not significantly correlated are the classes Ascidiacea and Bivalvia. The most evident difference, though, is the noticeable absence of Ctenophora with the P1 barcode. The alpha-diversity estimates based on Shannon Wiener Index of the P1 samples (2.6 ± 0.45) were not significantly different to the P2 samples (2.9 ± 0.38) (KW:

chi²= 43, df= 43, p= 0.47), and significantly correlated (Pearson's correlation: R= 0.8, p= 1.3e-9) (Figure C26A) as well as the taxa richness per sample (R= 0.6, p= 5.3e-5). The beta-diversity based on Bray-Curtis similarities was also significantly correlated (Mantel test based on Pearson's correlation: R= 0.9, p= 0.001). Within the very abundant group of copepods, the only genus detected with both barcodes, but not showing a significant correlation in its relative abundance between the two barcodes was the genus *Pseudodiaptomus* (*P. marinus*). At the same time, *Paracartia* was not detected with P1 and *Candacia* was not detected using the P2 system (even though previously detected with P2 in CHAPTER A). The relative abundance of copepods at genus level confirms that the two barcodes are highly correlated (R= 0.95, p < 2.2e-16) (Figure C26B).

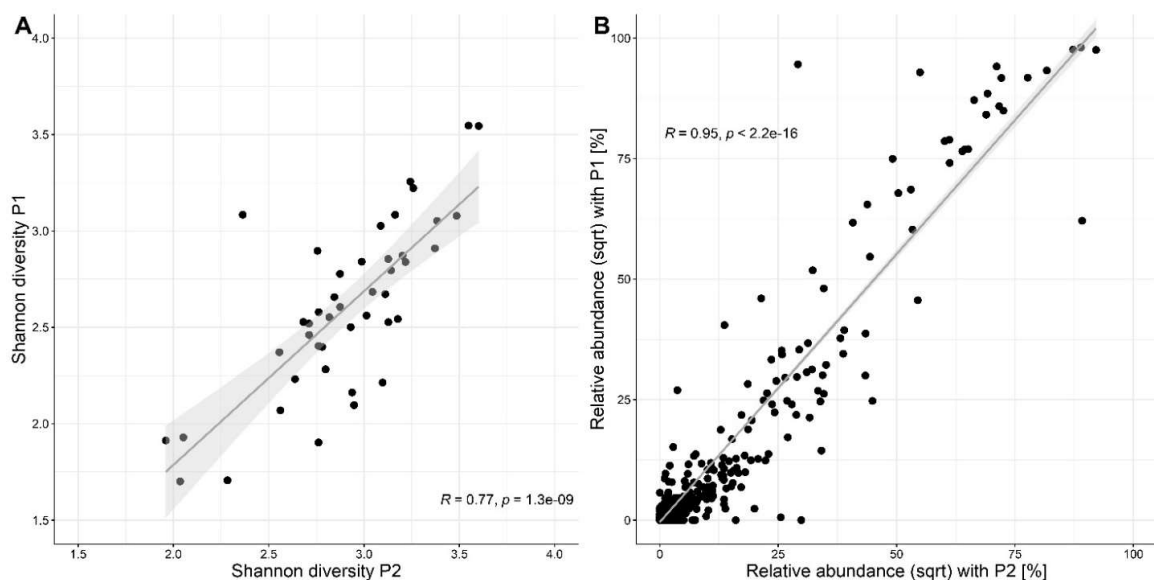


Figure C26: A) Alpha-diversity (Shannon Wiener Index (based on square-rooted data) and B) Relative abundance (based on square-rooted data) of copepods merged at genus level for P1 vs. P2 and its correlation (Pearson) and confidence interval (0.95) (grey shading).

Table C11: Mean relative abundance of all phyla and selected classes and orders and its standard deviation for each barcode and Pearson's correlation of the relative abundance between the two barcodes (based on square-rooted data). NA: group present in 1 single sample only (same sample for both barcodes). ***: highly significant ($p < 0.001$)

taxon	level	P1		P2		Pearson's correlation (df=42)			Sign.
		mean [%]	sd	mean [%]	sd	r	t	p	
Annelida	phylum	0.87	2.19	0.47	0.79	0.619	5.10	7.58e-06	***
Arthropoda	phylum	89.38	16.62	87.94	11.84	0.355	2.46	0.018	***
Branchiopoda	class	19.85	28.13	10.65	18.30	0.968	24.91	< 2.2e-16	***
Hexanauplia	class	60.83	29.99	72.68	21.06	0.799	8.62	7.8e-11	***
Calanoida	order	56.00	29.13	65.82	22.27	0.686	6.11	2.7e-07	***
Cyclopoida	order	0.47	1.44	0.03	0.05	0.635	5.32	3.7e-06	***
Harpacticoida	order	0.89	2.87	1.29	3.84	0.904	13.67	< 2.2e-16	***
Poecilostomatoida	order	0.02	0.05	0.28	0.79	0.823	9.38	7.4e-12	***
Sessilia	order	3.46	5.68	5.25	8.85	0.939	17.71	< 2.2e-16	***
Malacostraca	class	8.69	11.58	4.62	8.38	0.750	7.34	4.8e-09	***
Amphipoda	order	0.07	0.15	0.05	0.11	0.863	11.06	5.1e-14	***
Decapoda	order	8.61	11.55	4.54	8.41	0.765	7.71	1.4e-09	***
Isopoda	order	-	-	0.0001	0.001	-	-	-	-
Mysida	order	0.01	0.05	0.02	0.16	1	NA	< 2.2e-16	***
Pycnogonida	class	-	-	0.0004	0.003	-	-	-	-
Bryozoa	phylum	0.04	0.14	0.02	0.06	0.953	20.40	< 2.2e-16	***
Chaetognatha	phylum	0.13	0.27	1.42	1.85	0.764	7.67	1.6e-09	***
Chordata	phylum	2.90	12.45	1.51	4.59	0.768	7.77	1.2e-09	***
Actinopterygii	class	2.88	12.45	1.32	4.60	0.780	8.09	4.2e-10	***
Ascidiacea	class	0.02	0.05	0.20	0.44	0.054	0.35	0.729	
Cnidaria	phylum	2.05	4.87	1.16	1.87	0.823	9.39	7.04e-12	***
Anthozoa	class	0.78	3.84	0.06	0.29	0.985	37.26	< 2.2e-16	***
Hydrozoa	class	1.24	2.15	0.98	1.65	0.776	7.97	6.2e-10	***
Scyphozoa	class	0.03	0.09	0.12	0.35	0.846	10.27	5.0e-13	***
Ctenophora	phylum	-	-	6.14	10.53	-	-	-	-
Echinodermata	phylum	0.88	3.40	0.19	0.48	0.923	15.50	< 2.2e-16	***
Echinoidea	class	0.0002	0.0009	0.04	0.17	0.903	13.59	< 2.2e-16	***
Ophiuroidea	class	0.88	3.40	0.15	0.45	0.986	38.99	< 2.2e-16	***
Gastrotricha	phylum	0.0003	0.002	-	-	-	-	-	-
Mollusca	phylum	2.85	5.40	1.06	1.36	0.524	3.99	0.0003	***
Bivalvia	class	0.91	2.63	0.47	0.74	0.276	1.86	0.070	
Cephalopoda	class	0.0003	0.002	0.0004	0.003	0.813	9.03	2.1e-11	***
Gastropoda	class	1.94	3.97	0.58	1.09	0.746	7.30	5.5e-09	***
Scaphopoda	class	0.0003	0.002	0.0004	0.003	1	NA	< 2.2e-16	***
Nematoda	phylum	0.01	0.03	0.002	0.01	0.788	8.30	2.2e-10	***
Nemertea	phylum	0.02	0.04	0.01	0.01	0.561	4.40	7.4e-05	***
Phoronida	phylum	0.002	0.01	0.002	0.01	0.546	4.23	0.00012	***
Platyhelminthes	phylum	-	-	0.01	0.02	-	-	-	-
Porifera	phylum	0.87	3.14	0.06	0.18	0.971	26.09	< 2.2e-16	***
Rotifera	phylum	-	-	0.01	0.04	-	-	-	-

C.4 Discussion

The efficiency and suitability of the barcode proposed by Leray et al. (2013), the forward internal primer mCOIintF in combination with dgHCO2198 and jgHCO2198 (herein called P2), in assessing the zooplankton biodiversity was already verified by comparing it with morphological identifications in CHAPTER A and can therefore be considered a

reliable barcode for this type of studies. This study aims to test the efficiency of the second barcode proposed by Leray et al. (2013), the reverse internal primer mlCOIintR in combination jdgLCO1490, slightly modified and herein called P1, by comparing it with the P2 barcode. In contrast to the findings of Leray et al. (2013), which found the reverse mlCOIintR primer to “poorly perform” whether it was used with LCO1490, dgLCO1490 or jgLCO1490, this study could show that once modified, the P1 barcode seems to be a helpful and reliable barcode for zooplankton metabarcoding studies.

On the one hand, the two barcodes showed slight differences: i) while the proportions of taxonomically assigned vs. non-assigned sequences are comparable, P1 has slightly fewer assignments which can be a result of the missing detection of the relatively abundant ctenophore *M. leidy*. In fact, some phyla, like Ctenophora, Platyhelminthes and Rotifera were not detected by P1. Investigating on the primer binding sites of the P1 primers, no binding site for jdgLCO1490 was found for Ctenophora (tested on *M. leidy* (Acc.N. NC_016117) and *Boreo cucumis* (Acc.N. NC_045305)), as well as for Platyhelminthes (tested on *Benedenia humboldti* (Acc.N. CM028216), *Paragonimus westermani* (Acc.N. CM017921), *Schistosoma bovis* (Acc.N. CM014335), *Hymenolepis microstoma* (Acc.N. LR215992)), while in the phylum Rotifera, checked exemplarily on *Trichocera bimacula* (Acc.N. JN861750) the primer jdgLCO1490 could theoretically anneal. In fact, the mitochondrial genome of *M. leidy* strongly diverges from the “typical” mt genome as it is of minimal size (10–11 kb) (Pett et al., 2011) and reveals an extremely high evolutionary rate, and for Platyhelminthes COI was shown to have a poor primer performance for the Folmer region (Vanhove et al., 2013). These findings highlight that the suitability of a barcode, also in the case of the considered “universal” COI, depends on the target species, e.g., for cnidarians and ctenophores (Bucklin et al., 2011; Lindsay et al., 2015) and for groups such as Appendicularia, which in fact were neither detected with P1 nor with P2, and pelagic tunicates (Goodall-Copestake, 2017), COI has a proven difficulty in amplifying. This suggests opting for a multi-marker approach using both barcodes, P1/P2 or in combination with other genes, like 18S or 12S, instead of using the P1 as stand along marker. The benefit of using multiple markers has been shown in several studies (e.g. Stefanni et al., 2018 and Carroll et al., 2019 (both on COI and 18S-V9); Laroche et al., 2020 (COI and 18S-V4); Questel et al., 2021 (COI and 18S-V4+V9); Clarke et al., 2017 (COI, 18S-V4 and 16S); Lobo et al., 2017 (on different COI

markers) or Miya et al., 2020 (COI and 12S)). ii) Both in terms of numbers of sequences and OTUs for each level of assignment (“confidential” taxa, “cf.” taxa and “best matches”) the two barcodes performed similarly, but with a slightly higher proportion of 94%-only assignment (“cf.” assignments) for the P1 barcode. This finding could probably indicate a higher variability in the P1 region compared to P2. iii) The total number of OTUs was slightly different, and some could be detected only with one or the other barcode. For example, considering only species and genus level assignments, 38 taxa were detected only with P1, 161 were found with both barcodes and 85 were detected only with P2. However, most cases are explicable by very low abundances and may result from stochastic effects during the PCR. Indeed, 16 out of the 38 taxa detected only with P1 were detected in the dataset presented in CHAPTER A or in the large dataset comprehending the monthly sampling of all 16 stations (CHAPTER B). As for these datasets only the P2 barcode has been applied, no assumptions can be made on taxa detected with P2 only. iv) The largest differences in the mean relative abundance, were found in Branchiopoda (Cladocera), Decapoda, Actinopterygii, Anthozoa, Hydrozoa, Ophiuroidea, Bivalvia, Gastropoda and Porifera with higher relative abundance in P1 compared to P2, and in Calanoida, Sessilia and Chaetognatha with lower relative abundance in P1 compared to P2.

On the other hand, the two barcodes performed very comparably: i) the proportion of the different levels of taxonomic assignment are very similar, which depends both on the taxonomic level of the reference sequence as well as on the potential assignment of the same OTUs to different taxa, consequently assigned to the next higher taxonomic level due to the LCA algorithm. ii) The two taxonomic trees showed similar detail and proportions for each phylum, and iii) in terms of relative abundances, P1 and P2 showed similar patterns and the abundance was significantly correlated for almost all investigated groups. The only classes that were not significantly correlated, were Ascidiacea and Bivalvia. This suggests that for those, but especially for the phyla that were entirely missed by P1, the P2 barcode is probably the better option.

CHAPTER D: *IN-SITU* DIET ASSESSMENT OF THE INVASIVE CTENOPHORE *MNEMIOPSIS LEIDYI* BY DNA METABARCODING

D.1 Introduction and Aim

The increasing awareness of blooms of the invasive zooplanktivorous comb jellyfish *Mnemiopsis leidyi* (A. Agassiz 1865), which originated from the eastern American coasts, has led to a rising interest in their ecology because of its potentially severe impacts on the functioning of the marine systems (Brodeur et al., 2008) by exerting a top-down control (McNamara et al., 2013; Shiganova and Bulgakova, 2000) and by inducing trophic cascades (Roohi et al., 2010). The invasive power of this ctenophore is facilitated by its high plasticity due to its tolerance for wide ranges of temperature and salinity, its hermaphroditic reproduction (also self-fertilizing) and its regeneration ability (Purcell et al., 2001). The bloom of *M. leidyi* in the Black and Caspian Sea ecosystems in the late 1980s and early 1990s became probably possible due to a shortage of predators and competitors due to overfishing (Shiganova et al., 2001). Subsequently, the blooms of *Mnemiopsis* have been associated with severe declines in fish stocks (Shiganova and Bulgakova, 2000) and effects on the ecosystem production. *Mnemiopsis leidyi* has colonized most of the Mediterranean Sea, from the eastern to the western basin, and in 2016, this invasive species was firstly recorded in the Venice Lagoon (Malej et al., 2017), after being presumably introduced via ballast waters, a global vector in human-mediated invasions providing a fast dispersal mechanism for many marine taxa and therefore massively increasing the risk of NIS introduction (Marchini et al., 2015; Vidjak et al., 2019). Even once the invasion has occurred, the heavy maritime traffic in the VL presents a risk of continuous re-introduction via ballast waters and makes the VL a starting point and source of further dispersions.

As the Northern Adriatic is an important nursery and foraging area e.g., for sardines and anchovies, which together account for approximately 41% of total Adriatic marine catches (Morello & Arneri, 2009), the concerns regarding the impact *Mnemiopsis* could have on this ecosystem are enormous, both from an ecological as well as from an economic point of view. The Northern Adriatic coast, together with the Venice Lagoon,

however, is not only an important nursery area for fishes, but it is also one of the most important European area for mussel (*Mytilus*), clam (*Ruditapes* and *Chamaelea*) and crab (*Carcinus*) fishery and aquaculture (Cataudella et al., 2015). Being part of the zooplankton community as meroplankton during their larval stages, the predation on these organisms by *Mnemiopsis* may increase the pressure on this economic branch, both for small local businesses as well as for the industrial production. The pressures on the ichthyoplankton community can be various: direct predation on fish eggs and larvae, as well as predation on a wide range of zooplankton (Purcell et al., 2001) leading to a strong competition for food with zooplanktivorous fishes or their larvae which may indirectly affect the abundance of ichthyoplankton. In fact, *M. leidy* is known to feed on a variety of prey, depending on food availability as well as its live stage (Finenko et al., 2006; Javidpour et al., 2009a; Rapoza et al., 2005). Its complex feeding capacities permit to capture a wide range of zooplankton taxa and to selectively feed on i) slow-moving or immobile organisms, like mollusk and barnacle larvae or immobile eggs, collected by the cilia within the auricles creating an undetectable current which together with the mucus gets the prey to be trapped in their tentila, as well as ii) highly mobile preys, like copepods, captured by collision with the inside of the lobes (Colin et al., 2015; Haddock, 2007; Main, 1928; Presnell et al., 2016; Purcell et al., 1991; Waggett and Costello, 1999). Afterwards, the prey is transported to the mouth and pharynx.

In the past, the gut content of *Mnemiopsis* was mainly analyzed by morphological identification to study feeding preferences. However, this approach has its limits, as it allows to identify only un- or barely digested prey, in addition to the general impediments of species identification based on morphological features for some groups like larval stages or cryptic species. DNA metabarcoding has been previously used for gut content analyses, e.g., on fishes (Albaina et al., 2016) or the jellyfish *Chrysaora* (Meredith et al., 2016). This is the first study utilizing DNA metabarcoding for gut content analyses of *M. leidy*.

This chapter aims to identify the feeding preferences of the comb jellyfish *Mnemiopsis leidy* by DNA metabarcoding and to speculate on its potential impact on zooplankton abundances and biodiversity in the Lagoon of Venice. This will possibly give also new insights into the type of pressure on fish stocks, by indicating if it is due to competition for zooplankton as food source or to direct feeding of *Mnemiopsis* on fish eggs or larvae.

D.2 Material and Methods

D.2.1 Data collection

Mnemiopsis individuals were sampled from April 2018 to March 2019, together with the *in-situ* zooplankton community, in conjunction with the investigation described in CHAPTER B (Figure 1, Table 1). *Mnemiopsis* individuals (when >1.5cm length) were measured (total biovolume [ml]) and immediately frozen at -20°C, while zooplankton samples were preserved in 96% ethanol for genetic analyses. For the gut contents analyses, *Mnemiopsis* individuals were unfrozen in the laboratory, and the gut contents were extracted with a Pasteur pipette under a stereomicroscope (Zeiss, Discovery V8) and pooled to one for each station sample.

D.2.2 Molecular analysis

The molecular analysis of the zooplankton *in-situ* samples corresponds to the 44 samples analyzed in CHAPTER C. The manually obtained gut contents of *Mnemiopsis* were centrifuged to remove excess liquids and successively homogenized by bead-beating for one minute. The following procedures, including extraction, amplification, library preparation and sequencing again correspond to CHAPTER B and C. For this study, the barcode P1, the degenerated forward primer jdgLCO1490 (5'-TCAACAAAYCAYAARGAYATYGG-3') in combination with the modified reverse internal primer mlCO1intR proposed by Leray et al. (2013) with a target length of 319 bp (see Table C9), was used, having the advantage to not amplify *M. leidyi*.

D.2.3 Bioinformatic and statistical analysis

The bioinformatic analysis corresponds to CHAPTER B and C (Figure B14).

Spatial and temporal patterns of the environmental factors were assessed based on Euclidean distances of normalized data using repeated-measure permutational analysis of variance (PERMANOVA) with the sampling months as fixed factor and the stations as random factor (PRIMER 6 + and PERMANOVA software package; PRIMER-E, Ltd., UK). To visualize the similarities between the samples in terms of environmental conditions a PCoA (Principal coordinates analysis) has been computed. With the R software (R Core

Team, 2018), differences between months and stations were tested by the Kruskal-Wallis Test. Pearson's correlations between biovolume [ml/m^3] and environmental parameters, as well as of the relative abundance of groups (at different taxonomic level) between the *in-situ* zooplankton community and *Mnemiopsis*' gut contents (percentages of square-root transformed data) were calculated. To check for Pearson's correlations in the relative abundances at genus level, all taxa were collapsed at genus level and the relative abundance of all genera (excluding datapoints with absence in both datasets) was calculated. This was done also for the relative abundance of copepod genera within copepods, of mollusks genera within mollusks and of decapod genera within decapods (based on square-rooted data). The beta diversity was evaluated from dissimilarity matrices built according to Bray-Curtis distances using the *metaMDS* script with the *autotransform* function of the R package *vegan* (Oksanen et al., 2019).

D.3 Results

D.3.1 Biovolume of *Mnemiopsis leidyi*

Within the duration of this study, the first individuals of *M. leidyi*, including larval stages, were detected in June 2018 (~0.5cm length). Individuals larger than 1.5cm length were found in 44 samples, from June to February with variable total biovolumes ranging from 1.3 to 78 ml/m^3 (Figure D27A). Still, the highest biovolumes [ml/m^3] of *Mnemiopsis* were found during late summer, especially from July to October (Figure D27B). From November, only single individuals were found, and the presence of larval stages increased again. In fact, investigating on the correlation between *Mnemiopsis*' biomass and the environmental parameters (described in CHAPTER B), temperature shows a weak, but significant positive correlation to the biovolume of *Mnemiopsis* ($t= 3.55$, $df= 190$, $p= 0.0005$, $cor= 0.25$), while none of the other environmental parameters show significant correlations. Also, the abundance did differ between stations and seems to show slightly lower values close to the inlets (Figure D27C).

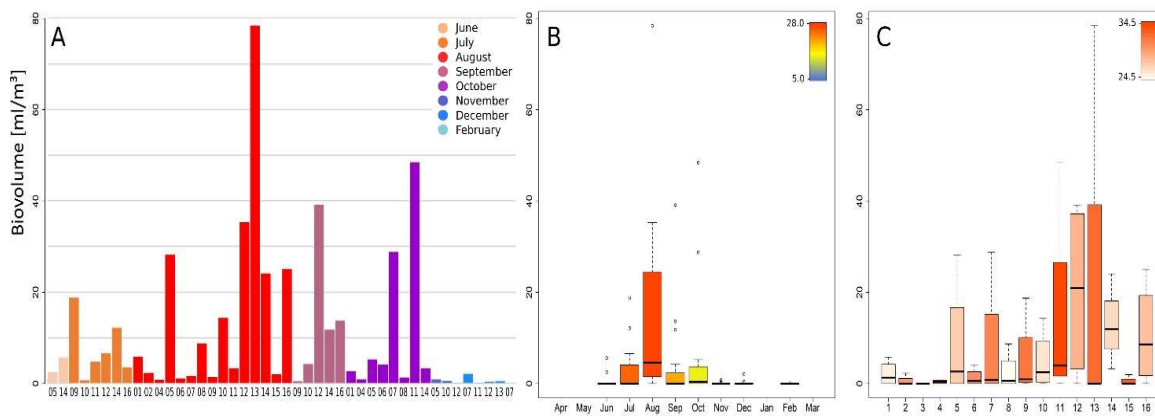


Figure D27: Relative biovolume of *M. leidy* in terms of ml/m³. A) biovolume of samples where *M. leidy* was present, B) Boxplot of biovolume through the year of observation (colors refer to median temperature [°C] per month), and C) at the 16 stations (July-October) (colors refer to median salinity per station).

D.3.2 Diet analysis

The number of raw sequences was 2.3×10^6 reads for the 44 samples of *Mnemiopsis* gut content and 3.2×10^6 reads for the 44 samples of *in-situ* mesozooplankton samples. After taxonomic assignments, the final number of sequences of the gut contents was 768,611 (assignments at 97%: 71.1%; at 94%: 14.9%; by the recovery of putative metazoans (“best match”): 14%) distributed between 122 OTUs, and of the mesozooplankton community, 233 OTUs representing 1,486,969 sequences (assignments at 97%: 87.5%; at 94%: 9.3%; by the recovery of putative metazoans: 3.2%). For the following analyses, the most stringent dataset was used, hence excluding the “best match” assignments, of 107 OTUs with 672,956 sequences of *Mnemiopsis* gut content and 213 OTUs with 1,464,823 sequences of *in-situ* mesozooplankton.

The taxonomic assignment of the gut content of *Mnemiopsis* indicates that it feeds on a variety of preys. The most abundant phylum of prey is Arthropoda (mean: $62\% \pm 31$), with the copepod order Calanoida as the most represented group ($25\% \pm 25$), followed by the classes of Decapoda ($20\% \pm 30$) and Branchiopoda (composed by cladocerans only) ($12\% \pm 26$). The second most abundant phylum is Mollusca ($21\% \pm 27$), composed mainly by Gastropoda ($15\% \pm 23$) and Bivalvia ($5\% \pm 10$); third is Annelida (composed by polychaetes only) ($12\% \pm 23$), and fourth is Nemertea ($3\% \pm 6$). As indicated by the high values of standard deviation, however, the samples show a high variability (Figure D28, Table D12).

The *in-situ* mesozooplankton community shows comparable compositions, as several groups show significant correlations between the gut content and the *in-situ*

mesozooplankton community: Cladocera, Cyclopoida, Amphipoda, Decapoda, Bryozoa, Anthozoa, Hydrozoa and Nemertea (Table D12). However, there are some differences: the relative abundance of arthropods is higher *in-situ* (89% vs. 62%), with higher proportions of calanoids (59% vs. 25%) and cladocerans (21% vs. 12%), but lower for decapods (5% vs. 20%), indicating a preference of *Mnemiopsis* of the latter one. Mollusks (3% vs. 21%), Nemertea (0.02% vs. 3%) and Polychaeta (1% vs. 12%) seem to be preferred as well.

When collapsing all taxa at genus level, the relative abundance of the *in-situ* zooplankton community and the gut content of *Mnemiopsis* show a significant correlation ($R= 0.55$, $p= 2.2e-16$) (Figure D29A). Considering the most abundant genera of copepods only (relative abundance calculated in relation to copepods), in the gut content of *Mnemiopsis* the genus *Acartia* contributed with 71.9% to the copepod community, followed by *Centropages* with 7.1%, *Oithona* with 6.6% and *Paracalanus* with 3.4%, whereas in the zooplankton community *Acartia* was again at the first rank with 76.9%, followed by *Paracalanus* with 8.2%, by *Centropages* with 5.6% and by *Temora* with 3.5%. While the three shared genera show significant correlations (*Acartia*: $R= 0.82$, *Centropages*: $R= 0.77$, and *Paracalanus*: $R= 0.68$) and equal distribution between the *in-situ* zooplankton community and the gut content, *Temora* is more abundant *in-situ*, indicating a reduced capture by *Mnemiopsis*, and *Oithona* and *Euterpina* are more abundant in the gut content, indicating possibly a preferential feeding by *Mnemiopsis* of the latter two (Figure D29B). Having a closer look at some meroplanktonic genera, especially the bivalve *Ruditapes*, which is of great commercial interest in the VL, shows a noticeable accumulation in the gut content (Figure D29C).

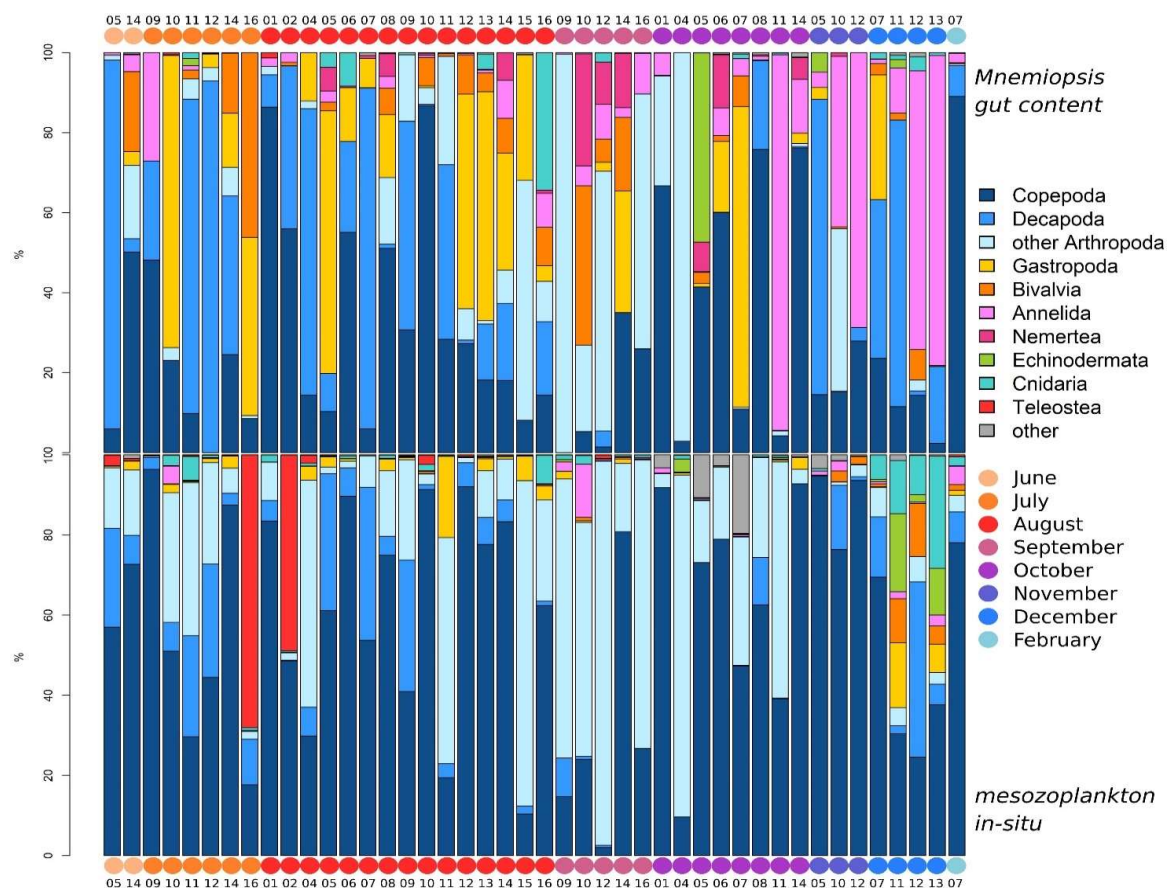


Figure D28: Barchart of relative abundance of different taxonomic groups in the gut content of *M. leidyi* (above) and of the in-situ mesozooplankton community (below) for the 44 samples where the presence of *Mnemiopsis* was detected. Colors of barcharts indicate taxonomic composition, while colored circles indicate the month of sampling.

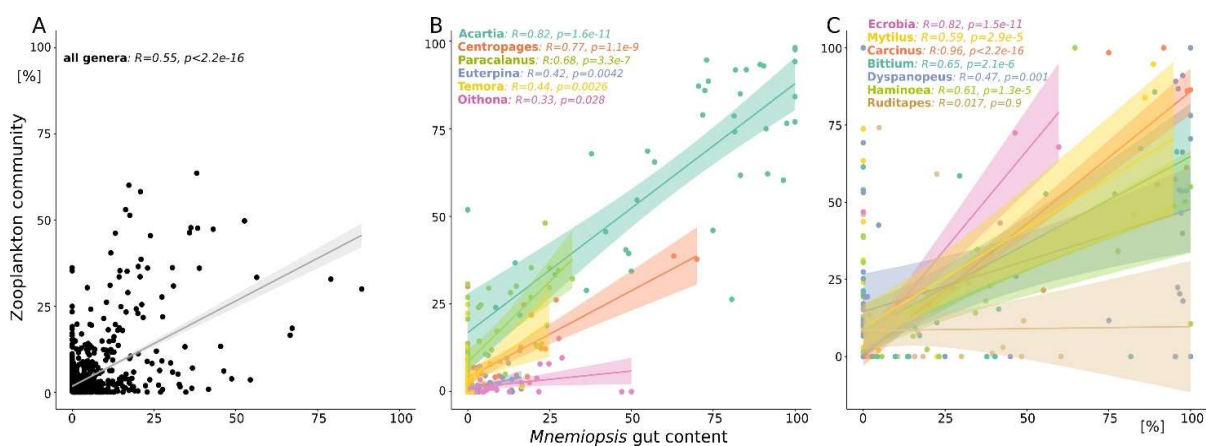


Figure D29: Correlation plot of A) all taxa (% based on square-rooted data) collapsed at genus level (excluding datapoints with absence of taxon in both datasets), B) most abundant copepod genera, and C) selected meroplanktonic genera. Pearson's correlations between the two datasets are given in the corresponding color.

Both the zooplankton community and the gut content showed a clear temporal differentiation by seasons as well as a spatial one by location (Figure D30A). The differences between the zooplankton samples are greater than between gut content samples (Figure D30B). However, when computing a Bray-Curtis matrix for both datasets together and plotting them on a single NMDS plot (Figure D30C), it emerges that they

are almost overlapping rather than creating two different clusters. This indicates that the feeding of *Mnemiopsis* depends mainly on the food availability at that specific moment and location.

Table D12: Mean values and standard deviation of relative abundances of taxonomic groups in the gut contents and the in-situ mesozooplankton community and its correlations (based on square-root transformed data).

taxon	level	<i>Mnemiopsis</i> gut		Zooplankton community		Pearson's correlation (df=42)		
		mean [%]	sd	mean [%]	sd	r	t	p
Annelida	p	11.68	22.80	0.89	2.25	0.196	1.30	0.201
Arthropoda	p	61.66	31.37	89.08	17.54	0.209	1.39	0.173
Branchiopoda	c	12.39	25.82	20.81	29.01	0.720	6.73	3.52e-08
Hexanauplia	c	29.52	26.65	63.63	30.17	0.407	2.89	0.006
Calanoida	o	24.96	24.80	58.64	29.52	0.412	2.93	0.0054
Cyclopoida	o	0.46	1.41	0.49	1.51	0.617	5.08	8.26e-06
Harpacticoida	o	0.20	0.48	0.92	2.96	0.130	0.85	0.399
Poecilostomatoida	o	0.41	1.30	0.02	0.05	0.234	1.56	0.126
Sessilia	o	3.49	11.63	3.56	5.81	0.441	3.18	0.003
Malacostraca	c	19.75	29.66	4.64	7.81	0.522	3.97	0.0003
Amphipoda	o	0.01	0.06	0.08	0.16	0.536	4.12	0.0002
Decapoda	o	19.74	29.67	4.55	7.76	0.564	4.43	6.63e-05
Mysida	o	0.00	0.00	0.01	0.05	-	-	-
Bryozoa	p	0.001	0.01	0.04	0.15	0.865	11.15	3.9e-14
Chaetognatha	p	0.09	0.25	0.13	0.28	0.405	2.87	0.006
Chordata	p	0.08	0.23	3.10	13.52	-0.166	-1.09	0.283
Actinopterygii	c	0.07	0.22	3.09	13.52	-0.140	-0.92	0.365
Ascidiacea	c	0.01	0.07	0.02	0.05	-0.050	-0.33	0.746
Cnidaria	p	1.52	5.35	2.14	5.06	0.462	3.37	0.002
Anthozoa	c	0.0001	0.0006	0.79	3.91	0.803	8.72	5.7e-11
Hydrozoa	c	1.43	5.35	1.31	2.41	0.516	3.90	0.0003
Scyphozoa	c	0.09	0.33	0.03	0.09	0.340	2.35	0.024
Echinodermata	p	1.53	8.47	0.90	3.44	0.019	0.125	0.901
Gastrotricha	p	0.00	0.00	0.0003	0.002	-	-	-
Mollusca	p	20.52	26.73	2.80	5.36	0.128	0.834	0.409
Bivalvia	c	5.35	10.26	0.98	2.92	0.094	0.61	0.543
Cephalopoda	c	0.00	0.00	0.0003	0.002	-	-	-
Gastropoda	c	15.17	22.92	1.83	3.67	0.242	1.61	0.114
Scaphopoda	c	0.00	0.00	0.0003	0.002	-	-	-
Nematoda	p	0.00	0.00	0.01	0.03	-	-	-
Nemertea	p	2.81	6.47	0.02	0.05	5.39	4.14	0.0002
Phoronida	p	0.00	0.00	0.002	0.01	-	-	-
Porifera	p	0.11	0.41	0.87	3.14	0.013	0.083	0.935

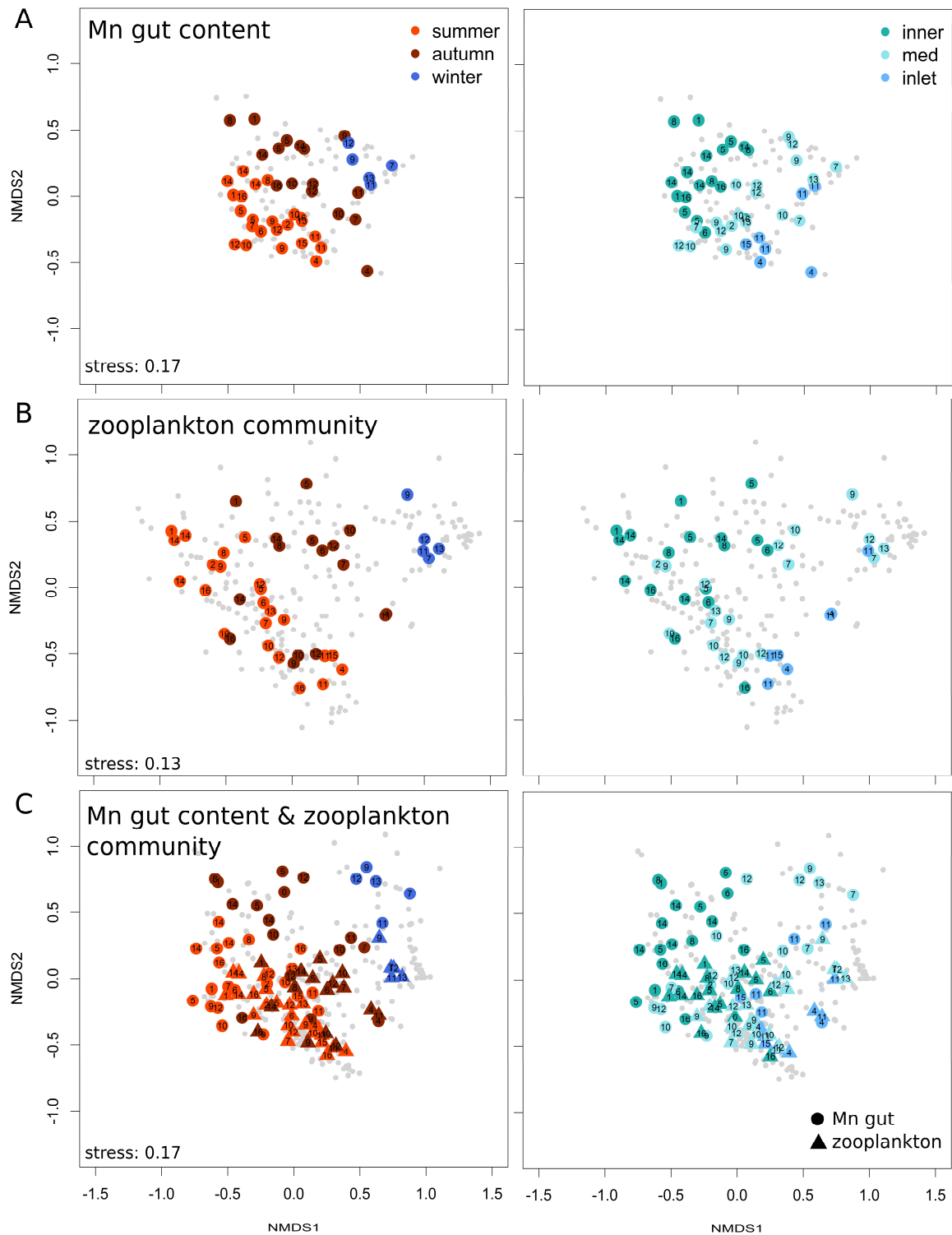


Figure D30: Beta diversity estimates based on Bray-Curtis similarities plotted on NMDS of A) *Mnemiopsis* gut content, B) in-situ mesozooplankton community and C) both datasets in a single plot. Colors of points refer to the sampling season or location of each sample.

D.4 Discussion

Understanding the characteristics of blooms of the zooplanktivorous invasive predator *M. leidy* is increasingly important, due to its ongoing successful global invasion and its potential impact on zooplankton communities, the faunal base of marine food webs with massive importance for the ecosystem production. The top-down effect of the predation pressure on zooplankton, which is especially significant during strong blooms of *M. leidy*, favors a substantial decrease in zooplankton and correlated increase in phytoplankton (Finenko et al., 2006; Shiganova, 1998; Tiselius and Møller, 2017), accompanied by a decline in fish stocks, as already experienced in the Black and Caspian Seas (Shiganova and Bulgakova, 2000). Considering the importance of the Venice Lagoon as nursery area, the massive blooms experienced in the last years in this area raise concerns regarding its already ongoing and future effects on ecosystem production and ecosystem services. Another important aspect of high densities of *Mnemiopsis* effecting the socio-economic functioning is the clogging of fishermen's nets and of the cooling systems of power plants by *Mnemiopsis* (Palmieri et al., 2014).

Mnemiopsis is a successful invader due to several characteristics, like hermaphroditism and the rapid development of fertility. Its known high ecological plasticity is conformed in this study, as *Mnemiopsis* was found to be present at all 16 investigated stations, representative for different environmental conditions in the Venice Lagoon, and throughout the whole year of sampling, although at different life stages. The seasonal persistence, tolerating the measured temperature range of 3.0 - 30.5 °C, indicates the VL as a suitable source habitat. The highest abundances in terms of biovolume [ml/m³] were detected during summer (July-October), with temperature as the main abiotic driver, likewise stated by many authors, e.g., Kremer (1994), who mentioned temperature and prey abundance as key factors affecting its seasonal patterns. Another factor typical for restricted lagoons are potential low oxygen levels, especially during summer. *Mnemiopsis leidy*, however, as many other gelatinous species, can potentially benefit from it as they are generally more tolerant to hypoxia compared to their preys. In fact, as shown by Decker et al. (2004) with a reduced jumping frequency of the copepod *A. tonsa* under hypoxic conditions, this favors higher capture rates for less-tolerant prey, making them more vulnerable to predation.

Although *M. leidy* was found to be present in the whole VL, some areas seem to show higher abundances. In general, its abundance was slightly lower in the inlets, which, however, could be partially explained by deficient sampling due to its vertical distribution in these deeper stations. Several studies investigated the vertical distribution of *M. leidy*, suggesting that certain conditions, such as water column stratification, diurnal prey migration, or surface disturbance, may influence its vertical distribution. The VL however, due to its generally low depths (favoring e.g., wind-induced mixing) and to its tidal influence, is characterized by relatively homogeneous water columns that allowed therefore to sample by horizontal surface tow. However, as some individuals may be located closer to the bottom, this type of sampling does not permit to fully assess the abundance. As stated by Costello and Mianzan (2003), biases inherent in conventional net sampling could limit quantification and reporting of these patterns. Hypotheses on the differences in abundance found within the lagoon could be those related to the availability of prey as well as to hydrodynamic processes that may tend to accumulate *M. leidy* in specific areas (Ghezzi et al., 2015).

Feeding preferences of *M. leidy* have been studied in the past by several authors, but this is the first study applying DNA metabarcoding, based on HTS technologies, to investigate its dietary composition.

Compared to gut content analyses based morphological identification, DNA metabarcoding has the benefit of identifying also partially digested prey. Nonetheless, the relative quantification of prey items that are more effortlessly, and therefore faster, digestible, e.g., soft organisms like fish larvae, or that have been ingested before times, may be underestimated. Also, as the used barcode (P1) does not amplify ctenophores, potential cannibalism as it has been reported by Javidpour et al. (2020) will not be detected with this approach.

In this study, in accordance with the literature (Granhag et al., 2011; Javidpour et al., 2009b; Madsen and Riisgård, 2010), *M. leidy*'s diet was very variable and reflected the composition of *in-situ* preys, mainly including copepods, decapods, cladocerans, gastropods, bivalves and polychaetes, but also echinoderms, Nemertea and cnidarians. Especially during winter, the dietary composition is dominated by polychaetes, in consistency with Larson (1987) and McNamara et al. (2010), which reported the ingestion of polychaetes larvae by *Mnemiopsis*. The noticeable difference in these

samples, however, may also be a result of higher uncertainty due to smaller sample size (see biovolume during winter).

Similarly to Decker et al. (2004) or Roohi et al. (2010), also in this study the copepods *A. tonsa* was the most abundant copepod species, both *in-situ* and in the gut content. However, copepods, as well as cladocerans, were less represented in the gut content than *in-situ*, while decapod and mollusk larvae were more abundant in the gut content, indicating a preferential feeding on the latter ones. In fact, due to the capture mechanisms of *Mnemiopsis*, less mobile organisms such as mollusk larvae seemed to be the most vulnerable prey of *M. leidy*, which is consistent with literature (e.g. Madsen and Riisgård, 2010; Marchessaux et al., 2021). Also species-specific differences in the mobility are of importance. Within copepods, for example, smaller species like *Oithona nana*, *O. davisae* or *Euterpina acutifrons* seemed to be captured preferentially. In comparison, the larger species *Temora stylifera*, being potentially faster, are less abundant in the gut content as they may escape from *M. leidy* more easily (Cowan et al., 1992; Suchman and Sullivan, 1998; Titelman, 2001). However, it is important to point out that, especially regarding the holoplanktonic copepods, DNA metabarcoding does not allow to differentiate between life stages. Therefore, more than size differences between copepod species, the actual life stage of each species at that specific moment may have a more significant effect on the vulnerability to the feeding pressure of *M. leidy*.

The diet of *Mnemiopsis* is known to differ at different life stages. Adults, as already mentioned, feed on a variety of holo- and meroplanktonic organisms (Shiganova and Bulgakova, 2000), like copepods (Colin et al., 2015; Javidpour et al., 2009b; Mianzan et al., 2010; Purcell et al., 2001), and meroplanktonic larvae of polychaetes, mollusks, decapods and barnacles (Marchessaux et al., 2021). Larvae and post-larvae of *Mnemiopsis* consume primarily microphyto- and microzooplankton prey like dinoflagellates or ciliates (Sullivan and Gifford, 2004). In this study, only individuals above 1.5 cm length were included in the gut content analysis, therefore the use of a standard mesozooplankton net with a mesh size of 200 μm should not have a strong bias on the comparison of the gut contents with the *in-situ* zooplankton community. Nonetheless, the ingested preys may include zooplankton smaller than 200 μm , like nauplii or bivalve larvae, which might be underestimated in the sampled zooplankton

community. In fact, the selectivity of the 200 µm mesh sized net could be another explanation for the higher relative abundance of small sized organisms in the gut content compared to the *in-situ* zooplankton assemblages. Hence, the additional use of e.g., an 80 µm mesh sized net to better describe the smaller size fraction of the community could be beneficial.

As previously mentioned, the VL represents an ecosystem of huge ecological but especially socio-economic importance. It is not only an important nursery area for fish species, but it is also an area for mussel, clam and crab aquaculture, as part of the traditional Venetian cousin and economy.

On the one hand, in this study, no significant correlation between the *in-situ* abundance of fish and its abundance the gut content was found, indicating no direct predation on fish larvae or eggs in this study. This is probably explained by the dominance of benthic fish species in the VL, and the fact that the spawning times, mainly during spring, may not coincide with the major blooming period of *Mnemiopsis*. Moreover, the lagoon resident fish species (e.g., some gobies (*Pomatoschistus marmoratus*, *P. canestrinii*, *Knipowitschia panizzae*, *Gobius niger*, *Zosterisessor ophiocephalus*), the pipefish *Syngnathus abaster*, the sand smelt *Atherina boyeri* and the peacock blenny *Salaria pavo*), spending their whole life cycle in the lagoon environment, adapted their reproductive strategy. They prevent seaward flushing of eggs and larvae by spawning demersal eggs attached to the aquatic vegetation or other substrates, while the planktonic larval stage is reduced or lacking (Dando, 1984; Franzoi et al., 2010). This significantly limits their availability as food source for *M. leidyi*. The marine migrant fish species (e.g. the European anchovy *Engraulis encrasicolus*, the European sprat and pilchard (*Sprattus sprattus*, *Sardina pilchardus*), the pipefish *Syngnathus acus*, the gilthead seabream *Sparus aurata*, the European flounder *Platichthys flesus* and grey mullets (fam. Mugilidae)) enter at the juvenile or sub-adult stages into transitional waters with a seasonal periodicity, mainly in spring–summer months, to take advantage of the high prey abundance available in these coastal systems (Elliott et al., 2007; Franzoi et al., 2010). This size class however, may not be a suitable prey size for *Mnemiopsis* (Jaspers et al., 2011). Therefore, both categories of fish may not represent a viable food source for *Mnemiopsis* in the Venice Lagoon. With this study we can therefore preliminarily conclude that in the VL, rather than direct predation on fish eggs

and larvae, competition for zooplankton may potentially have an impact on the fish stock.

On the other hand, the impact *Mnemiopsis* seems to have on the meroplanktonic compartment of the zooplankton community may increase the pressure on the local economy as well as the industrial production. In fact, the VL is the main Manila clam (*R. philippinarum*) production site in Europe (Brusà et al., 2013), with a period of larval recruitment from May to August (Pellizzato et al., 2011), which coincides with the blooming period of *Mnemiopsis*.

While in other geographic areas the major concern regarding the arrival and blooming of *Mnemiopsis* refers to the fish stocks and its associated economy, in the VL, *Mnemiopsis*' impact may in fact be greater on the meroplanktonic compartment, hence on its role in the trophic network and on the mussel, clam, and crab fishery and aquaculture.

CONCLUSION

The comparison of the classical morphology-based identification and the molecular identification based on DNA metabarcoding highlighted that the latter one can be a promising tool for zooplankton biodiversity assessments. However, although both techniques are highly informative, they give information of different nature. The method of choice may depend on the objectives of the study: while the morphology-based identification enables the analyses of population structure, identifying developmental state and sex, DNA metabarcoding offers the possibility of high spatial and temporal coverage, higher taxonomic resolution and broader taxonomic coverage, which is particularly useful when studying, e.g., invasive species, the ecology of larval dispersion or where high spatio-temporal resolution is preferred over the information on population structure. However, rather than alternative the two methods may be considered complementary. This comprehensive approach, defined as “integrative taxonomy” (Dayrat, 2005), combines molecular techniques with traditional identification based on morphological traits to increase the resolution of the identification process and to integrate taxonomy with information about, e.g., population structure.

In this study, after the evaluation of DNA metabarcoding for zooplankton biodiversity assessments, the method was applied on a higher spatial and temporal scale. This is especially important in ecosystems with high spatial and temporal variability, such as transitional environments, as demonstrated by the much greater number of taxa detected by monthly sampling in 16 stations (447) than by seasonal sampling in 6 stations (224).

Once the protocol (extraction, amplification, sequencing, bioinformatic) is defined, the metabarcoding analysis of 200 samples would require approximately one to two working months, an order of magnitude lower than morphological approach (depending on the sample complexity, 1-3 days per sample, approx. one working year for 200 samples). Moreover, both the extraction and the bioinformatic analysis will be probably faster in the near future by robotizing the wet-lab steps and with the automation of the codes paired with improved computational power.

CONCLUSION

Besides the already discussed benefit in increasing the monitoring effort, allowing to provide results of large datasets in “near real time”, DNA metabarcoding could find application also in institutional routine monitoring or in the framework of environmental impact assessment of major infrastructure projects (e.g., development of port infrastructures, offshore platforms), where fast results would support an adaptive management approach. Also, it could be applied on samples collected by automated zooplankton samplers installed on moored devices or autonomous vehicles. Moreover, the assessment and prediction of larval distribution patterns, especially of species of commercial interest, may be useful for management issues, such as the establishment of biological protection areas, rational management of nursery areas or for fisheries management measures, and may potentially increase the sustainability of, e.g., clam culture in the Venice Lagoon.

The comparison of a dual COI marker could successfully demonstrate the utility of the P1 barcode, the combination of the forward jdgLCO1490 primer with the modified reverse internal primer mlCOIintR, when studying zooplankton biodiversity, and probably valid for metazoans in general. First, the P1 barcode could be used in combination with P2: a large DNA marker sequenced in its entirety dramatically enhances the ability of a correct taxonomic assignment. Therefore, many hopes for a better taxonomic resolution lie in the sequencing of large DNA fragments with Pacbio (single-molecule real-time sequencing) and ONT (nanopore sequencing) platforms. Using P1 in combination with P2 could therefore have the benefit to not rely on one relatively short barcode only (319 and 313 bp), but rather having the variability of the whole Folmer region without the problem of sequencing a relatively large barcode (658 bp). Also, as the data showed some taxa specific primer selectivity like the missing primer binding site, e.g., for the forward primer jdgLCO1490 in ctenophores, combining P1 and P2 would reduce the risk of losing OTUs for a limited primer match in some metazoan groups. This will be overcome as at least the second half of the COI Folmer region, the P2, would be amplified, impeding to lose information on those taxa. Second, the missing amplification success for some taxa could be advantageously in particular cases. For example, excluding host sequences when studying the gut content can be beneficial to avoid unnecessarily sequence the host’s DNA. In the study presented in Chapter D, this barcode (P1), was successfully applied to investigate on the diet of *M. leidy* by

CONCLUSION

comparing its gut content with the *in-situ* mesozooplankton assemblage. The finding of this first study applying DNA metabarcoding on the diet assessment of *M. leidy* indicated that it mainly depends on the food availability *in-situ* designating *Mnemiopsis* as a generalist. However, especially meroplanktonic taxa, such as bivalves, gastropods and decapods seem to be preferentially fed, while fish larvae or eggs were not abundant in the gut contents. This indicates that the possible impact *Mnemiopsis* could have on local fish community in the VL may be by competition for zooplankton rather than by direct predation.

DNA metabarcoding is becoming a useful tool for biodiversity assessment, but it has its shortcomings too, as protocol biases and issues regarding the reference database reduce its reliability. Those limitations include the sensitivity to marker choice, incomplete and deficient reference databases, and biases caused by different bioinformatic approaches. These aspects among other technical issues, especially regarding the improvement of biomass estimations, should be one of the main future objectives in this field, e.g., by creating calibration curves for different taxa.

ACKNOWLEDGEMENTS

First, I wish to thank my supervisor Prof. Dr. Alberto Pallavicini and Dr. Elisa Camatti, without whose guidance and support I would not be here. They offered me the extraordinary opportunity to work on each step of the methodological process, from field samplings, to molecular and bioinformatic analyses, giving me the chance to work on various topics and with different colleagues. Their door was always open for scientific, as well as human, support and advice.

I would also like to thank Marco Pansera for sharing with me his passion for the world of zooplankton and its morphological identification, as well as for providing the morphology-based identification data used for the evaluation of DNA metabarcoding and for assisting me during the field samplings.

I would like to express my thankfulness to David Stanković for its precious guidance through the never-ending world of improving the bioinformatic analyses.

I would like to thank all the colleagues from the CNR ISMAR Venice, especially Fabrizio Bernardi Aubry and Gianni Zennaro for the technical support during fieldwork, as well as to the team of the Laboratory of Applied and Comparative Genomics at the University of Trieste, especially to Fabrizia Gionechetti and Fiorella Florian for the laboratory support.

Finally, I want to thank my husband Andrea for his unconditional love, support and for the numerous late-night discussions on ecology, our shared passion.

And a special mention goes to Jonas, my little boy, who was for sure the closest person to me in the last months of this journey...

REFERENCES

- Albaina, A., Aguirre, M., Abad, D., Santos, M., Estonba, A., 2016. 18S rRNA V9 metabarcoding for diet characterization: A critical evaluation with two sympatric zooplanktivorous fish species. *Ecol. Evol.* 6, 1809–1824. <https://doi.org/10.1002/ece3.1986>
- Amaral-Zettler, L.A., McCliment, E.A., Ducklow, H.W., Huse, S.M., 2009. A method for studying protistan diversity using massively parallel sequencing of V9 hypervariable regions of small-subunit ribosomal RNA *Genes. PLoS One* 4, 1–9. <https://doi.org/10.1371/journal.pone.0006372>
- Ardura, A., Planes, S., Garcia-Vazquez, E., 2013. Applications of DNA barcoding to fish landings: Authentication and diversity assessment. *Zookeys* 365, 49–65. <https://doi.org/10.3897/zookeys.365.6409>
- Bandelj, V., Socal, G., Park, Y.S., Lek, S., Coppola, J., Camatti, E., Capuzzo, E., Milani, L., Solidoro, C., 2008. Analysis of multitrophic plankton assemblages in the Lagoon of Venice. *Mar. Ecol. Prog. Ser.* 368, 23–40. <https://doi.org/10.3354/meps07565>
- Belmonte, G., Vaglio, I., Rubino, F., Alabiso, G., 2013. Zooplankton composition along the confinement gradient of the Taranto Sea System (Ionian Sea, south-eastern Italy). *J. Mar. Syst.* 128, 222–238. <https://doi.org/10.1016/j.jmarsys.2013.05.007>
- Bernardi-Aubry, F., Acri, F., Scarpa, G.M., Braga, F., 2020. Phytoplankton – Macrophyte Interaction in the Lagoon. *Water* 12, 2810.
- Bernardi Aubry, F., Acri, F., Bastianini, M., Bianchi, F., Cassin, D., Pugnetti, A., Socal, G., 2006. Seasonal and interannual variations of phytoplankton in the Gulf of Venice (Northern Adriatic Sea). *Chem. Ecol.* 22. <https://doi.org/10.1080/02757540600687962>
- Bianchi, F., Ravagnan, E., Acri, F., Bernardi-Aubry, F., Boldrin, A., Camatti, E., Cassin, D., Turchetto, M., 2004. Variability and fluxes of hydrology, nutrients and particulate matter between the Venice Lagoon and the Adriatic Sea. Preliminary results (years 2001-2002). *J. Mar. Syst.* 51, 49–64. <https://doi.org/10.1016/j.jmarsys.2004.05.007>
- Blanco-Bercial, L., 2020. Metabarcoding Analyses and Seasonality of the Zooplankton Community at BATS. *Front. Mar. Sci.* 7, 1–16. <https://doi.org/10.3389/fmars.2020.00173>
- Bolyen, E., Rideout, J.R., Dillon, M.R., Bokulich, N.A., Abnet, C.C., Al-Ghalith, G.A., Alexander, H., Alm, E.J., Arumugam, M., Asnicar, F., Bai, Y., Bisanz, J.E., Bittinger, K., Brejnrod, A., Brislawn, C.J., Brown, C.T., Callahan, B.J., Caraballo-Rodríguez, A.M., Chase, J., Cope, E.K., Da Silva, R., Diener, C., Dorrestein, P.C., Douglas, G.M., Durall, D.M., Duvallet, C., Edwardson, C.F., Ernst, M., Estaki, M., Fouquier, J., Gauglitz, J.M., Gibbons, S.M., Gibson, D.L., Gonzalez, A., Gorlick, K., Guo, J., Hillmann, B., Holmes,

REFERENCES

- S., Holste, H., Huttenhower, C., Huttley, G.A., Janssen, S., Jarmusch, A.K., Jiang, L., Kaehler, B.D., Kang, K. Bin, Keefe, C.R., Keim, P., Kelley, S.T., Knights, D., Koester, I., Kosciolk, T., Kreps, J., Langille, M.G.I., Lee, J., Ley, R., Liu, Y.X., Lofffield, E., Lozupone, C., Maher, M., Marotz, C., Martin, B.D., McDonald, D., Mclver, L.J., Melnik, A. V., Metcalf, J.L., Morgan, S.C., Morton, J.T., Naimey, A.T., Navas-Molina, J.A., Nothias, L.F., Orchanian, S.B., Pearson, T., Peoples, S.L., Petras, D., Preuss, M.L., Pruesse, E., Rasmussen, L.B., Rivers, A., Robeson, M.S., Rosenthal, P., Segata, N., Shaffer, M., Shiffer, A., Sinha, R., Song, S.J., Spear, J.R., Swafford, A.D., Thompson, L.R., Torres, P.J., Trinh, P., Tripathi, A., Turnbaugh, P.J., Ul-Hasan, S., van der Hooft, J.J.J., Vargas, F., Vázquez-Baeza, Y., Vogtmann, E., von Hippel, M., Walters, W., Wan, Y., Wang, M., Warren, J., Weber, K.C., Williamson, C.H.D., Willis, A.D., Xu, Z.Z., Zaneveld, J.R., Zhang, Y., Zhu, Q., Knight, R., Caporaso, J.G., 2019. Reproducible, interactive, scalable and extensible microbiome data science using QIIME 2. *Nat. Biotechnol.* 37, 852–857. <https://doi.org/10.1038/s41587-019-0209-9>
- Bourlat, S.J., Borja, A., Gilbert, J., Taylor, M.I., Davies, N., Weisberg, S.B., Griffith, J.F., Lettieri, T., Field, D., Benzie, J., Glöckner, F.O., Rodríguez-Ezpeleta, N., Faith, D.P., Bean, T.P., Obst, M., 2013. Genomics in marine monitoring: New opportunities for assessing marine health status. *Mar. Pollut. Bull.* 74, 19–31. <https://doi.org/10.1016/j.marpolbul.2013.05.042>
- Bragg, L.M., Stone, G., Butler, M.K., Hugenholtz, P., Tyson, G.W., 2013. Shining a Light on Dark Sequencing: Characterising Errors in Ion Torrent PGM Data. *PLoS Comput. Biol.* 9. <https://doi.org/10.1371/journal.pcbi.1003031>
- Brandon-Mong, G.J., Gan, H.M., Sing, K.W., Lee, P.S., Lim, P.E., Wilson, J.J., 2015. DNA metabarcoding of insects and allies: An evaluation of primers and pipelines. *Bull. Entomol. Res.* 105, 717–727. <https://doi.org/10.1017/S0007485315000681>
- Brannock, P.M., Waits, D.S., Sharma, J., Halanych, K.M., 2014. High-throughput sequencing characterizes intertidal meiofaunal communities in Northern Gulf of Mexico (Dauphin Island and Mobile Bay, Alabama). *Biol. Bull.* 227, 161–174. <https://doi.org/10.1086/BBLv227n2p161>
- Brodeur, R.D., Decker, M.B., Ciannelli, L., Purcell, J.E., Bond, N.A., Stabeno, P.J., Acuna, E., Hunt, G.L., 2008. Rise and fall of jellyfish in the eastern Bering Sea in relation to climate regime shifts. *Prog. Oceanogr.* 77, 103–111. <https://doi.org/10.1016/j.pocean.2008.03.017>
- Brusà, R.B., Cacciatore, F., Ponis, E., Molin, E., Delaney, E., 2013. Clam culture in the Venice lagoon: Stock assessment of Manila clam (*Venerupis philippinarum*) populations at a nursery site and management proposals to increase clam farming sustainability. *Aquat. Living Resour.* 26, 1–10. <https://doi.org/10.1051/alr/2013042>
- Bucklin, A., Lindeque, P.K., Rodríguez-Ezpeleta, N., Albaina, A., Lehtiniemi, M., 2016. Metabarcoding of marine zooplankton: Prospects, progress and pitfalls. *J. Plankton Res.* 38, 393–400. <https://doi.org/10.1093/plankt/fbw023>
- Bucklin, A., Ortman, B.D., Jennings, R.M., Nigro, L.M., Sweetman, C.J., Copley, N.J.,

REFERENCES

- Sutton, T., Wiebe, P.H., 2010. A “Rosetta Stone” for metazoan zooplankton: DNA barcode analysis of species diversity of the Sargasso Sea (Northwest Atlantic Ocean). *Deep. Res. Part II Top. Stud. Oceanogr.* 57, 2234–2247. <https://doi.org/10.1016/j.dsr2.2010.09.025>
- Bucklin, A., Peijnenburg, K.T.C.A., Kosobokova, K.N., O’Brien, T.D., Blanco-Bercial, L., Cornils, A., Falkenhaus, T., Hopcroft, R.R., Hosia, A., Laakmann, S., Li, C., Martell, L., Questel, J.M., Wall-Palmer, D., Wang, M., Wiebe, P.H., Weydmann-Zwolicka, A., 2021. Toward a global reference database of COI barcodes for marine zooplankton. *Mar. Biol.* 168, 1–26. <https://doi.org/10.1007/s00227-021-03887-y>
- Bucklin, A., Steinke, D., Blanco-Bercial, L., 2011. DNA barcoding of marine metazoa. *Ann. Rev. Mar. Sci.* 3, 471–508. <https://doi.org/10.1146/annurev-marine-120308-080950>
- Bucklin, A., Yeh, H.D., Questel, J.M., Richardson, D.E., Reese, B., Copley, N.J., Wiebe, P.H., 2019. Time-series metabarcoding analysis of zooplankton diversity of the NW Atlantic continental shelf. *ICES J. Mar. Sci.* 76, 1162–1176. <https://doi.org/10.1093/icesjms/fsz021>
- Cahill, A.E., Pearman, J.K., Borja, A., Carugati, L., Carvalho, S., Danovaro, R., Dashfield, S., David, R., Féral, J.P., Olenin, S., Šiaulys, A., Somerfield, P.J., Trayanova, A., Uyarra, M.C., Chenuil, A., 2018. A comparative analysis of metabarcoding and morphology-based identification of benthic communities across different regional seas. *Ecol. Evol.* 8, 8908–8920. <https://doi.org/10.1002/ece3.4283>
- Camacho, C., Coulouris, G., Avagyan, V., Ma, N., Papadopoulos, J., Bealer, K., Madden, T.L., 2009. BLAST+: Architecture and applications. *BMC Bioinformatics* 10, 1–9. <https://doi.org/10.1186/1471-2105-10-421>
- Camatti, E., Comaschi, A., De Olazabal, A., Fonda Umani, S., 2008. Annual dynamics of the mesozooplankton communities in a highly variable ecosystem (North Adriatic Sea, Italy). *Mar. Ecol.* 29, 387–398. <https://doi.org/10.1111/j.1439-0485.2008.00256.x>
- Camatti, E., Pansera, M., Bergamasco, A., 2019. The copepod *Acartia tonsa* Dana in a microtidal mediterranean Lagoon: History of a successful invasion. *Water (Switzerland)* 11. <https://doi.org/10.3390/w11061200>
- Caporaso, J.G., Kuczynski, J., Stombaugh, J., Bittinger, K., Bushman, F.D., Costello, E.K., Fierer, N., Peña, A.G., Goodrich, J.K., Gordon, J.I., Huttley, G.A., Kelley, S.T., Knights, D., Koenig, J.E., Ley, R.E., Lozupone, C.A., Mcdonald, D., Muegge, B.D., Pirrung, M., Reeder, J., Sevinsky, J.R., Turnbaugh, P.J., Walters, W.A., Widmann, J., Yatsunenko, T., Zaneveld, J., Knight, R., 2010. correspondence QIIME allows analysis of high-throughput community sequencing data Intensity normalization improves color calling in SOLiD sequencing. *Nat. Publ. Gr.* 7, 335–336. <https://doi.org/10.1038/nmeth0510-335>
- Cardinale, B.J., Duffy, J.E., Gonzalez, A., Hooper, D.U., Perrings, C., Venail, P., Narwani, A., MacE, G.M., Tilman, D., Wardle, D.A., Kinzig, A.P., Daily, G.C., Loreau, M., Grace,

REFERENCES

- J.B., Larigauderie, A., Srivastava, D.S., Naeem, S., 2012. Biodiversity loss and its impact on humanity. *Nature* 486, 59–67. <https://doi.org/10.1038/nature11148>
- Carroll, E.L., Gallego, R., Sewell, M.A., Zeldis, J., Ranjard, L., Ross, H.A., Tooman, L.K., O’Rorke, R., Newcomb, R.D., Constantine, R., 2019. Multi-locus DNA metabarcoding of zooplankton communities and scat reveal trophic interactions of a generalist predator. *Sci. Rep.* 9, 1–14. <https://doi.org/10.1038/s41598-018-36478-x>
- Cataudella, S., Crosetti, D., Massa, F., 2015. Mediterranean coastal lagoons: sustainable management and interactions among aquaculture, capture fisheries and the environment., General Fisheries Commission for the Mediterranean. *Studies and Reviews*.
- Chain, F.J.J., Brown, E.A., Macisaac, H.J., Cristescu, M.E., 2016. Metabarcoding reveals strong spatial structure and temporal turnover of zooplankton communities among marine and freshwater ports. *Divers. Distrib.* 22, 493–504. <https://doi.org/10.1111/ddi.12427>
- Chao, A., Colwell, R.K., Gotelli, N.J., Hsieh, T.C., Sander, E.L., Ma, K.H., Colwell, R.K., Ellison, A.M., 2014. Rarefaction and extrapolation with Hill numbers : A framework for sampling and estimation in species diversity studies. *Ecol. Monogr.* 84, 45–67. <https://doi.org/10.1890/13-0133.1>
- Clarke, K.R., Gorley, R.N., 2006. *PRIMERv6: User Manual/Tutorial*. PRIMER-E, Plymouth.
- Clarke, L.J., Beard, J.M., Swadling, K.M., Deagle, B.E., 2017. Effect of marker choice and thermal cycling protocol on zooplankton DNA metabarcoding studies. *Ecol. Evol.* 7, 873–883. <https://doi.org/10.1002/ece3.2667>
- Coissac, E., Riaz, T., Puillandre, N., 2012. Bioinformatic challenges for DNA metabarcoding of plants and animals. *Mol. Ecol.* 21, 1834–1847. <https://doi.org/10.1111/j.1365-294X.2012.05550.x>
- Colin, S.P., MacPherson, R., Gemmell, B., Costello, J.H., Sutherland, K., Jaspers, C., 2015. Elevating the predatory effect: Sensory-scanning foraging strategy by the lobate ctenophore *Mnemiopsis leidyi*. *Limnol. Oceanogr.* 60, 100–109. <https://doi.org/10.1002/lno.10007>
- Comtet, T., Sandionigi, A., Viard, F., Casiraghi, M., 2015. DNA (meta)barcoding of biological invasions: a powerful tool to elucidate invasion processes and help managing aliens. *Biol. Invasions* 17, 905–922. <https://doi.org/10.1007/s10530-015-0854-y>
- Costello, J.H., Mianzan, H.W., 2003. Sampling field distributions of *Mnemiopsis leidyi* (Ctenophora, Lobata): Planktonic or benthic methods? *J. Plankton Res.* 25, 455–459. <https://doi.org/10.1093/plankt/25.4.455>
- Cowan Jr, J. H., & Houde, E. D. (1992). Size-dependent predation on marine fish larvae by Ctenophores, Scyphomedusae, and Planktivorous fish. *Fisheries Oceanography*,

1(2), 113-126.

- Cristescu, M.E., 2014. From barcoding single individuals to metabarcoding biological communities: Towards an integrative approach to the study of global biodiversity. *Trends Ecol. Evol.* 29, 566–571. <https://doi.org/10.1016/j.tree.2014.08.001>
- Cucco, A., Umgiesser, G., 2006. Modeling the Venice Lagoon residence time. *Ecol. Modell.* 193, 34–51. <https://doi.org/10.1016/j.ecolmodel.2005.07.043>
- Dando, P. R., 1984. Reproduction in estuarine fish. *Fish reproduction: strategies and tactics.* Academic Press, London, 155-170.
- Darling, J.A., Martinson, J., Gong, Y., Okum, S., Pilgrim, E., Lohan, K.M.P., Carney, K.J., Ruiz, G.M., 2018. Ballast Water Exchange and Invasion Risk Posed by Intracoastal Vessel Traffic: An Evaluation Using High Throughput Sequencing. *Environ. Sci. Technol.* 52, 9926–9936. <https://doi.org/10.1021/acs.est.8b02108>
- Dayrat, B., 2005. Towards integrative taxonomy. *Biol. J. Linn. Soc.* 85, 407–415. <https://doi.org/10.1111/j.1095-8312.2005.00503.x>
- Deagle, B.E., Clarke, L.J., Kitchener, J.A., Polanowski, A.M., Davidson, A.T., 2018. Genetic monitoring of open ocean biodiversity: An evaluation of DNA metabarcoding for processing continuous plankton recorder samples. *Mol. Ecol. Resour.* 18, 391–406. <https://doi.org/10.1111/1755-0998.12740>
- Deagle, B.E., Eveson, J.P., Jarman, S.N., 2006. Quantification of damage in DNA recovered from highly degraded samples - A case study on DNA in faeces. *Front. Zool.* 3, 1–10. <https://doi.org/10.1186/1742-9994-3-11>
- Decker, M.B., Breitburg, D.L., Purcell, J.E., 2004. Effects of low dissolved oxygen on zooplankton predation by the ctenophore *Mnemiopsis leidyi*. *Mar. Ecol. Prog. Ser.* 280, 163–172. <https://doi.org/10.3354/meps280163>
- Djurhuus, A., Pitz, K., Sawaya, N.A., Rojas-Márquez, J., Michaud, B., Montes, E., Muller-Karger, F., Breitbart, M., 2018. Evaluation of marine zooplankton community structure through environmental DNA metabarcoding. *Limnol. Oceanogr. Methods* 16, 209–221. <https://doi.org/10.1002/lom3.10237>
- Elliott, M., Whitfield, A.K., Potter, I.C., Blaber, S.J.M., Cyrus, D.P., Nordlie, F.G., Harrison, T.D., 2007. The guild approach to categorizing estuarine fish assemblages: A global review. *Fish Fish.* 8, 241–268. <https://doi.org/10.1111/j.1467-2679.2007.00253.x>
- Evans, N.T., Li, Y., Renshaw, M.A., Olds, B.P., Deiner, K., Turner, C.R., Jerde, C.L., Lodge, D.M., Lamberti, G.A., Pfrender, M.E., 2017. Fish community assessment with eDNA metabarcoding: Effects of sampling design and bioinformatic filtering. *Can. J. Fish. Aquat. Sci.* 74, 1362–1374. <https://doi.org/10.1139/cjfas-2016-0306>
- Evans, N.T., Olds, B.P., Renshaw, M.A., Turner, C.R., Li, Y., Jerde, C.L., Mahon, A.R., Pfrender, M.E., Lamberti, G.A., Lodge, D.M., 2016. Quantification of mesocosm fish

REFERENCES

- and amphibian species diversity via environmental DNA metabarcoding. *Mol. Ecol. Resour.* 16, 29–41. <https://doi.org/10.1111/1755-0998.12433>
- Finenko, G.A., Kideys, A.E., Anninsky, B.E., Shiganova, T.A., Roohi, A., Tabari, M.R., Rostami, H., Bagheri, S., 2006. Invasive ctenophore *Mnemiopsis leidyi* in the Caspian Sea: Feeding, respiration, reproduction and predatory impact on the zooplankton community. *Mar. Ecol. Prog. Ser.* 314, 171–185. <https://doi.org/10.3354/meps314171>
- Flynn, J.M., Brown, E.A., Chain, F.J.J., Macisaac, H.J., Cristescu, M.E., 2015. Toward accurate molecular identification of species in complex environmental samples: Testing the performance of sequence filtering and clustering methods. *Ecol. Evol.* 5, 2252–2266. <https://doi.org/10.1002/ece3.1497>
- Franzoi, P., Franco, A., Torricelli, P., 2010. Fish assemblage diversity and dynamics in the Venice lagoon. *Rend. Lincei* 21, 269–281. <https://doi.org/10.1007/s12210-010-0079-z>
- Frøslev, T.G., Kjølner, R., Bruun, H.H., Ejrnæs, R., Brunbjerg, A.K., Pietroni, C., Hansen, A.J., 2017. Algorithm for post-clustering curation of DNA amplicon data yields reliable biodiversity estimates. *Nat. Commun.* 8. <https://doi.org/10.1038/s41467-017-01312-x>
- Gačić, M., Mancero Mosquera, I., Kovačević, V., Mazzoldi, A., Cardin, V., Arena, F., Gelsi, G., 2004. Temporal variations of water flow between the Venetian lagoon and the open sea. *J. Mar. Syst.* 51, 33–47. <https://doi.org/10.1016/j.jmarsys.2004.05.025>
- Gaston, K.J., 2009. Geographic range limits of species. *Proc. R. Soc. B Biol. Sci.* 276, 1391–1393. <https://doi.org/10.1098/rspb.2009.0100>
- Geller, J., Meyer, C., Parker, M., Hawk, H., 2013. Redesign of PCR primers for mitochondrial cytochrome c oxidase subunit I for marine invertebrates and application in all-taxa biotic surveys. *Mol. Ecol. Resour.* 13, 851–861. <https://doi.org/10.1111/1755-0998.12138>
- Ghezzi, M., De Pascalis, F., Umgiesser, G., Zemlys, P., Sigovini, M., Marcos, C., Pérez-Ruzafa, A., 2015. Connectivity in Three European Coastal Lagoons. *Estuaries and Coasts* 38, 1764–1781. <https://doi.org/10.1007/s12237-014-9908-0>
- Ghezzi, M., Guerzoni, S., Cucco, A., Umgiesser, G., 2010. Changes in Venice Lagoon dynamics due to construction of mobile barriers. *Coast. Eng.* 57, 694–708. <https://doi.org/10.1016/j.coastaleng.2010.02.009>
- Ghezzi, M., Sarretta, A., Sigovini, M., Guerzoni, S., Tagliapietra, D., Umgiesser, G., 2011. Modeling the inter-annual variability of salinity in the lagoon of Venice in relation to the water framework directive typologies, *Ocean and Coastal Management*. <https://doi.org/10.1016/j.ocecoaman.2011.06.007>
- Goetze, E., 2010. Species discovery in marine planktonic invertebrates through global

REFERENCES

- molecular screening. *Mol. Ecol.* 19, 952–967. <https://doi.org/10.1111/j.1365-294X.2009.04520.x>
- Goodall-Copestake, W.P., 2017. One tunic but more than one barcode: Evolutionary insights from dynamic mitochondrial DNA in *Salpa thompsoni* (Tunicata: Salpida). *Biol. J. Linn. Soc.* 120, 637–648. <https://doi.org/10.1111/bij.12915>
- Granhag, L., Møller, L.F., Hansson, L.J., 2011. Size-specific clearance rates of the ctenophore *Mnemiopsis leidyi* based on in situ gut content analyses. *J. Plankton Res.* 33, 1043–1052. <https://doi.org/10.1093/plankt/fbr010>
- Günther, B., Knebelberger, T., Neumann, H., Laakmann, S., Martínez Arbizu, P., 2018. Metabarcoding of marine environmental DNA based on mitochondrial and nuclear genes. *Sci. Rep.* 8, 1–13. <https://doi.org/10.1038/s41598-018-32917-x>
- Haddock, S.H.D., 2007. Comparative feeding behavior of planktonic ctenophores. *Integr. Comp. Biol.* 47, 847–853. <https://doi.org/10.1093/icb/icm088>
- Hänfling, B., Handley, L.L., Read, D.S., Hahn, C., Li, J., Nichols, P., Blackman, R.C., Oliver, A., Winfield, I.J., 2016. Environmental DNA metabarcoding of lake fish communities reflects long-term data from established survey methods. *Mol. Ecol.* 25, 3101–3119. <https://doi.org/10.1111/mec.13660>
- Harvey, J.B.J., Johnson, S.B., Fisher, J.L., Peterson, W.T., Vrijenhoek, R.C., 2017. Comparison of morphological and next generation DNA sequencing methods for assessing zooplankton assemblages. *J. Exp. Mar. Bio. Ecol.* 487, 113–126. <https://doi.org/10.1016/j.jembe.2016.12.002>
- Hays, G.C., Richardson, A.J., Robinson, C., 2005. Climate change and marine plankton. *Trends Ecol. Evol.* 20, 337–344. <https://doi.org/10.1016/j.tree.2005.03.004>
- Hebert, P.D.N., Cywinska, A., Ball, S.L., DeWaard, J.R., 2003. Biological identifications through DNA barcodes. *Proc. R. Soc. B Biol. Sci.* 270, 313–321. <https://doi.org/10.1098/rspb.2002.2218>
- Hirai, J., Kuriyama, M., Ichikawa, T., Hidaka, K., Tsuda, A., 2014. A metagenetic approach for revealing community structure of marine planktonic copepods. *Mol. Ecol. Resour.* 15, 68–80. <https://doi.org/10.1111/1755-0998.12294>
- Hirai, J., Shimode, S., Tsuda, A., 2013. Evaluation of ITS2-28S as a molecular marker for identification of calanoid copepods in the subtropical western North Pacific. *J. Plankton Res.* 35, 644–656. <https://doi.org/10.1093/plankt/fbt016>
- Hirai, J., Tachibana, A., Tsuda, A., 2020. Large-scale metabarcoding analysis of epipelagic and mesopelagic copepods in the Pacific. *PLoS One* 15, 1–24. <https://doi.org/10.1371/journal.pone.0233189>
- Hirai, J., Yasuike, M., Fujiwara, A., Nakamura, Y., Hamaoka, S., Katakura, S., Takano, Y., Nagai, S., 2015. Effects of plankton net characteristics on metagenetic community

REFERENCES

- analysis of metazoan zooplankton in a coastal marine ecosystem. *J. Exp. Mar. Bio. Ecol.* 469, 36–43. <https://doi.org/10.1016/j.jembe.2015.04.011>
- Hopkins, G.W., Freckleton, R.P., 2002. Declines in the numbers of amateur and professional taxonomists: Implications for conservation. *Anim. Conserv.* 5, 245–249. <https://doi.org/10.1017/S1367943002002299>
- Hsieh, T.C., Ma, K.H., Chao, A., 2019. iNEXT: iNterpolation and EXTrapolation for species diversity. R package version 2.0.19.
- Huson, D.H., Beier, S., Flade, I., Górska, A., El-Hadidi, M., Mitra, S., Ruscheweyh, H.J., Tappu, R., 2016. MEGAN Community Edition - Interactive Exploration and Analysis of Large-Scale Microbiome Sequencing Data. *PLoS Comput. Biol.* 12, 1–12. <https://doi.org/10.1371/journal.pcbi.1004957>
- Jaspers, C., Titelman, J., Hansson, L.J., Haraldsson, M., Ditlefsen, C.R., 2011. The invasive ctenophore *Mnemiopsis leidyi* poses no direct threat to Baltic cod eggs and larvae. *Limnol. Oceanogr.* 56, 431–439. <https://doi.org/10.4319/lo.2011.56.2.0431>
- Javidpour, J., Molinero, J.C., Lehmann, A., Hansen, T., Sommer, U., 2009a. Annual assessment of the predation of *Mnemiopsis leidyi* in a new invaded environment, the Kiel Fjord (Western Baltic Sea): A matter of concern? *J. Plankton Res.* 31, 729–738. <https://doi.org/10.1093/plankt/fbp021>
- Javidpour, J., Molinero, J.C., Peschutter, J., Sommer, U., 2009b. Seasonal changes and population dynamics of the ctenophore *Mnemiopsis leidyi* after its first year of invasion in the Kiel Fjord, Western Baltic Sea. *Biol. Invasions* 11, 873–882. <https://doi.org/10.1007/s10530-008-9300-8>
- Javidpour, J., Molinero, J.C., Ramírez-Romero, E., Roberts, P., Larsen, T., 2020. Cannibalism makes invasive comb jelly, *Mnemiopsis leidyi*, resilient to unfavourable conditions. *Commun. Biol.* 3, 1–7. <https://doi.org/10.1038/s42003-020-0940-2>
- Kasapidis, P., Siokou, I., Khelifi-Touhami, M., Mazzocchi, M.G., Matthaiaki, M., Christou, E., Fernandez De Puellas, M.L., Gubanova, A., Di Capua, I., Batziakas, S., Frangoulis, C., 2018. Revising the taxonomic status and distribution of the *Paracalanus parvus* species complex (Copepoda, Calanoida) in the Mediterranean and Black Seas through an integrated analysis of morphology and molecular taxonomy. *J. Plankton Res.* 40, 595–605. <https://doi.org/10.1093/plankt/fby036>
- Kim, K.C., Byrne, L.B., 2006. Biodiversity loss and the taxonomic bottleneck: Emerging biodiversity science. *Ecol. Res.* 21, 794–810. <https://doi.org/10.1007/s11284-006-0035-7>
- Krehenwinkel, H., Kennedy, S., Pekár, S., Gillespie, R.G., 2017. A cost-efficient and simple protocol to enrich prey DNA from extractions of predatory arthropods for large-scale gut content analysis by Illumina sequencing. *Methods Ecol. Evol.* 8, 126–134. <https://doi.org/10.1111/2041-210X.12647>

REFERENCES

- Kremer, P., 1994. Patterns of abundance for *Mnemiopsis* in US coastal waters: a comparative overview. *ICES Journal of Marine Science*, 51(4), 347-354.
- Laroche, O., Kersten, O., Smith, C.R., Goetze, E., 2020. Environmental DNA surveys detect distinct metazoan communities across abyssal plains and seamounts in the western Clarion Clipperton Zone. *Mol. Ecol.* 29, 4588–4604. <https://doi.org/10.1111/mec.15484>
- Larson, R.J., 1987. In Situ Feeding Rates of the Ctenophore *Mnemiopsis mccrady*. *Estuaries and Coasts* 10, 87–91.
- Lehtiniemi, M., Ojaveer, H., David, M., Galil, B., Gollasch, S., McKenzie, C., Minchin, D., Occhipinti-Ambrogi, A., Olenin, S., Pederson, J., 2015. Dose of truth-Monitoring marine non-indigenous species to serve legislative requirements. *Mar. Policy* 54, 26–35. <https://doi.org/10.1016/j.marpol.2014.12.015>
- Leray, M., Yang, J.Y., Meyer, C.P., Mills, S.C., Agudelo, N., Ranwez, V., Boehm, J.T., Machida, R.J., 2013. A new versatile primer set targeting a short fragment of the mitochondrial COI region for metabarcoding metazoan diversity: Application for characterizing coral reef fish gut contents. *Front. Zool.* 10, 1–14. <https://doi.org/10.1186/1742-9994-10-34>
- Lindeque, P.K., Harris, R.P., Jones, M.B., Smerdon, G.R., 1999. Simple molecular method to distinguish the identity of *Calanus* species (Copepoda: Calanoida) at any developmental stage. *Mar. Biol.* 133, 91–96. <https://doi.org/10.1007/s002270050446>
- Lindeque, P.K., Hay, S.J., Heath, M.R., Ingvarsdottir, A., Rasmussen, J., Smerdon, G.R., Waniek, J.J., 2006. Integrating conventional microscopy and molecular analysis to analyse the abundance and distribution of four *Calanus* congeners in the North Atlantic. *J. Plankton Res.* 28, 221–238. <https://doi.org/10.1093/plankt/fbi115>
- Lindeque, P.K., Parry, H.E., Harmer, R.A., Somerfield, P.J., Atkinson, A., 2013. Next generation sequencing reveals the hidden diversity of zooplankton assemblages. *PLoS One* 8, 1–14. <https://doi.org/10.1371/journal.pone.0081327>
- Lindsay, D., Grossmann, M.M., Nishikawa, J., Bentlage, B., Collins, A., LINDSAY, D., Matilda Grossmann, M., 2015. DNA barcoding of pelagic cnidarians: current status and future prospects. *Bull. Plankt. Soc. Japan* 62, 39–43. https://doi.org/10.24763/bpsj.62.1_39
- Lobo, J., Shokralla, S., Costa, M.H., Hajibabaei, M., Costa, F.O., 2017. DNA metabarcoding for high-throughput monitoring of estuarine macrobenthic communities. *Sci. Rep.* 7, 1–13. <https://doi.org/10.1038/s41598-017-15823-6>
- Lodge, D.M., Turner, C.R., Jerde, C.L., Barnes, M.A., Chadderton, L., Egan, S.P., Feder, J.L., Mahon, A.R., Pfrender, M.E., 2012. Conservation in a cup of water: Estimating biodiversity and population abundance from environmental DNA. *Mol. Ecol.* 21, 2555–2558. <https://doi.org/10.1111/j.1365-294X.2012.05600.x>

REFERENCES

- Lotze, H.K., Lenihan, H.S., Bourque, B.J., Bradbury, R.H., Cooke, R.G., Kay, M.C., Kidwell, S.M., Kirby, M.X., Peterson, C.H., Jackson, J.B.C., 2006. Depletion, Degradation, and Recovery Potential of Estuaries and Coastal Seas. *Science* (80-). 312, 1806 LP – 1809. <https://doi.org/10.1126/science.1128035>
- Machida, R.J., Hashiguchi, Y., Nishida, M., Nishida, S., 2009. Zooplankton diversity analysis through single-gene sequencing of a community sample. *BMC Genomics* 10, 438. <https://doi.org/10.1186/1471-2164-10-438>
- Madsen, C. V., Riisgård, H.U., 2010. Ingestion-rate method for measurement of clearance rates of the ctenophore *Mnemiopsis leidyi*. *Aquat. Invasions* 5, 357–361. <https://doi.org/10.3391/ai.2010.5.4.04>
- Main, R.J., 1928. Observations of the feeding mechanism of a ctenophore, *Mnemiopsis leidyi*. *Biol. Bull.* 55, 69–78. <https://doi.org/10.2307/1537150>
- Malej, A., Tirelli, V., Lučić, D., Paliaga, P., Vodopivec, M., Goruppi, A., Ancona, S., Benzi, M., Bettoso, N., Camatti, E., Ercolessi, M., Ferrari, C.R., Shiganova, T., 2017. *Mnemiopsis leidyi* in the northern Adriatic: here to stay? *J. Sea Res.* 124, 10–16. <https://doi.org/10.1016/j.seares.2017.04.010>
- Marchessaux, G., Belloni, B., Gadreaud, J., Thibault, D., 2021. Predation assessment of the invasive ctenophore *Mnemiopsis leidyi* in a French Mediterranean lagoon. *J. Plankton Res.* 43, 161–179. <https://doi.org/10.1093/plankt/fbab002>
- Marchini, A., Ferrario, J., Sfriso, A., Occhipinti-Ambrogi, A., 2015. Current status and trends of biological invasions in the Lagoon of Venice, a hotspot of marine NIS introductions in the Mediterranean Sea. *Biol. Invasions* 17, 2943–2962. <https://doi.org/10.1007/s10530-015-0922-3>
- Marinier, E., Brown, D.G., McConkey, B.J., 2015. Pollux: Platform independent error correction of single and mixed genomes. *BMC Bioinformatics* 16, 1–12. <https://doi.org/10.1186/s12859-014-0435-6>
- McNamara, M.E., Lonsdale, D.J., Cerrato, R.M., 2013. Top-down control of mesozooplankton by adult *Mnemiopsis leidyi* influences microplankton abundance and composition enhancing prey conditions for larval ctenophores. *Estuar. Coast. Shelf Sci.* 133, 2–10. <https://doi.org/10.1016/j.ecss.2013.04.019>
- McNamara, M.E., Lonsdale, D.J., Cerrato, R.M., 2010. Shifting abundance of the ctenophore *Mnemiopsis leidyi* and the implications for larval bivalve mortality. *Mar. Biol.* 157, 401–412. <https://doi.org/10.1007/s00227-009-1327-6>
- Medlin, L., Elwood, H.J., Stickel, S., Sogin, M.L., 1988. The characterization of enzymatically amplified eukaryotic 16S-like rRNA-coding regions. *Gene* 71, 491–499. [https://doi.org/10.1016/0378-1119\(88\)90066-2](https://doi.org/10.1016/0378-1119(88)90066-2)
- Meredith, R.W., Gaynor, J.J., Bologna, P.A.X., 2016. Diet assessment of the Atlantic Sea Nettle *Chrysaora quinquecirrha* in Barnegat Bay, New Jersey, using next-generation

- sequencing. *Mol. Ecol.* 25, 6248–6266. <https://doi.org/10.1111/mec.13918>
- Meyer, C.P., 2003. Molecular systematics of cowries (Gastropoda: Cypraeidae) and diversification patterns in the tropics. *Biol. J. Linn. Soc.* 79, 401–459. <https://doi.org/10.1046/j.1095-8312.2003.00197.x>
- Mianzan, H.W., Martos, P., Costello, J.H., Guerrero, R.A., 2010. Avoidance of hydrodynamically mixed environments by *Mnemiopsis leidyi* (Ctenophora: Lobata) in open-sea populations from Patagonia, Argentina. *Hydrobiologia* 645, 113–124. <https://doi.org/10.1007/s10750-010-0218-7>
- Milardi, M., Lanzoni, M., Gavioli, A., Fano, E.A., Castaldelli, G., 2018. Tides and moon drive fish movements in a brackish lagoon. *Estuar. Coast. Shelf Sci.* 215, 207–214. <https://doi.org/10.1016/j.ecss.2018.09.016>
- Miya, M., Gotoh, R.O., Sado, T., 2020. MiFish metabarcoding: a high-throughput approach for simultaneous detection of multiple fish species from environmental DNA and other samples, *Fisheries Science*. Springer Japan. <https://doi.org/10.1007/s12562-020-01461-x>
- Mohrbeck, I., Raupach, M.J., Arbizu, P.M., Knebelsberger, T., Laakmann, S., 2015. High-throughput sequencing—the key to rapid biodiversity assessment of marine metazoa? *PLoS One* 10, 1–24. <https://doi.org/10.1371/journal.pone.0140342>
- Molinaroli, E., Guerzoni, S., Sarretta, A., Cucco, A., Umgiesser, G., 2007. Links between hydrology and sedimentology in the Lagoon of Venice, Italy. *J. Mar. Syst.* 68, 303–317. <https://doi.org/10.1016/j.jmarsys.2006.12.003>
- Morabito, G., Mazzocchi, M.G., Salmaso, N., Zingone, A., Bergami, C., Flaim, G., Accoroni, S., Basset, A., Bastianini, M., Belmonte, G., Bernardi Aubry, F., Bertani, I., Bresciani, M., Buzzi, F., Cabrini, M., Camatti, E., Caroppo, C., Cataletto, B., Castellano, M., Del Negro, P., de Olazabal, A., Di Capua, I., Elia, A.C., Fornasaro, D., Giallain, M., Grilli, F., Leoni, B., Lipizer, M., Longobardi, L., Ludovisi, A., Lugliè, A., Manca, M., Margiotta, F., Mariani, M.A., Marini, M., Marzocchi, M., Obertegger, U., Oggioni, A., Padedda, B.M., Pansera, M., Piscia, R., Povero, P., Pulina, S., Romagnoli, T., Rosati, I., Rossetti, G., Rubino, F., Sarno, D., Satta, C.T., Sechi, N., Stanca, E., Tirelli, V., Totti, C., Pugnetti, A., 2018. Plankton dynamics across the freshwater, transitional and marine research sites of the LTER-Italy Network. Patterns, fluctuations, drivers. *Sci. Total Environ.* 627, 373–387. <https://doi.org/10.1016/j.scitotenv.2018.01.153>
- Morello, E. B., & Arneri, E., 2016. Anchovy and sardine in the Adriatic Sea—an ecological review. *Oceanography and marine biology*, 221-268.
- Oksanen, J., Blanchet, F.G., Friendly, M., Kindt, R., Legendre, P., Mcglinn, D., Minchin, P.R., O'hara, R.B., Simpson, G.L., Solymos, P., Henry, M., Stevens, H., Szoecs, E., Maintainer, H.W., 2019. Package “vegan”- Community ecology package. CRAN.
- Palmieri, M.G., Barausse, A., Luisetti, T., Turner, K., 2014. Jellyfish blooms in the Northern Adriatic Sea: Fishermen's perceptions and economic impacts on fisheries.

REFERENCES

- Fish. Res. 155, 51–58. <https://doi.org/10.1016/j.fishres.2014.02.021>
- Pansera, M., Camatti, E., Schroeder, A., Zagami, G., Bergamasco, A., 2021. The non-indigenous *Oithona davisae* in a Mediterranean transitional environment: coexistence patterns with competing species. *Sci. Rep.* 11, 1–14. <https://doi.org/10.1038/s41598-021-87662-5>
- Pearman, J.K., El-Sherbiny, M.M., Lanzén, A., Al-Aidaros, A.M., Irigoien, X., 2014. Zooplankton diversity across three Red Sea reefs using pyrosequencing. *Front. Mar. Sci.* 1, 1–11. <https://doi.org/10.3389/fmars.2014.00027>
- Pellizzato, M., Galvan, T., Lazzarini, R., Penzo, P., 2011. Recruitment of *Tapes philippinarum* in the Venice Lagoon (Italy) during 2002–2007. *Aquac. Int.* 19, 541–554. <https://doi.org/10.1007/s10499-010-9370-3>
- Pett, W., Ryan, J.F., Pang, K., Mullikin, J.C., Martindale, M.Q., Baxevanis, A.D., Lavrov, D. V, 2011. Extreme mitochondrial evolution in the ctenophore *Mnemiopsis leidyi*: Insights from mtDNA and the Nuclear Genome. *Fossils* 22, 130–142. <https://doi.org/10.3109/19401736.2011.624611>.Extreme
- Piñol, J., Senar, M.A., Symondson, W.O.C., 2019. The choice of universal primers and the characteristics of the species mixture determine when DNA metabarcoding can be quantitative. *Mol. Ecol.* 28, 407–419. <https://doi.org/10.1111/mec.14776>
- Presnell, J.S., Vandepas, L.E., Warren, K.J., Swalla, B.J., Amemiya, C.T., Browne, W.E., 2016. The presence of a functionally tripartite through-gut in Ctenophora has implications for metazoan character trait evolution. *Curr. Biol.* 26, 2814–2820. <https://doi.org/10.1016/j.cub.2016.08.019>
- Purcell, J.E., Cresswell, F.P., Cargo, D.G., Kennedy, V.S., 1991. Differential ingestion and digestion of bivalve larvae by the scyphozoan *Chrysaora quinquecirrha* and the ctenophore *Mnemiopsis leidyi*. *Biol. Bull.* 180, 103–111. <https://doi.org/10.2307/1542433>
- Purcell, J.E., Shiganova, T.A., Decker, M.B., Houde, E.D., 2001. The ctenophore *Mnemiopsis* in native and exotic habitats: U.S. estuaries versus the Black Sea basin. *Hydrobiologia* 451, 145–176. <https://doi.org/10.1023/A:1011826618539>
- Questel, J.M., Hopcroft, R.R., DeHart, H.M., Smoot, C.A., Kosobokova, K.N., Bucklin, A., 2021. Metabarcoding of zooplankton diversity within the Chukchi Borderland, Arctic Ocean: improved resolution from multi-gene markers and region-specific DNA databases. *Mar. Biodivers.* 51. <https://doi.org/10.1007/s12526-020-01136-x>
- Rapoza, R., Novak, D., Costello, J.H., 2005. Life-stage dependent, in situ dietary patterns of the lobate ctenophore *Mnemiopsis leidyi* Agassiz 1865. *J. Plankton Res.* 27, 951–956. <https://doi.org/10.1093/plankt/fbi065>
- Ratnasingham, S., Hebert, P.D.N., 2013. A DNA-Based Registry for All Animal Species: The Barcode Index Number (BIN) System. *PLoS One* 8.

- <https://doi.org/10.1371/journal.pone.0066213>
- Reizopoulou, S., Simboura, N., Barbone, E., Aleffi, F., Basset, A., Nicolaidou, A., 2014. Biodiversity in transitional waters: Steeper ecotone, lower diversity. *Mar. Ecol.* 35, 78–84. <https://doi.org/10.1111/maec.12121>
- Riccardi, N., 2010. Selectivity of plankton nets over mesozooplankton taxa: Implications for abundance, biomass and diversity estimation Selectivity of plankton nets over mesozooplankton taxa: implications for abundance, biomass and diversity estimation. *J. Limnol.* 69. <https://doi.org/10.3274/JL10-69-2-10>
- Richardson, A.J., 2008. In hot water: zooplankton and climate change. *ICES J. Mar. Sci.* 65, 279–295. <https://doi.org/https://doi.org/10.1093/icesjms/fsn028>.
- Rognes, T., Flouri, T., Nichols, B., Quince, C., Mahé, F., 2016. VSEARCH: A versatile open source tool for metagenomics. *PeerJ* 2016, 1–22. <https://doi.org/10.7717/peerj.2584>
- Roohi, A., Kideys, A.E., Sajjadi, A., Hashemian, A., Pourgholam, R., Fazli, H., Khanari, A.G., Eker-Develi, E., 2010. Changes in biodiversity of phytoplankton, zooplankton, fishes and macrobenthos in the Southern Caspian Sea after the invasion of the ctenophore *Mnemiopsis leidyi*. *Biol. Invasions* 12, 2343–2361. <https://doi.org/10.1007/s10530-009-9648-4>
- Sanger, F., Nicklen, S., Coulson, A., 1977. DNA sequencing with chain-terminating. *Proc Natl Acad Sci USA* 74, 5463–5467.
- Schroeder, A., Stanković, D., Pallavicini, A., Gionechetti, F., Pansera, M., Camatti, E., 2020. DNA metabarcoding and morphological analysis - Assessment of zooplankton biodiversity in transitional waters. *Mar. Environ. Res.* 160. <https://doi.org/10.1016/j.marenvres.2020.104946>
- Schulz, M.H., Weese, D., Holtgrewe, M., Dimitrova, V., Niu, S., Reinert, K., Richard, H., 2014. Fiona: A parallel and automatic strategy for read error correction. *Bioinformatics* 30, 356–363. <https://doi.org/10.1093/bioinformatics/btu440>
- Sfriso, A., Facca, C., Ghetti, P.F., 2003. Temporal and spatial changes of macroalgae and phytoplankton in a Mediterranean coastal area: The Venice lagoon as a case study. *Mar. Environ. Res.* 56, 617–636. [https://doi.org/10.1016/S0141-1136\(03\)00046-1](https://doi.org/10.1016/S0141-1136(03)00046-1)
- Sfriso, A., Marcomini, A., Pavoni, B., 1994. Annual nutrient exchanges between the central lagoon of Venice and the northern Adriatic Sea. *Sci. Total Environ.* 156, 77–92. [https://doi.org/10.1016/0048-9697\(94\)90421-9](https://doi.org/10.1016/0048-9697(94)90421-9)
- Shiganova, T.A., 1998. Invasion of the Black Sea by the ctenophore *Mnemiopsis leidyi* and recent changes in pelagic community structure. *Fish. Oceanogr.* 7, 305–310. <https://doi.org/10.1046/j.1365-2419.1998.00080.x>
- Shiganova, T.A., Bulgakova, Y. V., 2000. Effects of gelatinous plankton on Black Sea and

REFERENCES

- Sea of Azov fish and their food resources. *ICES J. Mar. Sci.* 57, 641–648. <https://doi.org/10.1006/jmsc.2000.0736>
- Shiganova, T.A., Mirzoyan, Z.A., Studenikina, E.A., Volovik, S.P., Siokou-Frangou, I., Zervoudaki, S., Christou, E.D., Skirta, A.Y., Dumont, H.J., 2001. Population development of the invader ctenophore *Mnemiopsis leidyi*, in the Black Sea and in other seas of the Mediterranean basin. *Mar. Biol.* 139, 431–445. <https://doi.org/10.1007/s002270100554>
- Shokralla, S., Porter, T.M., Gibson, J.F., Dobosz, R., Janzen, D.H., Hallwachs, W., Golding, G.B., Hajibabaei, M., 2015. Massively parallel multiplex DNA sequencing for specimen identification using an Illumina MiSeq platform. *Sci. Rep.* 5. <https://doi.org/10.1038/srep09687>
- Sigovini, M., 2011. Multiscale dynamics of zoobenthic communities and relationships with environmental factors in the Lagoon of Venice 207.
- Solidoro, C., Bandelj, V., Bernardi, F.A., Camatti, E., Ciavatta, S., Cossarini, G., Facca, C., Franzoi, P., Libralato, S., Canu, D.M., Pastres, R., Pranovi, F., Raicevich, S., Social, G., Sfriso, A., Sigovini, M., Tagliapietra, D., Torricelli, P., 2010. Response of the Venice Lagoon ecosystem to natural and anthropogenic pressures over the last 50 years. *Coast. Lagoons Crit. Habitats Environ. Chang.* 483–511. <https://doi.org/10.1201/EBK1420088304>
- Solidoro, C., Pastres, R., Cossarini, G., Ciavatta, S., 2004. Seasonal and spatial variability of water quality parameters in the lagoon of Venice. *J. Mar. Syst.* 51, 7–18. <https://doi.org/10.1016/j.jmarsys.2004.05.024>
- Sommer, S.A., Van Woudenberg, L., Lenz, P.H., Cepeda, G., Goetze, E., 2017. Vertical gradients in species richness and community composition across the twilight zone in the North Pacific Subtropical Gyre. *Mol. Ecol.* 26, 6136–6156. <https://doi.org/10.1111/mec.14286>
- Song, L., Huang, W., Kang, J., Huang, Y., Ren, H., Ding, K., 2017. Comparison of error correction algorithms for Ion Torrent PGM data: Application to hepatitis B virus. *Sci. Rep.* 7, 1–11. <https://doi.org/10.1038/s41598-017-08139-y>
- Stefanni, S., Stanković, D., Borme, D., de Olazabal, A., Juretić, T., Pallavicini, A., Tirelli, V., 2018. Multi-marker metabarcoding approach to study mesozooplankton at basin scale. *Sci. Rep.* 8, 1–13. <https://doi.org/10.1038/s41598-018-30157-7>
- Steinberg, D.K., Van Mooy, B.A.S., Buesseler, K.O., Boyd, P.W., Kobari, T., Karl, D.M., 2008. Bacterial vs. zooplankton control of sinking particle flux in the ocean's twilight zone. *Limnol. Oceanogr.* 53, 1327–1338. <https://doi.org/10.4319/lo.2008.53.4.1327>
- Suchman, C.L., Sullivan, B.K., 1998. Vulnerability of the copepod *Acartia tonsa* to predation by the scyphomedusa *Chrysaora quinquecirrha*: Effect of prey size and behavior. *Mar. Biol.* 132, 237–245. <https://doi.org/10.1007/s002270050389>

REFERENCES

- Sullivan, L.J., Gifford, D.J., 2004. Diet of the larval ctenophore *Mnemiopsis leidyi* A. Agassiz (Ctenophora, Lobata). J. Plankton Res. 26, 417–431. <https://doi.org/10.1093/plankt/fbh033>
- Taberlet, P., Coissac, E., Pompanon, F., Brochmann, C., Willerslev, E., 2012. Towards next-generation biodiversity assessment using DNA metabarcoding. Mol. Ecol. 21, 2045–2050. <https://doi.org/10.1111/j.1365-294X.2012.05470.x>
- Tagliapietra, D., Sigovini, M., Ghirardini, A.V., 2009. A review of terms and definitions to categorise estuaries, lagoons and associated environments. Mar. Freshw. Res. 60, 497–509. <https://doi.org/10.1071/MF08088>
- Tiselius, P., Møller, L.F., 2017. Community cascades in a marine pelagic food web controlled by the non-visual apex predator *Mnemiopsis leidyi*. J. Plankton Res. 39, 271–279. <https://doi.org/10.1093/plankt/fbw096>
- Titelman, J., 2001. Swimming and escape behavior of copepod nauplii: Implications for predator-prey interactions among copepods. Mar. Ecol. Prog. Ser. 213, 203–213. <https://doi.org/10.3354/meps213203>
- Tournois, J., Darnaude, A.M., Ferraton, F., Aliaume, C., Mercier, L., McKenzie, D.J., 2017. Lagoon nurseries make a major contribution to adult populations of a highly prized coastal fish. Limnol. Oceanogr. 62, 1219–1233. <https://doi.org/10.1002/lno.10496>
- Turner, J.T., 2015. Zooplankton fecal pellets, marine snow, phytodetritus and the ocean's biological pump. Prog. Oceanogr. 130, 205–248. <https://doi.org/10.1016/j.pocean.2014.08.005>
- Unal, E., Frost, B.W., Armbrust, V., Kideys, A.E., 2006. Phylogeography of *Calanus helgolandicus* and the Black Sea copepod *Calanus euxinus*, with notes on *Pseudocalanus elongatus* (Copepoda, Calanoida). Deep. Res. Part II Top. Stud. Oceanogr. 53, 1961–1975. <https://doi.org/10.1016/j.dsr2.2006.03.017>
- Vanhove, M.P.M., Tessens, B., Schoelinck, C., Jondelius, U., Littlewood, D.T.J., Artois, T., Huyse, T., 2013. Problematic barcoding in flatworms: A case-study on monogeneans and rhabdocoels (Platyhelminthes). Zookeys 365, 355–379. <https://doi.org/10.3897/zookeys.365.5776>
- Vences, M., Lyra, M.L., Perl, R.G.B., Bletz, M.C., Stanković, D., Lopes, C.M., Jarek, M., Bhujju, S., Geffers, R., Haddad, C.F.B., Steinfartz, S., 2016. Freshwater vertebrate metabarcoding on Illumina platforms using double-indexed primers of the mitochondrial 16S rRNA gene. Conserv. Genet. Resour. 8, 323–327. <https://doi.org/10.1007/s12686-016-0550-y>
- Vidjak, O., Bojanić, N., de Olazabal, A., Benzi, M., Brautović, I., Camatti, E., Hure, M., Lipej, L., Lučić, D., Pansera, M., Pećarević, M., Pestorić, B., Pigozzi, S., Tirelli, V., 2019. Zooplankton in Adriatic port environments: Indigenous communities and non-indigenous species. Mar. Pollut. Bull. 147, 133–149. <https://doi.org/10.1016/j.marpolbul.2018.06.055>

REFERENCES

- Waggett, R., Costello, J.H., 1999. Capture mechanisms used by the lobate ctenophore, *Mnemiopsis leidyi*, preying on the copepod *Acartia tonsa*. *J. Plankton Res.* 21, 2037–2052. <https://doi.org/10.1093/plankt/21.11.2037>
- Wang, X., Hua, F., Wang, L., Wilcove, D.S., Yu, D.W., 2019. The biodiversity benefit of native forests and mixed-species plantations over monoculture plantations. *Divers. Distrib.* 25, 1721–1735. <https://doi.org/10.1111/ddi.12972>
- Ward, B.A., Dutkiewicz, S., Jahn, O., Follows, M.J., 2012. A size-structured food-web model for the global ocean. *Limnol. Oceanogr.* 57, 1877–1891. <https://doi.org/10.4319/lo.2012.57.6.1877>
- Weigand, H., Beermann, A.J., Čiampor, F., Costa, F.O., Csabai, Z., Duarte, S., Geiger, M.F., Grabowski, M., Rimet, F., Rulik, B., Strand, M., Szucsich, N., Weigand, A.M., Willassen, E., Wyler, S.A., Bouchez, A., Borja, A., Čiamporová-Zaťovičová, Z., Ferreira, S., Dijkstra, K.D., Eisendle, U., Freyhof, J., Gadawski, P., Graf, W., Haegerbaeumer, A., van der Hoorn, B.B., Japoshvili, B., Keresztes, L., Keskin, E., Leese, F., Macher, J., Mamos, T., Paz, G., Pešić, V., Pfannkuchen, D.M., Pfannkuchen, M.A., Price, B.W., Rinkevich, B., Teixeira, M.A.L., Várbíró, G., Ekrem, T., 2019. DNA barcode reference libraries for the monitoring of aquatic biota in Europe: Gap-analysis and recommendations for future work. *bioRxiv*. <https://doi.org/10.1101/576553>
- Yu, G., Smith, D.K., Zhu, H., Guan, Y., Lam, T.T.Y., 2017. Ggtree: an R Package for Visualization and Annotation of Phylogenetic Trees With Their Covariates and Other Associated Data. *Methods Ecol. Evol.* 8, 28–36. <https://doi.org/10.1111/2041-210X.12628>
- Zaiko, A., Samuiloviene, A., Ardura, A., Garcia-Vazquez, E., 2015. Metabarcoding approach for nonindigenous species surveillance in marine coastal waters. *Mar. Pollut. Bull.* 100, 53–59. <https://doi.org/10.1016/j.marpolbul.2015.09.030>
- Zirino, A., Elwany, H., Neira, C., Maicu, F., Mendoza, G., Levin, L.A., 2014. Salinity and its variability in the Lagoon of Venice, 2000–2009. *Adv. Oceanogr. Limnol.* 5, 41–59. <https://doi.org/10.1080/19475721.2014.900113>
- Zuliani, A., Zaggia, L., Collavini, F., Zonta, R., 2005. Freshwater discharge from the drainage basin to the Venice Lagoon (Italy). *Environ. Int.* 31, 929–938. <https://doi.org/10.1016/j.envint.2005.05.004>

LIST OF FIGURES

- Figure 1:** Study area - Overview and bathymetry of the 16 sampling stations within the Venice lagoon, and one in the Gulf of Venice. Orange dots: Long-Term Ecological Research (LTER) stations; Yellow dots: additional stations for the PhD project. 11
- Figure A2:** A) Heatmap based on the abundance of assignments for different taxonomic groups at similarity thresholds ranging from 100% to 90%, together with a similarity dendrogram. B) Barchart of summed taxonomic assignments of most the abundant phyla at different similarity thresholds (from 100% to 90%). 17
- Figure A3:** Flowchart of the bioinformatic multistep approach. 19
- Figure A4:** A) Histogram of read lengths after quality check and chimera filtering. B) Number of reads per sample of the 24 samples. Two samples (st.S autumn; st.1, autumn) have less than 20% (black #) and one sample (st.5, winter) less than 5% (red #) of reads in relation to the sample with the highest number of reads. C) Taxonomic level of assignment using the molecular approach (MBC) and the morphological approach (MOI). 21
- Figure A5:** Pie chart of assignments with 97% (1.3×10^6) and 94% (0.94×10^6) similarity threshold of the 24 samples divided by phyla. 21
- Figure A6:** Sample-size-based rarefaction/extrapolation curves along with a bridging sample completeness curve of the 6 stations per seasons (R package ggiNEXT). 22
- Figure A7:** Taxonomic tree representing the taxonomic richness revealed with the molecular approach (MBC) and the morphological approach (MOI), respectively (R package ggtree). 23
- Figure A8:** Relative read abundance of main phyla and of zooplanktonic groups by A) the molecular approach (MBC) and B) the morphological approach (MOI). 24
- Figure A9:** Venn diagram of A) list of copepod families; and B) number of taxa (species, genus, family) found with the molecular approach (MBC) and the morphological approach (MOI); and Shannon Wiener Index of C) MOI vs. MBC; and D) copepods vs. whole dataset. 26
- Figure A10:** Barcharts of relative abundances grouped by phyla (colors) and classes (patterns) and averaged by stations (st.S, st.1–5) and by seasons with A) the molecular approach (MBC) and B) the morphological approach (MOI). Barchart of relative abundance per sample with C) MBC and D) MOI. Those samples are marked with a #, that have less than 20% (black) or less than 5% (red) of reads compared to the maximum number of reads in a sample (st.2 winter). 28
- Figure A11:** Relative abundance of reads for molecular data (MBC) and of individual counts for morphological data (MOI) (percent based on square-rooted

data) of (A) most abundant phyla; (B) most abundant classes of Arthropoda (Hexanauplia, Malacostraca, Branchiopoda) and (C) 21 selected species present in both datasets (AT: *Acartia tonsa*, AC: *Acartia clausi*, PP: *Paracalanus parvus*, PA: *Penilia avirostris*, Eng: *Engraulis* sp., OS: *Oithona similis*, CV: *Ctenocalanus vanus*, CP: *Centropages ponticus*, TS: *Temora stylifera*, PM: *Pseudodiaptomus marinus*, LB: *Labidocera brunescens*; species with lowest abundances are not labelled (*Centropages typicus*, *Clausocalanus jobei*, *Oithona plumifera*, *Nannocalanus minor*, *Paracartia latisetosa*, *Temora longicornis*, *Clausocalanus furcatus*, *Diaixis* sp.). Pearson’s correlations between the two methods are given in the corresponding color. 30

Figure A12: Beta diversity estimates based on Bray-Curtis similarities plotted on NMDS plots based on molecular (MBC) and morphological (MOI) data, respectively. Colors of points refer to the sampling season of each sample. The three locations (sea, inlet, lagoon) are highlighted plotting the distance to their centroid and the standard deviations of the points per location with the respective colors. Salinity and temperature are superimposed (brown and grey contour lines) on the NMDS plots according to the CTD measurements during sampling..... 31

Figure A13: Relative abundance within specific taxa with A) DNA metabarcoding (MBC) and B) morphological identification (MOI); and of zooplankton groups with C) MBC and D) MOI divided by seasons calculating the fluctuation in abundances for each taxon along the year..... 32

Figure B14: Bioinformatic workflow. Green boxes: taxa considered as “confidential”, yellow boxes: considered as less confidential (“cf.” taxa), orange boxes: even less confidential and therefore not considered in some analyses (“best match”), red boxes: OTUs were excluded as they were not considered putative metazoan sequences. 44

Figure B15: A) PCoA (Principal coordinates analysis) of environmental parameters colored by sampling month (left) and by location (right). B) Boxplot of Temperature, Salinity and Turbidity measured during sampling activities. 46

Figure B16: Proportion of taxa and sequences of A) the different degrees of taxonomic assignments and B) different taxonomic level of assignment. And C), number of sequences per sample, divided by assigned and unassigned ones, and number of taxa per sample (black bar)..... 48

Figure B17: Barchart of mean relative abundances grouped by phyla (colors) and classes (patterns) averaged by stations (left) and by months/seasons (right)..... 49

Figure B18: Barchart of relative abundances of all 192 samples grouped by phyla (colors) and classes (patterns). 50

Figure B19: Beta diversity estimates based on Bray-Curtis similarities plotted on NMDS plots. Colors of points refer to the sampling season (left) and sampling month (right). The three locations (inner, med, inlet) are

highlighted plotting the distance to their centroid and the standard deviations of the points per location with the respective colors. Salinity and temperature are superimposed (brown and grey contour lines) according to the CTD measurements during sampling..... 51

Figure B20: Beta diversity estimates based on Bray-Curtis similarities plotted on NMDS plots divided by sampling location, inner (top), med (center) and inlet (bottom) stations. Colors refer to the sampling month. To highlight the circular succession of months, a colored ring was manually added. The taxa best describing the ordination pattern ($r^2 > 0.2$ and $p = 0.001$) are plotted as vectors. 52

Figure B21: Correlation between alpha diversity (Shannon Wiener Index) and the two environmental parameters, temperature, and salinity. Colors of points refer to the sampling month (left) and location (right)..... 53

Figure C22: Schematic representation of the primer regions..... 57

Figure C23: Barchart of proportion of A) sequences and B) OTUs for each degree of taxonomic assignments, and C) of OTUs for each taxonomic level of assignment, for each barcode, P1 and P2. D) Venn diagram of OTUs assigned at species or genus level (above) and, below, those aggregated at family level, detected with P1 only, with both barcodes, or with P2 only..... 60

Figure C24: Taxonomic tree representing the taxonomic richness revealed with the barcodes P1 and P2, respectively. 61

Figure C25: Barchart of relative abundance of the most abundant phyla (colors) and their classes (pattern) for each sample for P1 and P2..... 62

Figure C26: A) Alpha-diversity (Shannon Wiener Index (based on square-rooted data) and B) Relative abundance (based on square-rooted data) of copepods merged at genus level for P1 vs. P2 and its correlation (Pearson) and confidence interval (0.95) (grey shading)..... 63

Figure D27: Relative biovolume of *M. leidy* in terms of ml/m³: A) biovolume of samples where *M. leidy* was present, B) Boxplot of biovolume through the year of observation (colors refer to median temperature [°C] per month), and C) at the 16 stations (July-October) (colors refer to median salinity per station). 72

Figure D28: Barchart of relative abundance of different taxonomic groups in the gut content of *M. leidy* (above) and of the *in-situ* mesozooplankton community (below) for the 44 samples where the presence of *Mnemiopsis* was detected. Colors of barcharts indicate taxonomic composition, while colored circles indicate the month of sampling..... 74

Figure D29: Correlation plot of A) all taxa (% based on square-rooted data) collapsed at genus level (excluding datapoints with absence of taxon in both datasets), B) most abundant copepod genera, and C) selected meroplanktonic genera. Pearson’s correlations between the two datasets are given in the corresponding color. 74

Figure D30: Beta diversity estimates based on Bray-Curtis similarities plotted on NMDS of A) *Mnemiopsis* gut content, B) *in-situ* mesozooplankton community and C) both datasets in a single plot. Colors of points refer to the sampling season or location of each sample. 76

LIST OF TABLES

Table 1: Name, coordinates, type, location, and chapter in which the stations were investigated.....	12
Table A2: Primers used in this chapter.....	16
Table A3: Query for the creation of the marine metazoan reference database.	16
Table A4: Relative abundances in percent (mean value and standard deviation) of main phyla and of main classes of arthropods per station, location (sea, inlet, lagoon) and per season for molecular (MBC) and morphological (MOI) data.....	29
Table A5: Differences between relative abundances (square-rooted data in percent) of the most abundant phyla and the most abundant classes of arthropods over seasons and locations (lagoon (st.1, 2, 3, 4) and sea (st.S)) and in specific cases, additional tests were assessed with the non-parametric Kruskal-Wallis Test. Correlations between the two methods were assessed with Pearson's correlation coefficient.....	29
Table A6: Seasonal variation (relative abundances in percent) of selected taxa and of the three groups holo-, mero- and ichthyoplankton by metabarcoding (MBC) and morphological identification (MOI).	32
Table B7: Spatial and temporal patterns of the environmental factors based on Euclidean distances assessed using repeated-measure PERMANOVA with the sampling months as fixed factor and the stations as random factor.....	46
Table B8: Number and percentage of taxa and sequences at different degrees of taxonomic assignment.	47
Table C9: Primers used in this chapter.	58
Table C10: Stepwise change in number of sequences and OTUs through bioinformatic analyses and taxonomic assignment.	59
Table C11: Mean relative abundance of all phyla and selected classes and orders and its standard deviation for each barcode and Pearson's correlation of the relative abundance between the two barcodes (based on square-rooted data). NA: group present in 1 single sample only (same sample for both barcodes). ***: highly significant ($p < 0.001$).....	64
Table D12: Mean values and standard deviation of relative abundances of taxonomic groups in the gut contents and the <i>in-situ</i> mesozooplankton community and its correlations (based on square-root transformed data).	75

SUPPLEMENTARY MATERIAL

Table S1: List of taxa detected with DNA metabarcoding (MBC) and morphological identification (MOI). Taxa identified with MBC as singletons are marked with an x.

phylum	class	order	family	genus	species	de-novo best match <94%	MBC	MOI	sing.
Annelida	Clitellata	Haplotaxida	Naididae	<i>Paranais</i>	<i>frici</i>		+		
		Haplotaxida	Naididae			<i>Tubificoides cf. brownae</i>	+		
	Polychaeta	-	-	-	-			+	
		-	Capitellidae			<i>Capitella cf. capitata</i>	+		
		-	Magelonidae	<i>Magelona</i>	<i>minuta</i>		+		
		Amphinomida	Amphinomidae	<i>Hermodice</i>	<i>carunculata</i>		+		
		Canalipalpata	Sabellariidae	<i>Sabellaria</i>	<i>spinulosa</i>		+		
		Eunicida	Eunicidae	<i>Marphysa</i>			+		
					<i>sanguinea</i>		+		x
		Phyllodocida	Phyllodocidae			<i>Phyllodoce cf. groenlandica</i>	+		
				<i>Phyllodoce</i>	<i>longipes</i>		+		
			Nephtyidae			<i>Nephtys cf. hombergii</i>	+		
			Nereididae	<i>Hediste</i>	<i>diversicolor</i>		+		
		Sabellida	Oweniidae	<i>Galathowenia</i>	<i>oculata</i>		+		
				<i>Owenia</i>	<i>fusiformis</i>		+		
			Serpulidae	<i>Hydroides</i>	<i>dianthus</i>		+		
				<i>Spirobranchus</i>	<i>triqueter</i>		+		
		Spionida	Spionidae	<i>Streblospio</i>			+		
						<i>Dipolydora cf. capensis</i>	+		
						<i>Scoelelis cf. eltaninae</i>	+		
				<i>Polydora</i>	<i>cornuta</i>		+		
					<i>websteri</i>		+		
			Paraonidae			<i>Aricidea cf.</i>	+		
Arthropoda	Branchiopoda	Ctenopoda	Sididae	<i>Penilia</i>	<i>avirostris</i>		+	+	
		Onychopoda	Podonidae					+	
				<i>Pleopis</i>	<i>polyphemoides</i>		+		
				<i>Podon</i>	<i>intermedius</i>		+		
				<i>Pseudevadne</i>	<i>tergestina</i>		+	+	
				<i>Evadne</i>	<i>nordmanni</i>		+		
					<i>spinifera</i>		+		
		Anomopoda	Daphniidae	<i>Daphnia</i>			+		
			Macrothricidae			<i>Macrothrix cf. sp.</i>	+		
	Collembola	Poduromorpha	Neanuridae	<i>Anurida</i>	<i>maritima</i>		+		
	Hexanauplia	Copepoda (subclass)						+	
		Calanoida						+	
			Acartiidae	<i>Acartia</i>				+	
					<i>tonsa</i>		+	+	
					<i>clausii</i>		+	+	
					<i>margalefi</i>		+	+	
				<i>Paracartia</i>	<i>latisetosa</i>		+	+	
			Calanidae					+	
				<i>Calanus</i>	<i>euxinus</i>		+		
					<i>helgolandicus</i>			+	
				<i>Mesocalanus</i>	<i>tenuicornis</i>			+	
				<i>Nannocalanus</i>	<i>minor</i>		+	+	
			Candaciidae	<i>Candacia</i>				+	
					<i>giesbrechti</i>			+	
			Centropagidae	<i>Centropages</i>				+	
					<i>kröyeri</i>			+	
					<i>ponticus</i>		+	+	
					<i>typicus</i>		+	+	

phylum	class	order	family	genus	species	de-novo best match <94%	MBC	MOI	sing.
				<i>Isias</i>				+	
					<i>clavipes</i>			+	
			Clausocalanidae	<i>Clausocalanus</i>				+	
					<i>furcatus</i>			+	+
					<i>jobei</i>			+	+
					<i>lividus</i>			+	x
					<i>mastigophorus</i>			+	
					<i>parapergens</i>			+	
					<i>paululus</i>			+	x
				<i>Ctenocalanus</i>	<i>vanus</i>			+	+
				<i>Pseudocalanus</i>	<i>elongatus</i>			+	
			Corycaeidae					+	
				<i>Ditrichocorycaeus</i>	<i>anglicus</i>			+	
			Diaixidae	<i>Diaixis</i>	<i>hibernica</i>			+	
					<i>pygmaea</i>			+	
			Metridinidae	<i>Pleuromamma</i>	<i>gracilis</i>			+	x
			Paracalanidae	<i>Paracalanus</i>				+	+
					<i>indicus</i>			+	
					<i>parvus</i>			+	+
					<i>quasimodo</i>			+	
				<i>Calocalanus</i>				+	
					<i>pavo</i>			+	
					<i>styliremis</i>			+	
			Peltidiidae	<i>Clytemnestra</i>	<i>scutellata</i>			+	
			Pontellidae	<i>Labidocera</i>				+	
					<i>brunescens</i>			+	+
					<i>wollastoni</i>			+	
						<i>Pontellina cf. plumata</i>		+	
			Pseudodiaptomidae	<i>Calanipeda</i>	<i>aquaedulcis</i>			+	
						<i>Pseudodiaptomus cf. malayalus</i>		+	
				<i>Pseudodiaptomus</i>	<i>marinus</i>			+	+
			Scolecitrichidae	<i>Scolecithricella</i>	<i>dentata</i>			+	x
			Subeucalanidae	<i>Subeucalanus</i>	<i>pileatus</i>			+	
			Temoridae	<i>Temora</i>				+	
					<i>longicornis</i>			+	+
					<i>stylifera</i>			+	+
		Cyclopoida						+	
			Lichomolgidae	<i>Zygomoligus</i>	<i>dentatus</i>			+	
			Oithonidae					+	
						<i>Oithonidae cf.</i>		+	
				<i>Oithona</i>				+	
					<i>davisae</i>			+	
					<i>nana</i>			+	
					<i>plumifera</i>			+	+
					<i>setigera</i>			+	
					<i>similis</i>			+	+
					<i>tenuis</i>			+	
			Oncaeidae					+	
				<i>Oncaea</i>				+	
					<i>mediterranea</i>			+	
					<i>scottodicarloi</i>			+	
					<i>venusta</i>			+	
					<i>waldemari</i>			+	x
		Harpacticoida						+	+
			Ectinosomatidae	<i>Microsetella</i>	<i>rosea</i>			+	
			Harpacticidae	<i>Harpacticella</i>	<i>jejuensis</i>			+	
			Peltidiidae	<i>Goniopsyllus</i>	<i>rostratus</i>			+	
			Tachidiidae	<i>Euterpina</i>	<i>acutifrons</i>			+	
			Thalestridae	<i>Eudactylopus</i>	<i>spectabilis</i>			+	
		Siphonostomatoida						+	
		Cirripedia (infraclass)						+	
		Sessilia	Balanidae					+	

phylum	class	order	family	genus	species	de-novo best match <94%	MBC	MOI	sing.
				<i>Amphibalanus</i>			+		
					<i>amphitrite</i>		+		
					<i>eburneus</i>		+		
					<i>improvisus</i>		+		
	Malacostraca	Amphipoda	Chthamalidae	<i>Chthamalus</i>	<i>montagui</i>		+		
			Gammaridae			<i>Echinogammarus cf. foxi</i>	+		
			Aoridae	<i>Grandidierella</i>	<i>japonica</i>		+		
			Caprellidae	<i>Caprella</i>	<i>scaura</i>		+		
				<i>Paracaprella</i>	<i>pusilla</i>		+		
			Corophiidae	<i>Monocorophium</i>	<i>acherusicum</i>		+		
					<i>insidiosum</i>		+	x	
			Ischyroceridae	<i>Jassa</i>	<i>slatteryi</i>		+		
		Decapoda					+		
			Paguridae			<i>Paguridae cf.</i>	+		
			Alpheidae	<i>Athanas</i>	<i>nitescens</i>		+		
			Astacidae	<i>Austropotamobius</i>	<i>torrentium</i>		+		
			Carcinidae	<i>Carcinus</i>	<i>aestuarii</i>		+		
						<i>Carcinus cf. maenas</i>	+		
			Crangonidae	<i>Philocheras</i>	<i>bispinosus</i>		+		
						<i>Philocheras cf. bispinosus</i>	+		
				<i>Philocheras</i>	<i>trispinosus</i>		+		
			Galatheidae				+		
			Goneplacidae	<i>Goneplax</i>	<i>rhomboides</i>		+		
			Inachidae	<i>Inachus</i>	<i>communissimus</i>		+		
			Palaemonidae	<i>Palaemon</i>			+		
					<i>adpersus</i>		+		
					<i>elegans</i>		+		
					<i>macrodactylus</i>		+		
			Panopeidae	<i>Dyspanopeus</i>	<i>sayi</i>		+		
				<i>Rhithropanopeus</i>	<i>harrisi</i>		+		
			Penaeidae	<i>Penaeus</i>	<i>kerathurus</i>		+		
			Pilumnidae	<i>Pilumnus</i>			+		
					<i>aestuarii</i>		+		
			Polybiidae	<i>Liocarcinus</i>	<i>vernalis</i>		+		
			Processidae	<i>Processa</i>	<i>modica</i>		+		
					<i>nouveli</i>		+		
			Sicyoniidae	<i>Sicyonia</i>	<i>carinata</i>		+		
			Thoridae	<i>Eualus</i>	<i>cranchii</i>		+		
			Upogebiidae			<i>Upogebia cf. pusilla</i>	+		
		Isopoda					+		
			Idoteidae			<i>Idotea cf. metallica</i>	+		
		Mysida					+		
			Mysidae	<i>Mesopodopsis</i>	<i>slabberi</i>		+		
		Cumacea					+		
	Ostracoda						+		
		Halocyprida	Halocyprididae	<i>Mikroconchoecia</i>			+		
				<i>Porroecia</i>	<i>spirostris</i>		+		
				<i>Proceroecia</i>	<i>microprocera</i>		+	x	
Bryozoa							+		
	Gymnolaemata	Cheilostomatida	Candidae	<i>Tricellaria</i>	<i>occidentalis</i>		+		
		Ctenostomatida	Vesiculariidae	<i>Amathia</i>	<i>verticillata</i>		+		
Chaetognatha							+		
	Sagittoidea	Aphragmophora	Sagittidae	<i>Pseudosagitta</i>	<i>lyra</i>		+	x	
				<i>Sagitta</i>	<i>enflata</i>		+		
					<i>setosa</i>		+		
Chordata	Actinopterygii						+		
		Syngnathiformes	Syngnathidae	<i>Syngnathus</i>	<i>acus</i>		+		
		Atheriniformes	Atherinidae	<i>Atherina</i>	<i>boyeri</i>		+		
		Clupeiformes	Clupeidae	<i>Sardina</i>	<i>pilchardus</i>		+	x	

phylum	class	order	family	genus	species	de-novo best match <94%	MBC	MOI	sing.
				<i>Sprattus</i>	<i>sprattus</i>		+		
			Engraulidae	<i>Engraulis</i>			+		
					<i>encrasicolus</i>		+	+	
		Myctophiformes	Myctophidae	<i>Notoscopelus</i>	<i>bolini</i>		+		x
		Perciformes	Blenniidae	<i>Salaria</i>	<i>pavo</i>		+		
			Gobiidae	<i>Deltentosteus</i>	<i>quadrifasciatus</i>		+		
				<i>Gobius</i>	<i>niger</i>		+		
				<i>Knipowitschia</i>			+		x
				<i>Ninnigobius</i>			+		
				<i>Proterorhinus</i>	<i>semilunaris</i>		+		
				<i>Zosterisessor</i>	<i>ophiocephalus</i>		+		
			Mugilidae	<i>Liza</i>	<i>aurata</i>		+		
				<i>Mugil</i>	<i>cephalus</i>		+		
				<i>Chelon</i>	<i>saliens</i>		+		
			Sparidae	<i>Diplodus</i>	<i>annularis</i>		+		
		Pleuronectiformes	Bothidae	<i>Arnoglossus</i>			+		
			Pleuronectidae	<i>Platichthys</i>	<i>flesus</i>		+		
			Soleidae	<i>Solea</i>	<i>solea</i>		+		x
	Appendicularia							+	
	Asciacea							+	
		Stolidobranchia	Pyuridae	<i>Pyura</i>	<i>dura</i>		+		
				<i>Polyandrocarpa</i>	<i>zorritensis</i>		+		
				<i>Styela</i>	<i>plicata</i>		+		
		Phlebobranchia	Asciidiidae	<i>Ascidia</i>	<i>ahodori</i>		+		
					<i>virginea</i>		+		
				<i>Ascidiella</i>	<i>aspersa</i>		+		
			Cionidae	<i>Ciona</i>			+		x
	Leptocardii	-	Branchiostomatidae	<i>Branchiostoma</i>				+	
					<i>lanceolatum</i>		+		
	Thaliacea							+	
Cnidaria								+	
	Anthozoa	Actiniaria	Aiptasiidae	<i>Aiptasia</i>	<i>pulchella</i>		+		
		Actiniaria	Metridiidae	<i>Metridium</i>	<i>senile</i>		+		
		Actiniaria	Diadumenidae	<i>Diadumene</i>	<i>leucolena</i>		+		
		Actiniaria	Actiniidae	<i>Anthopleura</i>	<i>elegantissima</i>		+		
	Hydrozoa							+	
		Anthoathecata	Rathkeidae	<i>Podocorynoides</i>	<i>minima</i>		+		
			Zanclidae	<i>Zanclaea</i>			+		
			Bougainvilliidae	<i>Bougainvillia</i>	<i>muscus</i>		+		
			Corynidae	<i>Sarsia</i>	<i>tubulosa</i>		+		
			Rathkeidae	<i>Lizzia</i>	<i>blondina</i>		+		
			Tubulariidae	<i>Ectopleura</i>	<i>dumortierii</i>		+		
		Leptothecata	Campanulariidae			<i>Orthopyxis cf. integra</i>	+		
			Tiaropsidae	<i>Tiaropsis</i>	<i>multicirrata</i>		+		
			Blackfordiidae	<i>Blackfordia</i>	<i>virginica</i>		+		
			Campanulariidae	<i>Campanularia</i>	<i>hincksii</i>		+		
				<i>Clytia</i>			+		
					<i>gracilis</i>		+		
				<i>Obelia</i>			+		
					<i>bidentata</i>		+		
					<i>dichotoma</i>		+		
			Laodiceidae			<i>Laodicea cf. undulata</i>	+		
		Siphonophorae		<i>Siphonophorae</i>				+	
			Diphyidae			<i>Muggiaea cf. Atlantica</i>	+		
				<i>Lensia</i>	<i>campanella</i>		+		
			Sphaeronectidae	<i>Sphaeronectes</i>	<i>gracilis</i>		+		
	Scyphozoa							+	
		Rhizostomeae	Rhizostomatidae	<i>Rhizostoma</i>	<i>pulmo</i>		+		
		Semaeostomeae	Ulmaridae	<i>Aurelia</i>			+		
Ctenophora								+	
	Tantaculata	Lobata	Bolinopsidae	<i>Mnemiopsis</i>	<i>leidyi</i>		+		
		Cydidippa	Pleurobrachiidae	<i>Pleurobrachia</i>	<i>pileus</i>		+		

phylum	class	order	family	genus	species	de-novo best match <94%	MBC	MOI	sing.
Echinodermata									+
	Asteroidea	Paxillosida	Astropectinidae			<i>Astropecten cf. irregularis complex</i>	+		
Echinodermata	Echinoidea	Camarodonta	Parechinidae	<i>Psammechinus</i>	<i>miliaris</i>		+		
				<i>Paracentrotus</i>	<i>lividus</i>		+		
		Clypeasteroidea	Echinocyamidae	<i>Echinocyamus</i>	<i>pusillus</i>		+		
		Spatangoida	Loveniidae	<i>Echinocardium</i>	<i>cordatum</i>		+		
			Brissidae	<i>Brissopsis</i>	<i>lyrifera</i>		+		
			Loveniidae	<i>Echinocardium</i>	<i>mediterraneum</i>		+		
			Schizasteridae			<i>Paraster cf. doederleini</i>	+		
	Holothuroidea	Dendrochirotida	Cucumariidae			<i>Plesiocolochirus cf. challengerii</i>	+		
	Ophiuroidea	Amphilepidida	Amphiuridae	<i>Amphiura</i>	<i>filiformis</i>		+		
			Ophiotrichidae	<i>Ophiothrix</i>			+		
					<i>fragilis</i>		+		
		Ophiurida	Ophiuridae	<i>Ophiura</i>	<i>albida</i>		+		
					<i>ophiura</i>		+		
Gastrotricha	-	Macrodasysida	Macrodasysidae	<i>Urodasys</i>			+		
Mollusca	Bivalvia								+
		-	Gastrochaenidae				+		
		-	Lasaeidae	<i>Kurtiella</i>	<i>bidentata</i>		+		
		Adapedonta	Hiatellidae	<i>Hiatella</i>			+		
		Myida	Corbulidae	<i>Corbula</i>	<i>gibba</i>		+		
			Teredinidae	<i>Lyrodus</i>	<i>pedicellatus</i>		+		
						<i>Teredo cf. navalis</i>	+		
		Mytilida	Mytilidae	<i>Arcuatula</i>	<i>senhousia</i>		+		
				<i>Modiolula</i>	<i>phaseolina</i>		+		x
				<i>Mytilus</i>	<i>galloprovincialis</i>		+		
				<i>Xenostrobus</i>	<i>securis</i>		+		
		Ostreida	Ostreidae	<i>Magallana</i>	<i>gigas</i>		+		
				<i>Ostrea</i>	<i>stentina</i>		+		
			Pinnidae	<i>Atrina</i>	<i>fragilis</i>		+		
		Venerida	Veneridae	<i>Polititapes</i>	<i>aureus</i>		+		
				<i>Ruditapes</i>	<i>philippinarum</i>		+		
				<i>Chamelea</i>	<i>gallina</i>		+		
		Veneroidea	Cardiidae	<i>Cerastoderma</i>	<i>glaucum</i>		+		
	Gastropoda								+
		Heterobranchia (subclass)					+		
		-	Limapontiidae	<i>Ercolania</i>	<i>viridis</i>		+		
		Aplysiida	Aplysiidae			<i>Aplysia cf. cervina</i>	+		
		Caenogastropoda	Cerithiidae	<i>Bittium</i>	<i>reticulatum</i>		+		
		Cephalaspidea	Aglajidae			<i>Chelidonura cf. sandrana</i>	+		
			Philinidae			<i>Philine cf. aperta</i>	+		
			Retusidae			<i>Retusa cf. umbilicata</i>	+		
			Haminoeidae	<i>Haminoea</i>	<i>japonica</i>		+		
					<i>navicula</i>		+		
						<i>Haminoea cf. navicula</i>	+		
		Littorinimorpha	Aporrhaidae	<i>Aporrhais</i>	<i>pespelecani</i>		+		
			Rissoidae	<i>Rissoa</i>			+		
			Hydrobiidae	<i>Ecrobia</i>	<i>ventrosa</i>		+		
		Neogastropoda	Mangeliidae	<i>Mangelia</i>	<i>attenuata</i>		+		
		Neogastropoda	Fascioliariidae			<i>Chryseofusus cf. acherusius</i>	+		
		Nudibranchia	Aeolidiidae	<i>Spurilla</i>	<i>neapolitana</i>		+		
			Eubranthidae	<i>Eubranthus</i>	<i>exiguus</i>		+		
			Onchidorididae	<i>Acanthodoris</i>	<i>pilosa</i>		+		x

phylum	class	order	family	genus	species	de-novo best match <94%	MBC	MOI	sing.
		Neogastropoda	Nassariidae			<i>Reticunassa cf. simoni</i>	+		
				<i>Tritia</i>	<i>incrassata</i>		+		
					<i>nitida</i>		+		
						<i>Tritia cf. nitida</i>	+		
		Opisthobranchia	Elysiidae	<i>Elysia</i>			+		
		Pleurobranchomorpha	Pleurobranchidae	<i>Berthella</i>			+		
			Pleurobranchaeidae	<i>Pleurobranchaea</i>	<i>meckeli</i>		+		
		Pteropoda						+	
Nematoda								+	
	Chromadorea	Monhysterida	Linhomoeidae	<i>Terschellingia</i>	<i>longicaudata</i>		+		x
	Secernentea	Rhabditida	Rhabditidae	<i>Caenorhabditis</i>	<i>brenneri</i>		+		x
Nemertea	Palaeonemertea	-	Hubrechtidae	<i>Hubrechtella</i>	<i>dubia</i>		+		
		-	Tubulanidae			<i>Tubulanus cf. sp.</i>	+		x
		-	Cephalothricidae	<i>Cephalothrix</i>			+		
Phoronida								+	
	-	-	Phoronidae			<i>Philocheras cf. trispinosus</i>	+		
	-	-				<i>Phoronis cf. hippocrepi</i>	+		
	-	-				<i>Phoronis cf. ijimai</i>	+		
Platyhelminthes		-	-				+		x
	Rhabditophora	Dolichomicrostomida	Microstomidae	<i>Microstomum</i>			+		x
Porifera	Demospongiae	Poecilosclerida	Coelosphaeridae	<i>Lissodendoryx</i>	<i>isodictyalis</i>		+		
			Tedaniidae	<i>Tedania</i>	<i>ignis</i>		+		
		Spongillida					+		x
		Suberitida	Halichondriidae	<i>Halichondria</i>	<i>panicea</i>		+		
				<i>Hymeniacion</i>			+		
			Suberitidae	<i>Protosuberites</i>	<i>mereui</i>		+		
	Homoscleromorpha	Homosclerophorida	Oscarellidae	<i>Oscarella</i>			+		
Rotifera	Eurotatoria	-	Philodinidae	<i>Philodina</i>			+		x
		Ploima	Brachionidae	<i>Keratella</i>	<i>quadrata</i>		+		

Table S2: List of taxa detected with P1 and P2, respectively. Indicating the level of taxonomic assignment, with which barcode the taxon was detected, if it was a “cf.” assignment (94% similarity threshold) and, in case, if it was a singleton assignment.

phylum	class	order	family	genus	species	level	presence	cf.	singl.	
Annelida	Polychaeta					cl	P1			
		Aspidosiphonidormes	Aspidosiphonidae	<i>Aspidosiphon</i>	<i>Aspidosiphon muelleri</i>	sp	P1			
		Capitellida	Capitellidae	<i>Capitella</i>	<i>Capitella teleta</i>	sp	P2			
			Maldanidae	<i>Clymenura</i>	<i>Clymenura clypeata</i>	sp	P1+P2	P1/P2	P2	
		Echiuroidea	Bonelliidae	<i>Maxmuelleria</i>	<i>Maxmuelleria lankesteri</i>	sp	P2			
		Eunicida	Eunicidae	<i>Marphysa</i>	<i>Marphysa sanguinea</i>	sp	P1		P1	
			Onuphidae	<i>Diopatra</i>	<i>Diopatra neapolitana</i>	sp	P1+P2			
		Phyllodocida	Glyceridae	<i>Glycera</i>	<i>Glycera unicornis</i>	sp	P1	P1		
			Nereididae	<i>Alitta</i>	<i>Alitta succinea</i>	sp	P2			
				<i>Hediste</i>	<i>Hediste diversicolor</i>	sp	P1+P2			
			Polynoidae	<i>Harmothoe</i>	<i>Harmothoe imbricata</i>	sp	P1+P2			
			Syllidae	<i>Odontosyllis</i>	<i>Odontosyllis gibba</i>	sp	P2		P2	
		Sabellida	Oweniidae	<i>Owenia</i>	<i>Owenia fusiformis</i>	sp	P1+P2			
			Sabellariidae	<i>Sabellaria</i>	<i>Sabellaria spinulosa</i>	sp	P1+P2			
			Serpulidae	<i>Hydroides</i>	<i>Hydroides dianthus</i>	sp	P2			
		<i>Hydroides elegans</i>			sp	P2				
		Spionida	Chaetopteridae	<i>Chaetopterus</i>	<i>Chaetopterus variopedatus</i>	sp	P2			
			Spionidae	<i>Polydora</i>	<i>Polydora cf. nuchalis</i>	sp	P2			
					<i>Polydora cornuta</i>	sp	P2			
					<i>Polydora websteri</i>	sp	P2			
			<i>Prionospio</i>		g	P2				
			<i>Pseudopolydora</i>		g	P2				
			<i>Spiophanes</i>	<i>Spiophanes bombyx</i>	sp	P1	P1			
			<i>Streblospio</i>		g	P1+P2				
				<i>Streblospio shrubsolii</i>	sp	P2				
			Terebellida	Terebellidae			f	P2		P2
		<i>Nicolea</i>				g	P1+P2			
		Arthropoda	Branchiopoda	Diplostraca	Daphniidae	<i>Simocephalus</i>		g	P2	P2
					Macrotrichidae	<i>Macrotrix</i>		g	P1+P2	
					Podonidae	<i>Evadne</i>	<i>Evadne spinifera</i>	sp	P1+P2	
						<i>Pleopis</i>	<i>Pleopis polyphemoides</i>	sp	P1+P2	
						<i>Podon</i>	<i>Podon intermedius</i>	sp	P1+P2	P2
						<i>Pseudevadne</i>	<i>Pseudevadne tergestina</i>	sp	P1+P2	
Sididae	<i>Penilia</i>			<i>Penilia avirostris</i>	sp	P1+P2				
Hexanauplia	Calanoida			Acartiidae	<i>Acartia</i>	<i>Acartia clausii</i>	sp	P1+P2		
						<i>Acartia tonsa</i>	sp	P1+P2		
					<i>Paracartia</i>	<i>Paracartia latisetosa</i>	sp	P2		
			Calanidae	<i>Calanus</i>	<i>Calanus helgolandicus/euxinus complex</i>	sp	P1+P2			
					<i>Ctenocalanus</i>	<i>Ctenocalanus vanus</i>	sp	P1+P2		
					<i>Nannocalanus</i>	<i>Nannocalanus minor</i>	sp	P1+P2		
			Calocalanidae	<i>Calocalanus</i>	<i>Calocalanus pavo</i>	sp	P1+P2	P1		
			Candaciidae	<i>Candacia</i>	<i>Candacia bipinnata</i>	sp	P1	P1		
			Centropagidae	<i>Centropages</i>	<i>Centropages ponticus</i>	sp	P1+P2			
					<i>Centropages typicus</i>	sp	P1+P2			
Clausocalanidae	<i>Clausocalanus</i>		<i>Clausocalanus furcatus</i>	sp	P1+P2					
			<i>Clausocalanus jobei</i>	sp	P1+P2					
<i>Pseudocalanus</i>	<i>Pseudocalanus elongatus</i>		sp	P1+P2						
Diaixidae	<i>Diaixis</i>	<i>Diaixis hibernica/pygmea</i>	sp	P1+P2						
Paracalanidae	<i>Paracalanus</i>		g	P1+P2						

phylum	class	order	family	genus	species	level	presence	cf.	singl.
					<i>Paracalanus indicus</i>	sp	P1+P2		
					<i>Paracalanus parvus</i>	sp	P1+P2		
					<i>Paracalanus quasimodo</i>	sp	P1+P2		
			Pontellidae	<i>Anomalocera</i>	<i>Anomalocera patersonii</i>	sp	P1+P2		
				<i>Labidocera</i>	<i>Labidocera brunescens</i>	sp	P1+P2		
			Pseudodiaptomidae	<i>Pseudodiaptomus</i>	<i>Pseudodiaptomus marinus</i>	sp	P1+P2		P1
			Temoridae	<i>Temora</i>	<i>Temora stylifera</i>	sp	P1+P2		
		Cyclopoida	Cyclopidae	<i>Mesocyclops</i>	<i>Mesocyclops pelpeiensis</i>	sp	P2		
			Oithonidae	<i>Oithona</i>	<i>Oithona davisae</i>	sp	P2		
					<i>Oithona nana</i>	sp	P1+P2		
					<i>Oithona plumifera</i>	sp	P2		
					<i>Oithona similis</i>	sp	P1+P2		
		Harpacticoida				or	P1+P2		
			Ectinosomatidae			f	P1+P2		
			Euterpinidae	<i>Euterpina</i>	<i>Euterpina acutifrons</i>	sp	P1+P2		
			Harpacticidae	<i>Harpacticella</i>	<i>Harpacticella jejuensis</i>	sp	P1+P2	P1	
			Longipediidae	<i>Longipedia</i>		g	P1+P2		
			Peltidiidae	<i>Goniopsyllus</i>	<i>Goniopsyllus rostratus</i>	sp	P1+P2		
			Thalestridae	<i>Eudactylopus</i>	<i>Eudactylopus spectabilis</i>	sp	P1+P2		
		Poecilostomatoida	Corycaeidae	<i>Ditrichocorycaeus</i>	<i>Ditrichocorycaeus anglicus</i>	sp	P2		
			Lichomolgidae	<i>Zygomoligus</i>	<i>Zygomoligus dentatus</i>	sp	P1+P2		
			Oncaea	<i>Oncaea</i>		g	P1+P2		
					<i>Oncaea curta</i>	sp	P1	P1	P1
					<i>Oncaea scottodicaloi</i>	sp	P2		
					<i>Oncaea venusta</i>	sp	P2		
					<i>Oncaea waldemari</i>	sp	P1+P2		
		Sessilia	Balanidae	<i>Amphibalanus</i>	<i>Amphibalanus reticulatus</i>	f	P1+P2		P2
					<i>Amphibalanus amphitrite</i>	sp	P1+P2		
					<i>Amphibalanus eburneus</i>	sp	P1+P2		
					<i>Amphibalanus improvisus</i>	sp	P1+P2		
					<i>Perforatus</i>	<i>Perforatus perforatus</i>	sp	P1+P2	
			Chthamalidae	<i>Chthamalus</i>	<i>Chthamalus montagui</i>	sp	P1+P2		
					<i>Chthamalus stellatus</i>	sp	P2		
					<i>Microeuraphia</i>	<i>Microeuraphia depressa</i>	sp	P1+P2	
			Coronulidae	<i>Chelonibia</i>	<i>Chelonibia testudinaria</i>	sp	P2		
	Malacostraca	Amphipoda	Caprellidae	<i>Caprella</i>	<i>Caprella equilibra</i>	sp	P1+P2		
					<i>Caprella scaura</i>	sp	P1+P2		
			Corophiidae	<i>Grandidierella</i>	<i>Grandidierella japonica</i>	sp	P1+P2		
				<i>Laticorophium</i>	<i>Laticorophium baconi</i>	sp	P1		
				<i>Monocorophium</i>	<i>Monocorophium acherusicum</i>	sp	P1+P2		
					<i>Monocorophium insidiosum</i>	sp	P1+P2		
			Gammaridae	<i>Elasmopus</i>		g	P1+P2		
				<i>Gammarus</i>		g	P1+P2		
			Ischyroceridae	<i>Jassa</i>	<i>Jassa slatteryi</i>	sp	P1+P2		
			Melitidae	<i>Gammarella</i>	<i>Gammarella fucicola</i>	sp	P1+P2		P2
				<i>Melita</i>	<i>Melita palmata</i>	sp	P1+P2		
		Decapoda	Alpheidae	<i>Athanas</i>	<i>Athanas nitescens</i>	sp	P1+P2		
			Carcinidae	<i>Carcinus</i>	<i>Carcinus aestuarii</i>	sp	P1+P2		
			Grapsidae	<i>Pachygrapsus</i>	<i>Pachygrapsus marmoratus</i>	sp	P1+P2		
			Hippolytidae	<i>Hippolyte</i>		g	P1+P2		

phylum	class	order	family	genus	species	level	presence	cf.	singl.
			Paguridae			f	P1+P2		
			Palaemonidae	<i>Palaemon</i>	<i>Palaemon adspersus</i>	sp	P1+P2		
					<i>Palaemon elegans</i>	sp	P1+P2		
					<i>Palaemon macrodactylus</i>	sp	P1	P1	P1
			Panopeidae	<i>Dyspanopeus</i>	<i>Dyspanopeus sayi</i>	sp	P1+P2		
				<i>Lophopanopeus</i>	<i>Lophopanopeus bellus</i>	sp	P1	P1	
				<i>Rhithropanopeus</i>	<i>Rhithropanopeus harrisi</i>	sp	P1+P2		
			Parthenopidae	<i>Derilambrus</i>	<i>Derilambrus angulifrons</i>	sp	P2		
			Penaeidae	<i>Penaeus</i>	<i>Penaeus kerathurus</i>	sp	P1+P2		
			Pilumnidae	<i>Pilumnus</i>	<i>Pilumnus aestuarii</i>	sp	P2		
					<i>Pilumnus hirtellus</i>	sp	P1+P2		
					<i>Pilumnus spinifer</i>	sp	P1	P1	P1
			Polybiidae	<i>Liocarcinus</i>	<i>Liocarcinus vernalis</i>	sp	P1+P2		
			Sicyoniidae	<i>Sicyonia</i>	<i>Sicyonia carinata</i>	sp	P1+P2		
			Upogebiidae	<i>Upogebia</i>	<i>Upogebia pusilla</i>	sp	P2		
			Xanthidae			f	P1	P1	
				<i>Xantho</i>	<i>Xantho porea</i>	sp	P2		
		Isopoda	Janiridae	<i>Ianiropsis</i>	<i>Ianiropsis epilittoralis</i>	sp	P2		
		Mysida	Mysidae	<i>Mesopodopsis</i>	<i>Mesopodopsis slabberi</i>	sp	P1+P2		
Bryozoa	Gymnolaemata	Cheilostomatida	Bugulidae			f	P1		P1
				<i>Bugula</i>	<i>Bugula neritina</i>	sp	P1+P2		
			Candidae	<i>Tricellaria</i>	<i>Tricellaria occidentalis</i>	sp	P2		
		Ctenostomatida	Vesiculariidae	<i>Amathia</i>		g	P1+P2		
					<i>Amathia verticillata</i>	sp	P1+P2		
	Phylactolaemata	-	Plumatellidae	<i>Plumatella</i>	<i>Plumatella fungosa</i>	sp	P1+P2		P2
					<i>Plumatella repens</i>	sp	P1	P1	P1
Chaetognatha	Sagittoidea	Aphragmophora	Sagittidae	<i>Flaccisagitta</i>	<i>Flaccisagitta enflata</i>	sp	P1+P2		
				<i>Sagitta</i>	<i>Sagitta setosa</i>	sp	P1+P2		
Chordata	Actinopterygii	Atheriniformes	Atherinidae	<i>Atherina</i>	<i>Atherina boyeri</i>	sp	P1+P2		
		Beloniformes	Belonidae	<i>Belone</i>	<i>Belone belone</i>	sp	P2		
			Blenniidae	<i>Parablennius</i>	<i>Parablennius incognitus</i>	sp	P2		
					<i>Parablennius tentacularis</i>	sp	P2		
				<i>Salaria</i>	<i>Salaria pavo</i>	sp	P1+P2	P1	
		Carangiformes	Carangidae	<i>Lichia</i>	<i>Lichia amia</i>	sp	P1+P2		
		Clupeiformes	Clupeidae	<i>Sprattus</i>	<i>Sprattus sprattus</i>	sp	P1		P1
			Engraulidae	<i>Engraulis</i>	<i>Engraulis encrasicolus</i>	sp	P1+P2		
		Gadiformes	Gadidae	<i>Merlangius</i>	<i>Merlangius merlangus</i>	sp	P2		P2
		Gobiiformes	Gobiidae	<i>Gobius</i>	<i>Gobius niger</i>	sp	P1+P2		
				<i>Knipowitschia</i>	<i>Knipowitschia panizae</i>	sp	P2		
				<i>Ninnigobius</i>	<i>Ninnigobius canestrinii</i>	sp	P2		P2
				<i>Pomatoschistus</i>	<i>Pomatoschistus marmoratus</i>	sp	P2		
				<i>Zosterisessor</i>	<i>Zosterisessor ophiocephalus</i>	sp	P1+P2		
		Mugiliformes	Mugilidae	<i>Chelon</i>	<i>Chelon auratus</i>	sp	P1+P2	P1	
					<i>Chelon labrosus</i>	sp	P2		
					<i>Chelon ramada</i>	sp	P1		
					<i>Chelon saliens</i>	sp	P1+P2		
				<i>Mugil</i>	<i>Mugil cephalus</i>	sp	P2		P2
		Perciformes	Serranidae	<i>Serranus</i>	<i>Serranus hepatus</i>	sp	P1		
		Spariformes	Sparidae	<i>Lithognathus</i>	<i>Lithognathus mormyrus</i>	sp	P1		
				<i>Sparus</i>	<i>Sparus aurata</i>	sp	P1		
		Syngnathiformes	Syngnathidae	<i>Syngnathus</i>	<i>Syngnathus acus</i>	sp	P2		P2
		Tetraodontiformes	Tetraodontidae	<i>Tetraodon</i>	<i>Tetraodon nigroviridis</i>	sp	P2	P2	

phylum	class	order	family	genus	species	level	presence	cf.	singl.		
	Ascidacea	Enterogona	Asciidiidae	<i>Asciidiella</i>	<i>Asciidiella aspersa</i>	sp	P2		P2		
			Cionidae	<i>Ciona</i>		g	P2				
			Clavelinidae	<i>Clavelina</i>	<i>Clavelina oblonga</i>	sp	P2				
			Didemnidae	<i>Didemnum</i>		g	P2	P2	P2		
				<i>Diplosoma</i>	<i>Diplosoma listerianum</i>	sp	P2				
		Stolidobranchia	Molgulidae	<i>Molgula</i>	<i>Molgula manhattensis</i>	sp	P2				
			Pyuridae			f	P2				
				<i>Pyura</i>	<i>Pyura dura</i>	sp	P2				
			Styelidae	<i>Botrylloides</i>		g	P2				
				<i>Botryllus</i>	<i>Botryllus schlosseri</i>	sp	P2				
		<i>Polyandrocarpa</i>		<i>Polyandrocarpa zorritensis</i>	sp	P1+P2					
			<i>Styela</i>	<i>Styela plicata</i>	sp	P1+P2					
		Cnidaria	Anthozoa	Actiniaria	Actiniidae	<i>Anemonia</i>	<i>Anemonia viridis</i>	sp	P1		
						<i>Anthopleura</i>	<i>Anthopleura elegantissima</i>	sp	P1+P2		
					Diadumenidae	<i>Diadumene</i>	<i>Diadumene leucolena</i>	sp	P1		
<i>Diadumene lineata</i>	sp						P1+P2		P2		
Edwardsiidae	<i>Edwardsia</i>				<i>Edwardsia longicornis</i>	sp	P2		P2		
Metridiidae	<i>Metridium</i>				<i>Metridium senile</i>	sp	P1+P2	P2			
Sagartiidae						f	P1+P2				
	<i>Cereus</i>				<i>Cereus pedunculatus</i>	sp	P1				
	<i>Sagartiogeton</i>					g	P2				
<i>Sagartiogeton laceratus</i>					sp	P1+P2					
Hydrozoa	Anthoathecata			Bougainvilliidae	<i>Bougainvillia</i>		g	P1+P2			
						<i>Bougainvillia carolinensis</i>	sp	P2			
						<i>Lizzia</i>	<i>Lizzia blondina</i>	sp	P1+P2		
				Corymorphidae	<i>Corymorpha</i>	<i>Corymorpha bigelowi</i>	sp	P1+P2	P1	P1	
				Corynidae	<i>Sarsia</i>	<i>Sarsia tubulosa</i>	sp	P2			
				Oceaniidae	<i>Turritopsis</i>		g	P1			
				Rathkeidae	<i>Podocorynoides</i>	<i>Podocorynoides minima</i>	sp	P1+P2			
				Tubulariidae	<i>Ectopleura</i>	<i>Ectopleura dumortierii</i>	sp	P1+P2			
				Zanclidae	<i>Zanclia</i>		g	P1+P2	P1		
				Leptothecata			or	P1+P2	P1/P2	P1	
		Blackfordiidae	<i>Blackfordia</i>		<i>Blackfordia polytentaculata</i>	sp	P1+P2				
		Campanulariidae	<i>Campanularia</i>		<i>Campanularia hincksii</i>	sp	P1	P1			
		Campanulariidae	<i>Eucheilota</i>		<i>Eucheilota maculata</i>	sp	P2				
		Clytiidae	<i>Clytia</i>		<i>Clytia gracilis</i>	sp	P1+P2				
						g	P1+P2				
Eirenidae	<i>Eugymnanthea</i>	<i>Eugymnanthea inquilina</i>	sp		P1+P2	P1					
Eutimidae	<i>Tima</i>	<i>Tima formosa</i>	sp		P1	P1/P2	P1				
Obeliidae	<i>Laomedea</i>	<i>Laomedea angulata</i>	sp		P1+P2						
		<i>Obelia</i>			g	P2					
			<i>Obelia bidentata</i>		sp	P1+P2					
			<i>Obelia dichotoma</i>		sp	P1+P2					
	<i>Obelia geniculata</i>	sp	P1+P2	P1	P1						
Tiaropsidae	<i>Tiaropsis</i>	<i>Tiaropsis multicirrata</i>	sp	P1+P2		P2					
Limnomedusae	Olindiidae	<i>Gonionemus</i>		g	P2		P2				
Siphonophorae	Agalmatidae	<i>Nanomia</i>	<i>Nanomia bijuga</i>	sp	P1+P2						
	Diphyidae	<i>Lensia</i>	<i>Lensia campanella</i>	sp	P1+P2						
<i>Muggiaea</i>		<i>Muggiaea atlantica</i>	sp	P1+P2	P1						
Scyphozoa	Rhizostomeae	Rhizostomatidae	<i>Rhizostoma</i>	<i>Rhizostoma pulmo</i>	g	P1+P2					
	Semaeostomeae	Ulmaridae	<i>Aurelia</i>		g	P1+P2					
Ctenophora	Tentaculata	Cydippida	Pleurobrachiidae	<i>Pleurobrachia</i>	<i>Pleurobrachia pileus</i>	sp	P2				
		Lobata	Bolinopsidae	<i>Mnemiopsis</i>	<i>Mnemiopsis leidyi</i>	sp	P2				

phylum	class	order	family	genus	species	level	presence	cf.	singl.		
Echinodermata	Echinoidea	Echinoida	Echinidae	<i>Paracentrotus</i>	<i>Paracentrotus lividus</i>	sp	P1+P2				
		Spatangoida	Loveniidae	<i>Echinocardium</i>	<i>Echinocardium cordatum</i>	sp	P2				
	Ophiuroidea	Ophiurida	Amphiuridae	<i>Amphiura</i>	<i>Amphiura filiformis</i>	sp	P1+P2				
			Ophiodermatidae	<i>Ophioderma</i>		g	P2	P2	P2		
			Ophiotrichidae	<i>Ophiotrix</i>	<i>Ophiotrix fragilis</i>	sp	P1+P2				
			Ophiuridae	<i>Ophiura</i>	<i>Ophiura albida</i>	sp	P1+P2				
	<i>Ophiura ophiura</i>	sp		P1+P2							
Gastrotricha	-	Macrodasysida	Macrodasysidae	<i>Urodasys</i>	<i>Urodasys calicostylis</i>	ph	P1	P1			
Mollusca	Bivalvia	Arcoida	Arcidae	<i>Anadara</i>	<i>Anadara transversa</i>	sp	P2				
		Limoida	Limidae	<i>Limaria</i>	<i>Limaria hians</i>	sp	P2		P2		
		Myoida	Corbulidae	<i>Corbula</i>	<i>Corbula gibba</i>	sp	P1+P2				
				Hiatellidae	<i>Hiatella</i>		g	P2			
				Teredinidae	<i>Lyrodus</i>	<i>Lyrodus pedicellatus</i>	sp	P2			
					<i>Teredo</i>	<i>Teredo navalis</i>	sp	P2			
		Mytiloida	Mytilidae	<i>Arcuatula</i>	<i>Arcuatula senhousia</i>	sp	P2		P2		
				<i>Lithophaga</i>	<i>Lithophaga lithophaga</i>	sp	P2				
				<i>Modiolus</i>	<i>Modiolus barbatus</i>	sp	P1+P2	P1			
				<i>Mytilaster</i>	<i>Mytilaster solidus</i>	sp	P2				
				<i>Mytilus</i>			g	P1+P2			
					<i>Mytilus edulis</i>		sp	P1			
					<i>Mytilus galloprovincialis</i>		sp	P1+P2			
				<i>Xenostrobus</i>	<i>Xenostrobus securis</i>	sp	P1+P2				
		Ostreoida	Ostreidae	<i>Crassostrea</i>	<i>Crassostrea gigas</i>	sp	P1+P2				
				<i>Ostrea</i>	<i>Ostrea stentina</i>	sp	P1+P2				
		Pterioida	Pinnidae	<i>Atrina</i>	<i>Atrina fragilis</i>	sp	P1+P2				
				<i>Pinna</i>	<i>Pinna nobilis</i>	sp	P2				
		Veneroida	Cardiidae	<i>Cerastoderma</i>	<i>Cerastoderma glaucum</i>	sp	P1+P2				
			Gastrochaenidae			f	P2				
			Mactridae	<i>Mactra</i>	<i>Mactra corallina</i>	sp	P2				
			Montacutidae	<i>Entovalva</i>		g	P1	P1	P1		
				<i>Kurtiella</i>	<i>Kurtiella bidentata</i>	sp	P2	P2			
			Solenidae	<i>Solen</i>	<i>Solen marginatus</i>	sp	P1	P2	P1		
			Veneridae	<i>Chamelea</i>	<i>Chamelea gallina</i>	sp	P1+P2				
				<i>Polititapes</i>	<i>Polititapes aureus</i>	sp	P1+P2	P1	P1		
		<i>Ruditapes</i>		<i>Ruditapes philippinarum</i>	sp	P1+P2					
		Cephalopoda	Octopoda	Octopodidae	<i>Octopus</i>	<i>Octopus maya</i>	sp	P1		P1	
			Sepiida	Sepiidae	<i>Sepia</i>	<i>Sepia officinalis</i>	sp	P1+P2	P1	P1	
		Gastropoda	-	Acteonidae	<i>Acteon</i>	<i>Acteon tornatilis</i>	sp	P2		P2	
				Cerithiidae	<i>Bittium</i>	<i>Bittium reticulatum</i>	sp	P1+P2			
				Cerithiopsidae	<i>Cerithiopsis</i>	<i>Cerithiopsis tubercularis</i>	sp	P2			
				Limapontiidae	<i>Ercolania</i>	<i>Ercolania viridis</i>	sp	P1+P2			
					<i>Placida</i>	<i>Placida dendritica</i>	sp	P1		P1	
				Turritellidae	<i>Turritella</i>	<i>Turritella communis</i>	sp	P1+P2			
				Cephalaspidea	Aglajidae	<i>Philinopsis</i>	<i>Philinopsis depicta</i>	sp	P2		P2
					Haminoeidae	<i>Haminoea</i>	<i>Haminoea hydatis</i>	sp	P1+P2	P1	P1
						<i>Haminoea japonica</i>	sp	P1+P2			
			<i>Haminoea navicula</i>			sp	P1+P2				
			<i>Haminoea ortei</i>			sp	P1+P2				
			<i>Roxaniella</i>	<i>Roxaniella jeffreysi</i>	sp	P1+P2					
			Philimidae	<i>Philine</i>		g	P2				
			Littorinimorpha	Aporrhaidae	<i>Aporrhais</i>	<i>Aporrhais pespelecani</i>	sp	P1+P2			
				Hydrobiidae	<i>Ecrobia</i>	<i>Ecrobia grimmi</i>	sp	P2			
					<i>Ecrobia maritima</i>	sp	P1+P2				
					<i>Ecrobia ventrosa</i>	sp	P1+P2		P2		
			<i>Hydrobia</i>	<i>Hydrobia acuta</i>	sp	P1+P2					

phylum	class	order	family	genus	species	level	presence	cf.	singl.								
		Neogastropoda	Littorinidae	<i>Melarhaphe</i>	<i>Melarhaphe neritoides</i>	sp	P1										
			Rissoidae	<i>Rissoa</i>		g	P1+P2										
			Muricidae	<i>Rapana</i>	<i>Rapana venosa</i>	sp	P1+P2										
			Nassariidae	<i>Tritia</i>	<i>Tritia nitida</i>	sp	P1+P2										
		<i>Tritia neritea</i>			sp	P1											
		Nudibranchia	Aeolidiidae	<i>Spurilla</i>	<i>Spurilla neapolitana</i>	sp	P1+P2		P1								
			Goniodorididae	<i>Okenia</i>	<i>Okenia aspersa</i>	sp	P1+P2										
			Polyceridae	<i>Polycera</i>	<i>Polycera hedgpethi</i>	sp	P1+P2										
				<i>Polycerella</i>	<i>Polycerella emertoni</i>	sp	P1+P2		P2								
		Pteropoda	Creseidae	<i>Creseis</i>	<i>Creseis acicula</i>	sp	P1+P2		P2								
					<i>Creseis virgula</i>	sp	P1+P2										
		Scaphopoda	Dentaliida	Dentaliidae			f	P1	P1								
<i>Antalis</i>	<i>Antalis dentalis</i>				sp	P2											
Nematoda	Chromadorea	Monhysterida	Linhomoeidae	<i>Terschellingia</i>	<i>Terschellingia longicaudata</i>	sp	P1+P2	P1									
			Monhysteridae	<i>Diplolaimella</i>	<i>Diplolaimella dievengatensis</i>	sp	P1	P1	P1								
		Rhabditida	Toxocaridae	<i>Toxocara</i>	<i>Toxocara cati</i>	sp	P2	P2	P2								
Nemertea	Palaeonemertea	-	Cephalothricidae	<i>Cephalothrix</i>		g	P1+P2										
			Tubulanidae	<i>Tubulanus</i>	<i>Tubulanus superbus</i>	g	P2										
	Pilidiophora	-	Hubrechtidae	<i>Hubrechtella</i>	<i>Hubrechtella dubia</i>	sp	P1+P2	P1	P1								
Heteronemertea				Lineidae	<i>Lineus</i>	<i>Lineus bilineatus</i>	sp	P1+P2									
Phoronida	-	-	-	<i>Phoronis</i>	<i>Phoronis hippocrepia</i>	sp	P1+P2										
					<i>Phoronis muelleri</i>	sp	P1	P1									
Platyhelminthes	Trematoda	Strigeidida	Bucephalidae	<i>Bucephalus</i>	<i>Bucephalus minimus</i>	sp	P2	P2									
							ph	P2									
Porifera	Demospongiae					cl	P1	P1									
						Bubarida	Dictyonellidae	<i>Scopalina</i>	<i>Scopalina lophyropoda</i>	sp	P1						
						Clionaida	Clionaidae	<i>Pione</i>	<i>Pione vastifica</i>	sp	P1+P2		P2				
						Haplosclerida					or	P1					
											Callyspongiidae	<i>Callyspongia</i>		g	P1		P1
											Chalinidae	<i>Haliclona</i>	<i>Haliclona simulans</i>	sp	P1	P1	
						Poecilosclerida	Tedaniidae	<i>Tedania</i>	<i>Tedania ignis</i>	sp			P2				
						Suberitida	Halichondriidae				<i>Halichondria</i>	g	P1				
											<i>Halichondria panicea</i>	sp	P1+P2				
											<i>Hymeniacion</i>	g	P1+P2				
											<i>Hymeniacion perlevis</i>	sp	P1+P2				
						Tethyida	Tethyidae	<i>Tethya</i>	<i>Tethya citrina</i>	sp	P1		P1				
Homoscleromorpha	Homosclerophorida	Oscarellidae	<i>Oscarella</i>		g	P2	P2										
Monogononta	Ploima	Trichocercidae	<i>Trichocerca</i>		g	P2											